Soft and Hard X-ray Microscopy

Ian McNulty

Advanced Photon Source,
Argonne National Laboratory

Cheiron School 2008

SPring-8

Outline

1. Fundamentals

resolution

contrast

sources

optics

2. Direct methods

projection imaging

full-field imaging

scanning

3. Indirect methods

microdiffraction

coherent diffraction

holography

References:

1. M. Howells, "Soft-x-ray microscopes," Physics Today 38, 22 (Aug. 1985).
2. J. Kirz, "Soft X-ray microscopes and their biological applications," Q. Rev. Biophys. 28, 1 (1995).
3. J. Als-Nielsen and D. McMorrow, *Elements of Modern X-ray Physics* (Wiley, New York, 2000).
4. D. Attwood, *Soft X-Rays and Extreme Ultraviolet Radiation: Principles and Applications* (Cambridge, 2007).

Image formation as a scattering process

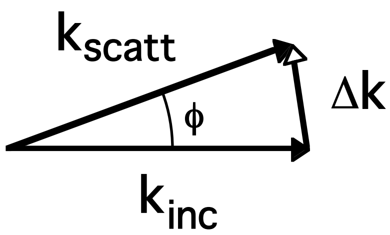

Incident waves with initial momentum k_{inc} are elastically scattered into new direction k_{scatt} with momentum transfer Δk.

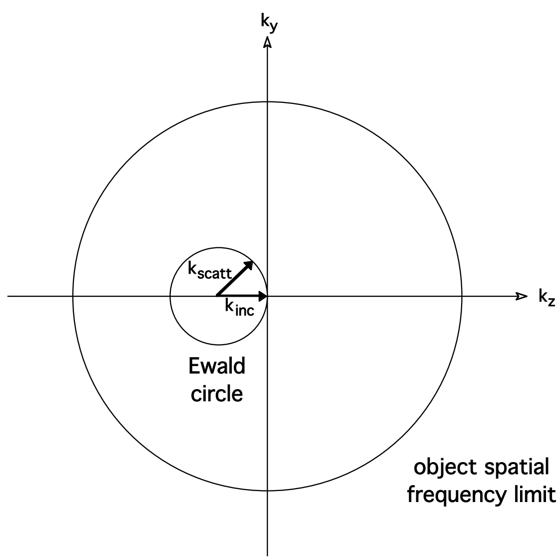

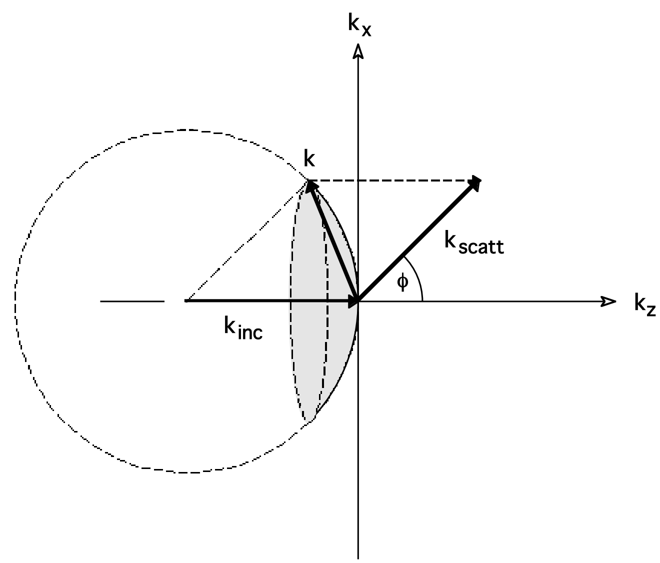

Ewald sphere is defined by conservation of momentum. Only spatial frequencies on the Ewald sphere are accessible to the imaging process, limiting attainable resolution.

Diffraction limits to resolution

Point-spread function

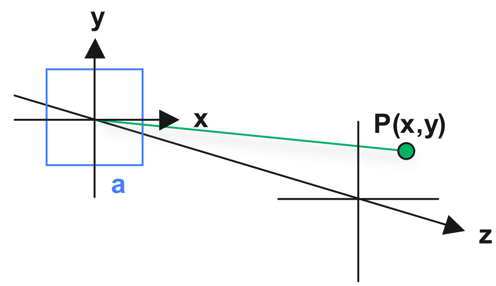

$$P(x,y) = \frac{\sin x}{x}\,\frac{\sin y}{y}$$

with $x = \dfrac{kax}{z}$, $y = \dfrac{kay}{z}$

Transverse $\boxed{R = 0.5\,\dfrac{\lambda}{NA}}$

where $NA \sim \dfrac{a}{z}$

$$k = \frac{2\pi}{\lambda}$$

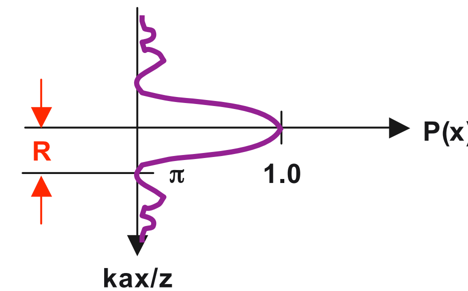

Bragg's law

$$\Delta\vec{k} = \vec{k}_{inc} - \vec{k}_{scatt} \qquad (0 \le \Delta k \le 2k_{inc}) \qquad k_x^2 + k_y^2 + (k_z + k_{inc})^2 = k_{inc}^2$$

For extreme-angle ray (xz plane, $k_y = 0$) with $k_x = \dfrac{2\pi}{2R} = \dfrac{2\pi}{\lambda}NA$

Longitudinal $\boxed{DOF = \dfrac{\lambda}{(NA)^2}}$ **and** $k_z = \dfrac{k_x^2}{2k_{inc}} \qquad (k_z << k_{inc})$

What do we mean by "resolution"?

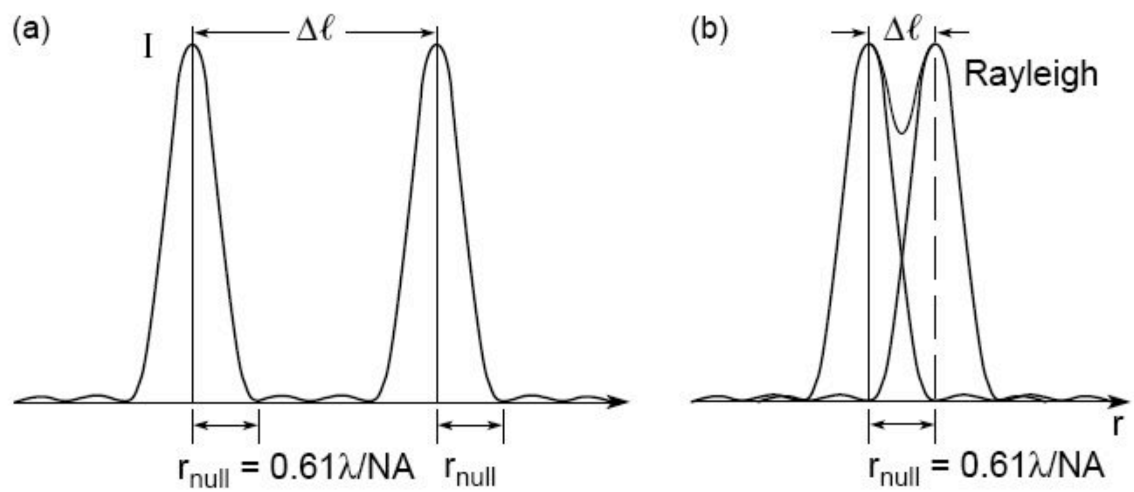

- Point sources are spatially coherent
- Mutually incoherent
- Intensities add
- Rayleigh criterion (26.5% dip)

Conclusion: With spatially coherent illumination, objects are "just resolvable" when

$$\mathrm{Res}|_{\mathrm{coh}} = \frac{0.61\,\lambda}{\mathrm{NA}} = 1.22\,\Delta r$$

Coherence

longitudinal coherence

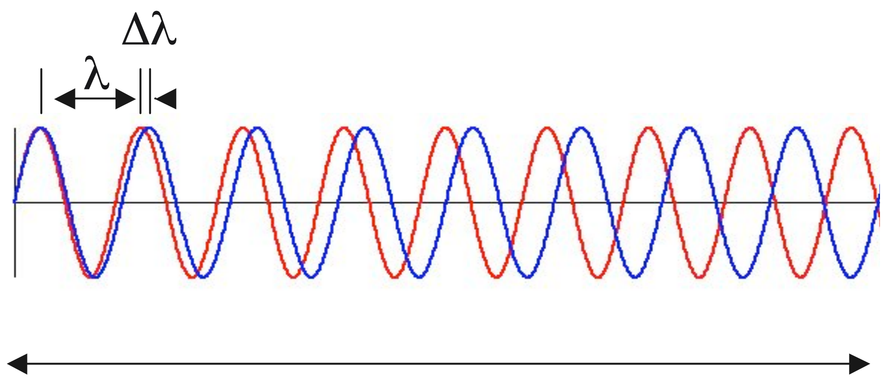

$$l_c \sim \frac{\lambda^2}{\Delta\lambda}$$

$$\tau_c \sim \frac{\lambda^2}{c\Delta\lambda}$$

transverse coherence

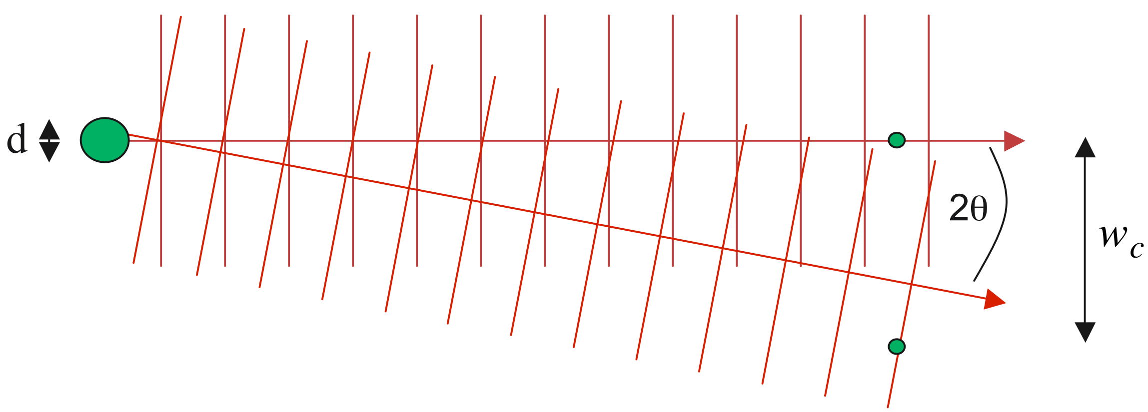

$$w_c \sim \frac{\lambda z}{d}$$

$$d \cdot \theta = \lambda / 2\pi$$

$$\Delta x \, \Delta p \geq \hbar / 2$$

Coherent vs. incoherent

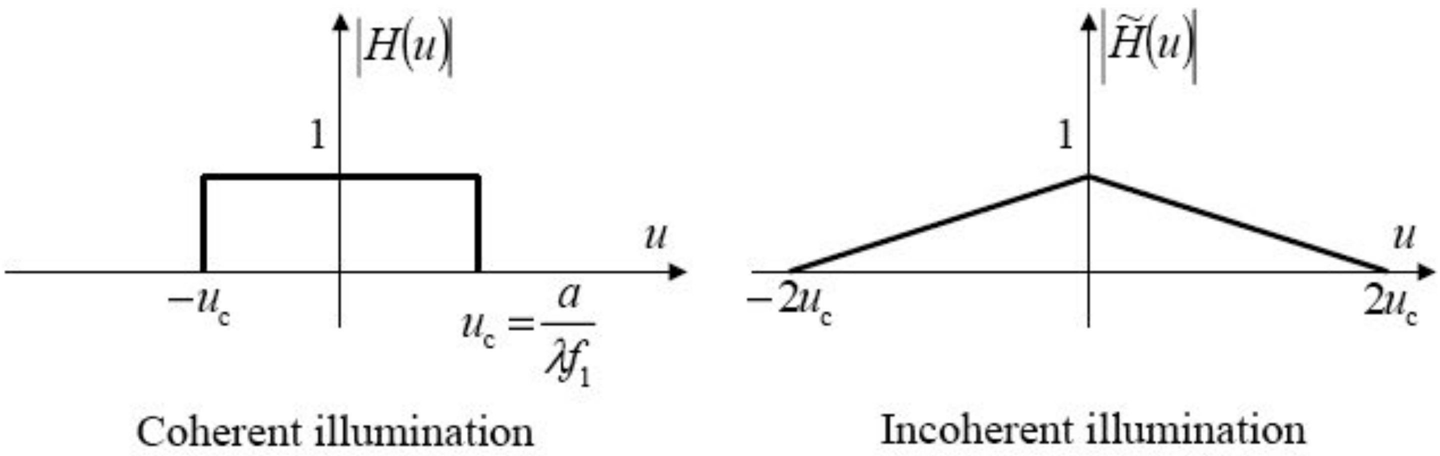

Scanning and full-field microscopy are *incoherent* methods

- **Transfer function is linear in the field *intensities***
- **Characterized by sloping function down to 2NA**

Diffraction and holographic microscopy are *coherent* methods

- **Transfer function is linear in the field *amplitudes***
- **Characterized by flat top, sharp cutoff at limiting NA**

Why use x-rays?

- Penetration through whole cells and thick materials with minimal multiple scattering: “clean” images and spectra
- Short wavelengths, so high spatial resolution is possible
- Short pulses, so high time resolution is possible
- Coupling to core-level electrons: element detection, “clean” measurement of electronic and chemical states
- Coupling to electronic spin via polarization: probe magnetic states and ordering

But: ionizing radiation, so repeated high-resolution imaging of radiation-sensitive samples (e.g. live cells) is not possible.

Contrast mechanisms in x-ray microscopy

- **Access a wealth of information**
  - Absorption — measure electron density
  - Phase — measure real part of refractive index
  - Fluorescence — measure elemental distribution
  - Spectroscopy — extract chemical state, spin state
  - Diffraction — reveal structure, strain, mag. charge

- **Natural sample contrast is possible; staining not required**
- **Image structure of thick samples, sectioning not required**
- **More penetrating, less damage, less charging than with electrons**

Refractive index and contrast

$$n = 1 - \delta - i\beta = 1 - \frac{r_e}{2\pi}\lambda^2 \sum_i n_i f_i(0)$$

$$A = A_0 \exp(-inkt)$$
$$k = 2\pi / \lambda$$

- Absorption contrast:

  sensitive to *Im(n)*

  $\sim 2\pi\delta(x,y)t/\lambda$

- Phase contrast:

  sensitive to *Re(n)*

  $\sim 4\pi\beta(x,y)t/\lambda$

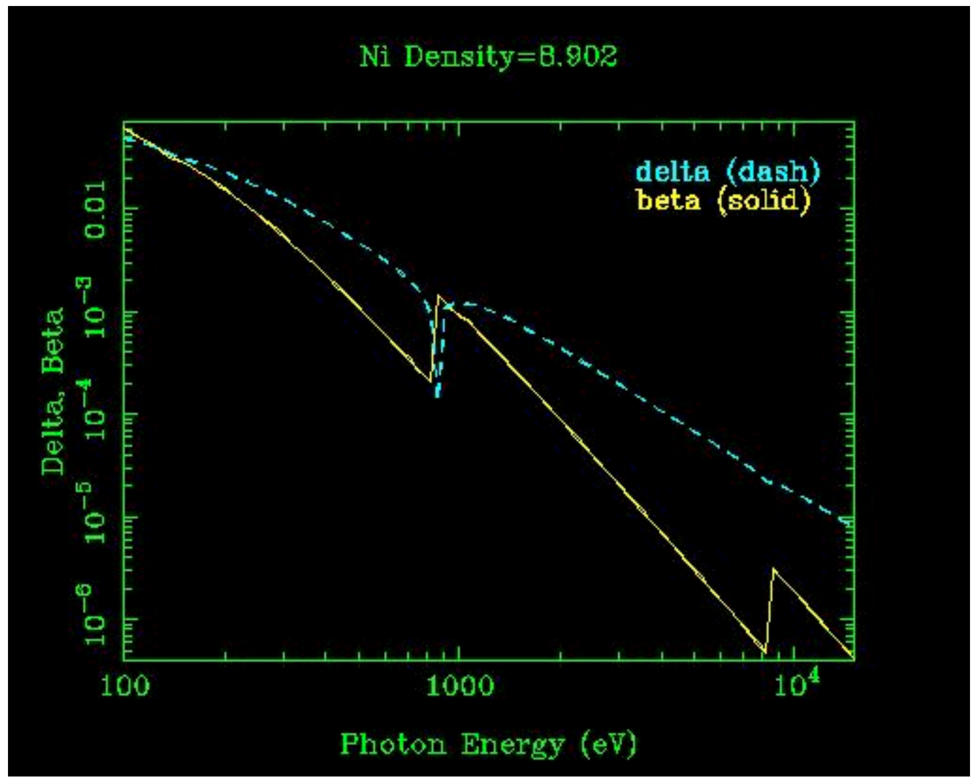

Elemental sensitivity at absorption edges

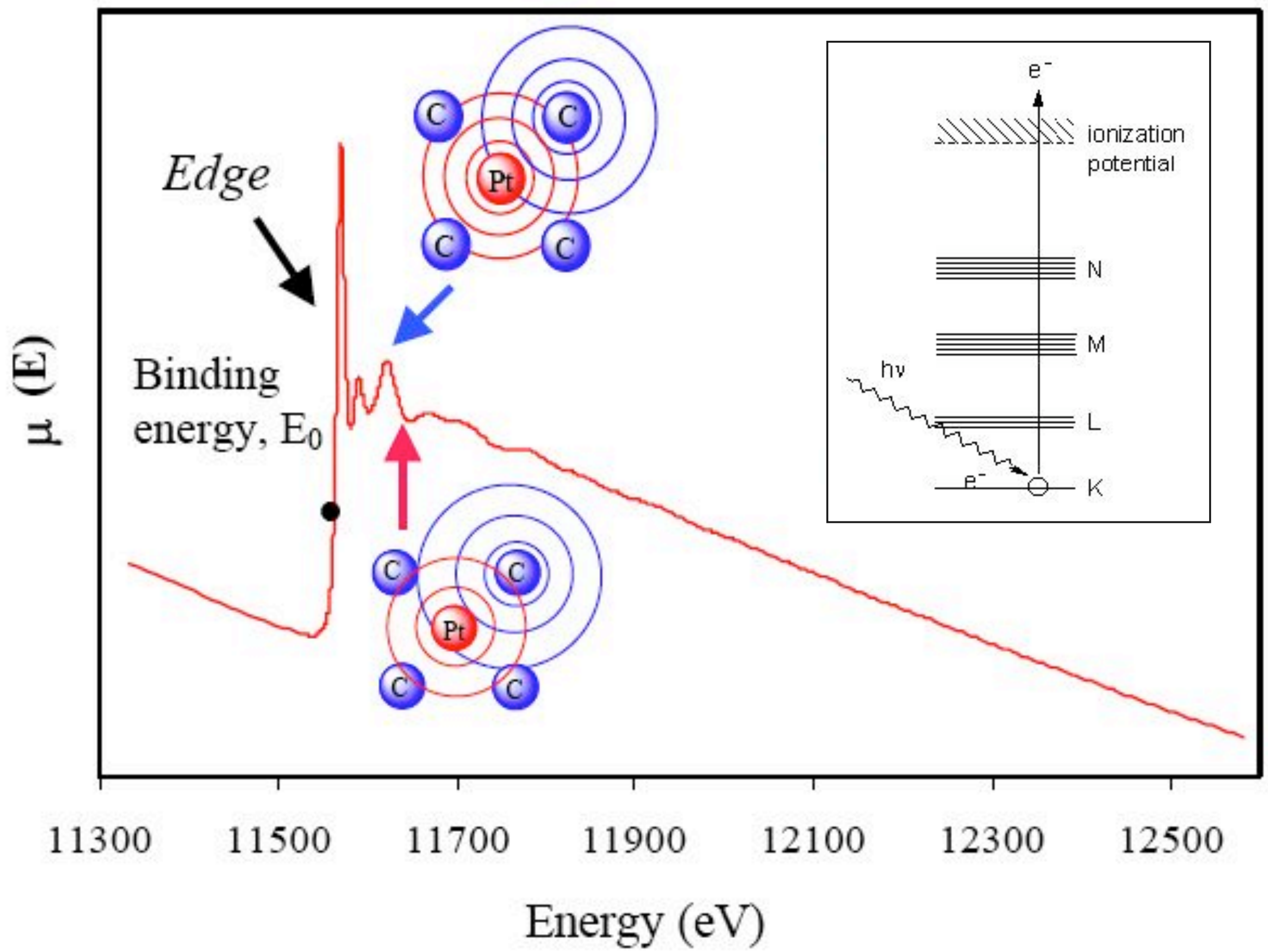

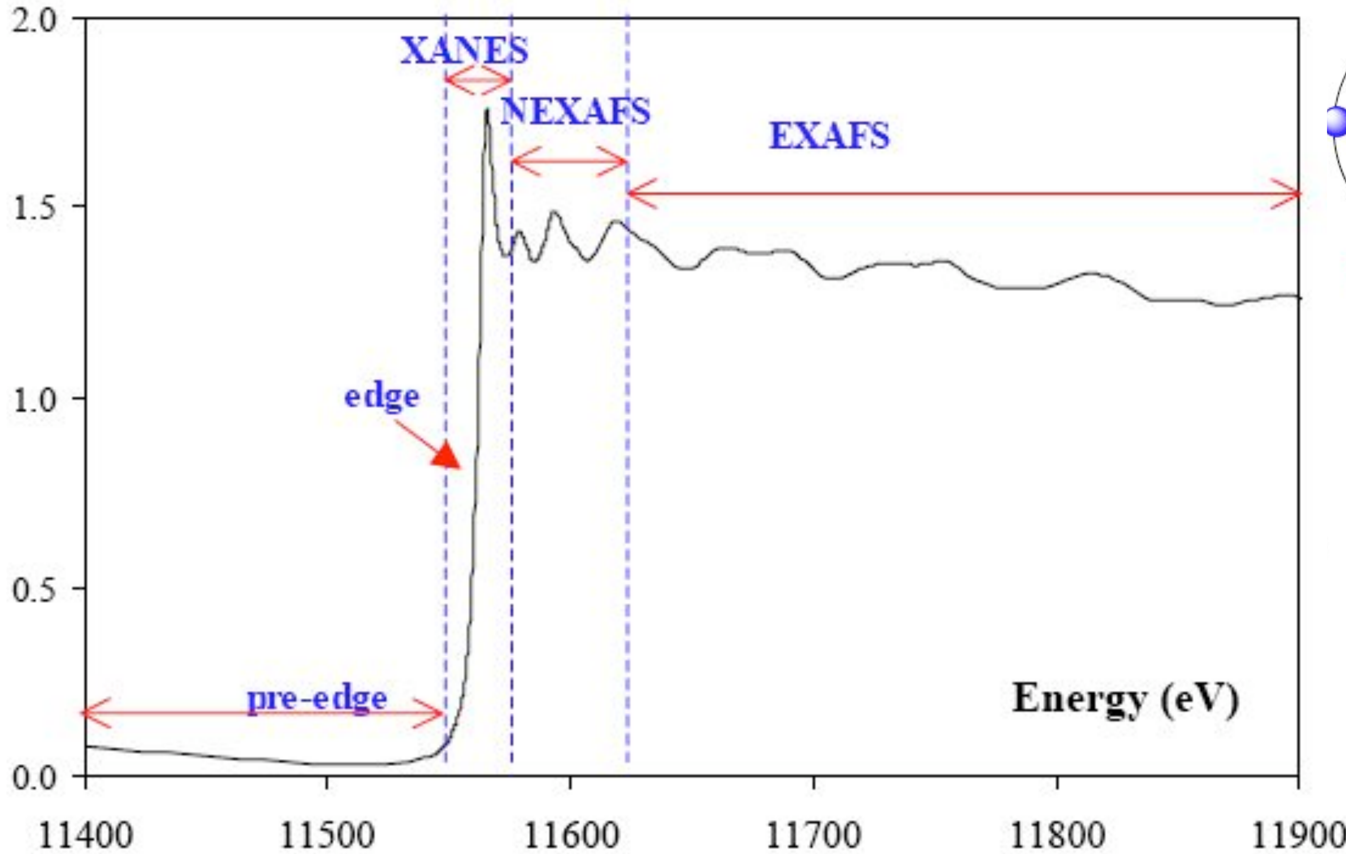

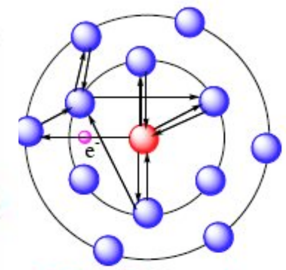

Multiple scattering

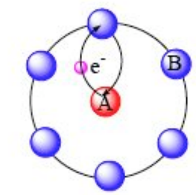

Single scattering

The "water window"

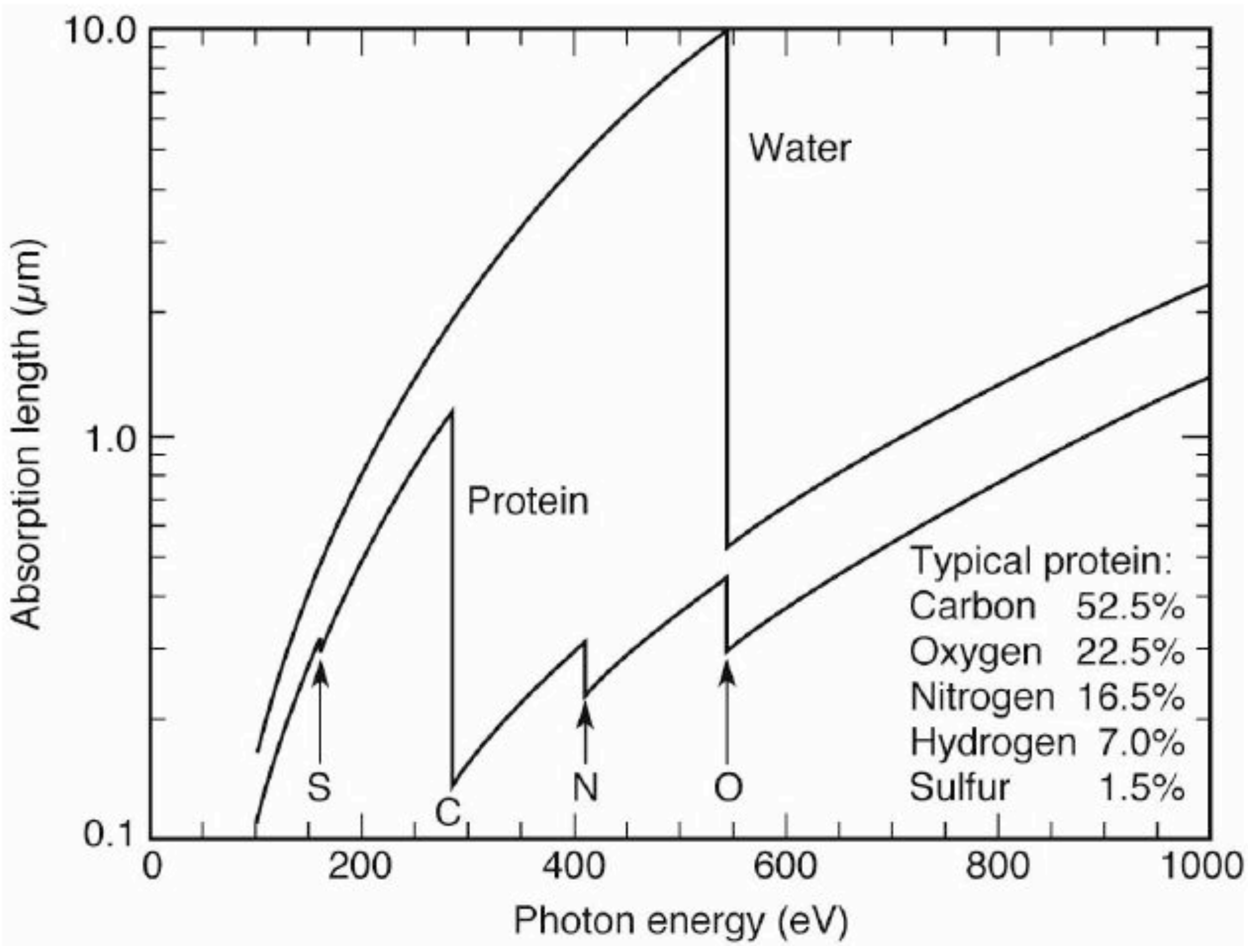

Fluorescence spectroscopy

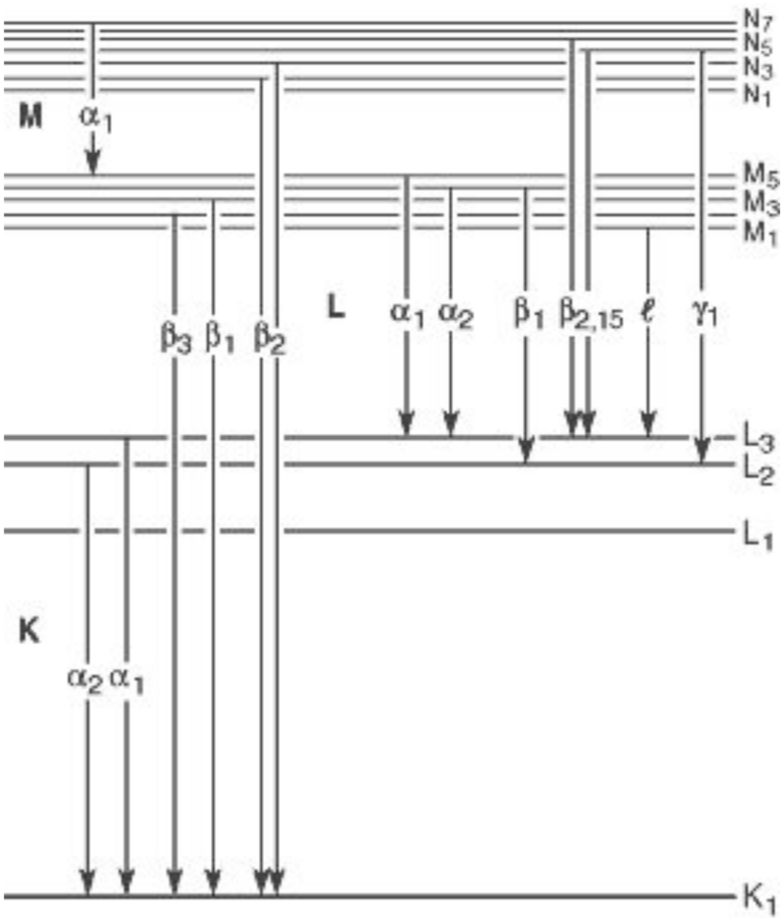

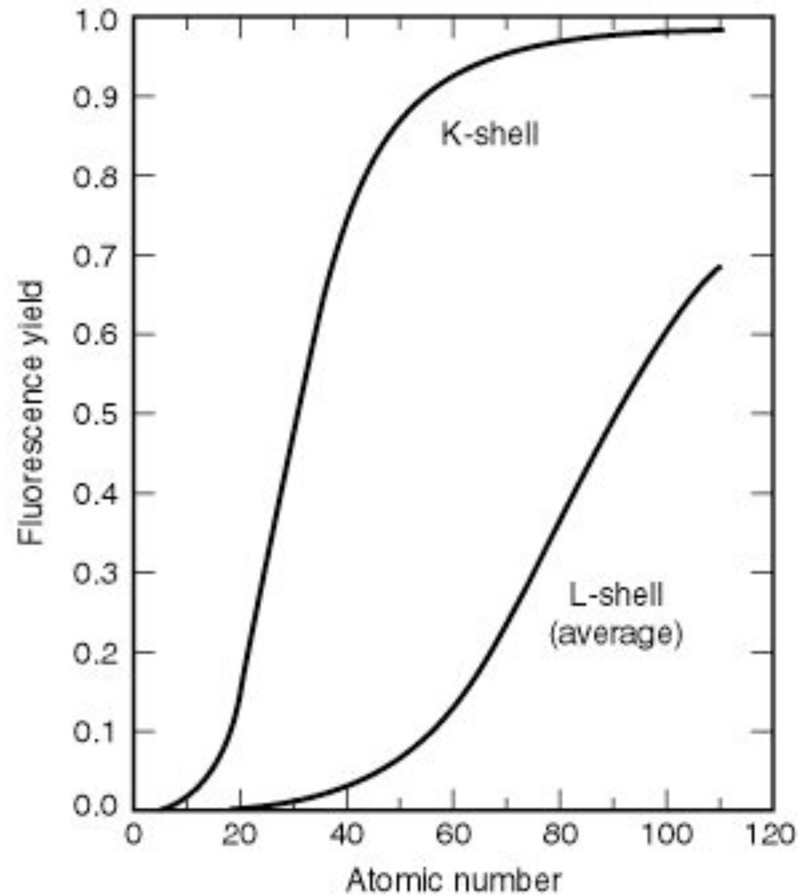

Why use synchrotrons?

Synchrotron sources offer

- **Brilliance (small source, collimated)**
- **Tunability (IR to hard x-rays)**
- **Polarization (linear, circular)**
- **Time structure (short pulses)**

➢ **Undulators produce the most brilliant x-ray beams available**

B = photons/source area, divergence, bandwidth

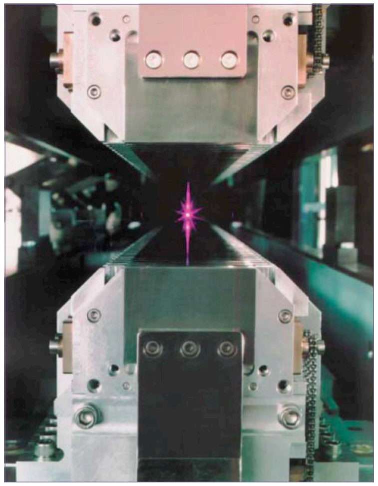

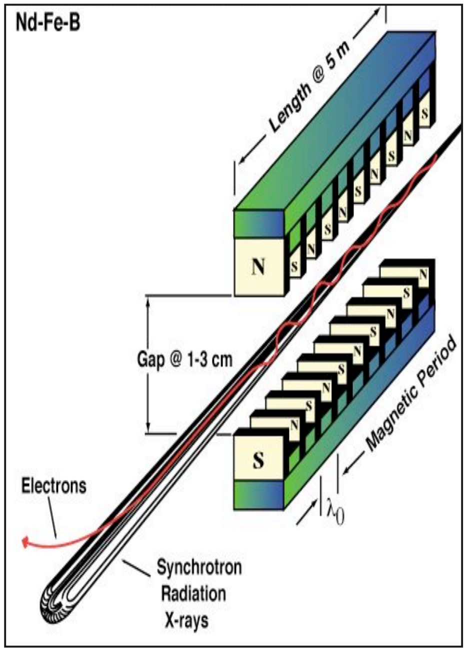

Undulator radiation

- **SR sources (except FEL) are incoherent, but highly forward directed due to relativistic effects** $\theta \sim 1/\gamma$

- **Spatial and temporal filtering (pinholes, monochromators) is needed to select the coherent flux** $F_c \sim \lambda^2 B$

- **Only the coherent flux can be focused into a diffraction-limited spot or be used to form interference fringes**

Focusing optics for x-rays

Achieving high NA is challenging because x-rays interact weakly

$n = 1 - \delta - i\beta$ $\qquad$ $\delta, \beta \sim 10^{-3}$ to 10^{-6} $\qquad \Rightarrow \qquad$ $|n| \approx 1$

Refractive (compound refractive lenses) ~ 50 nm

Low efficiency, highly chromatic, aberrations

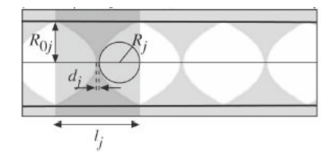

Reflective (Kirkpatrick-Baez mirrors) ~ 40 nm

High efficiency, achromatic, limited to ~10 nm

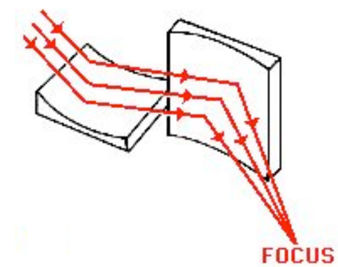

Diffractive (Fresnel zone plates, MLLs) ~ 20 nm

Moderate efficiency, limited to ~10 nm except MLL

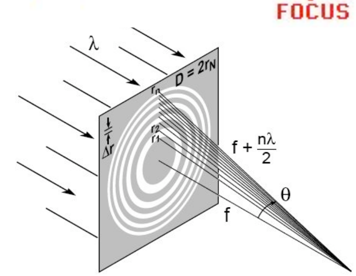

Waveguides ~ 20 nm

Low efficiency, 2D is challenging

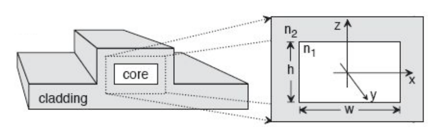

SCIENTIFIC
AMERICAN

Established 1845

CONTENTS FOR MARCH 1949 VOLUME 180, NUMBER 3

2. Direct methods

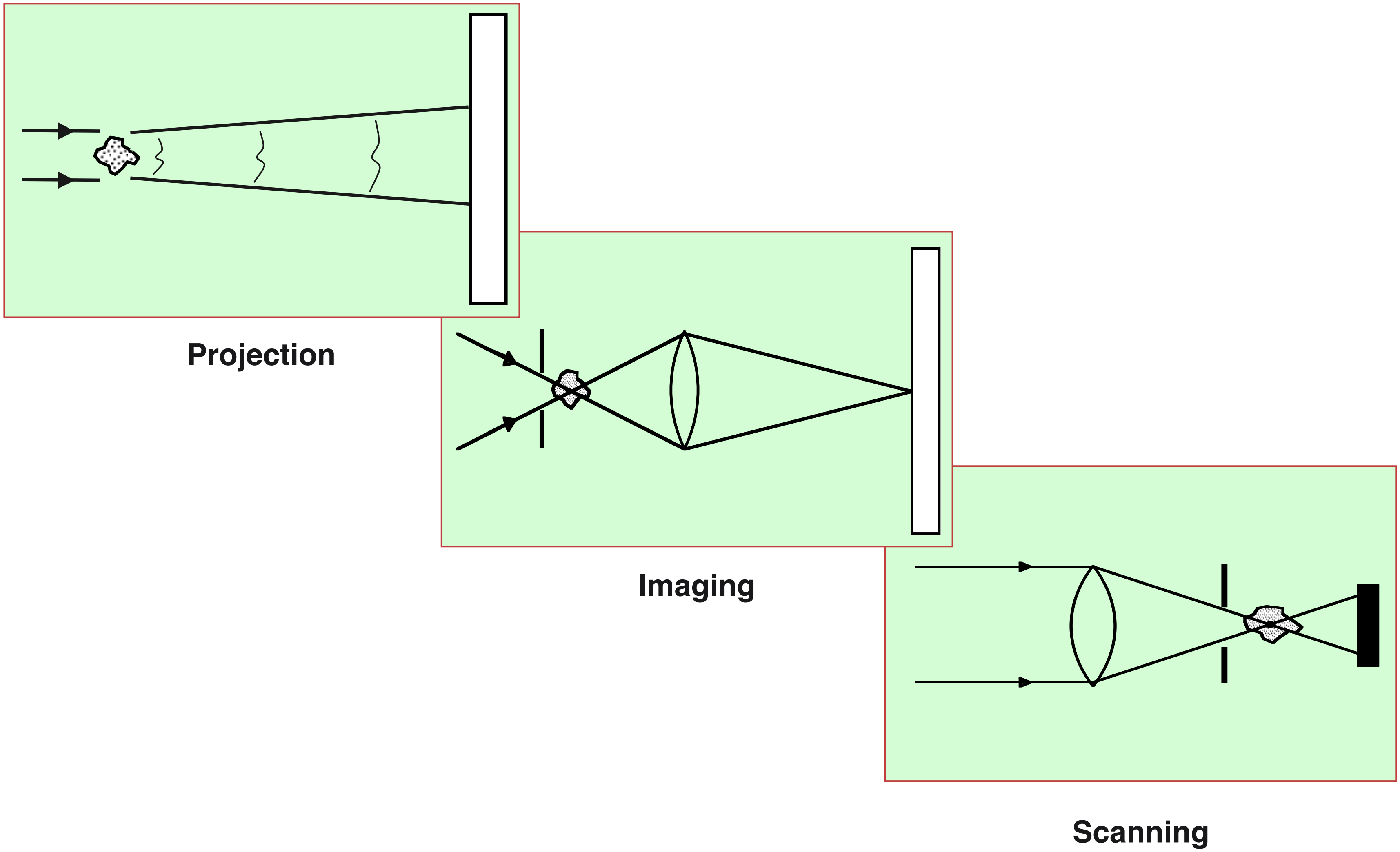

Different regimes of x-ray imaging

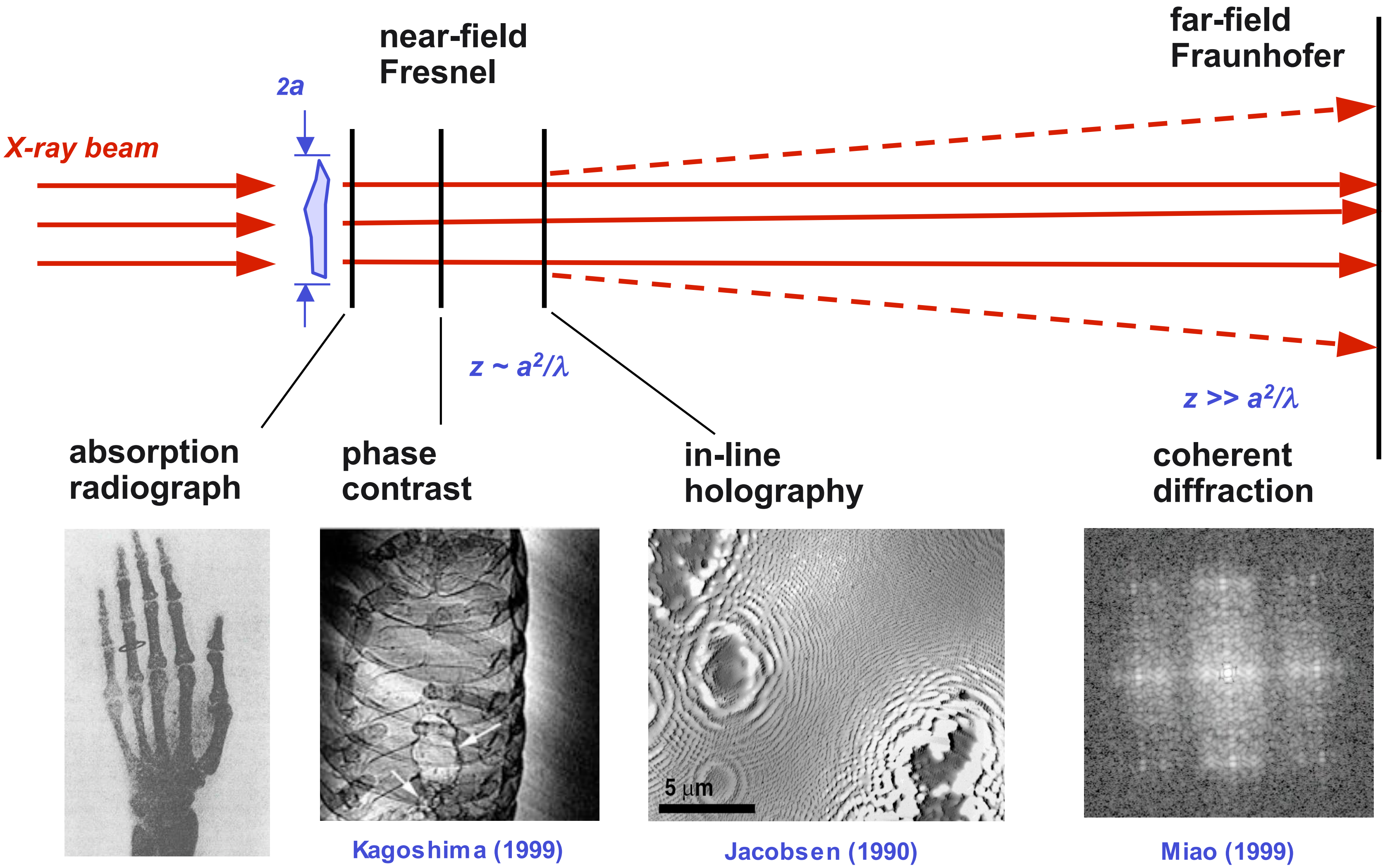

Phase contrast: tool of choice for low-absorption samples

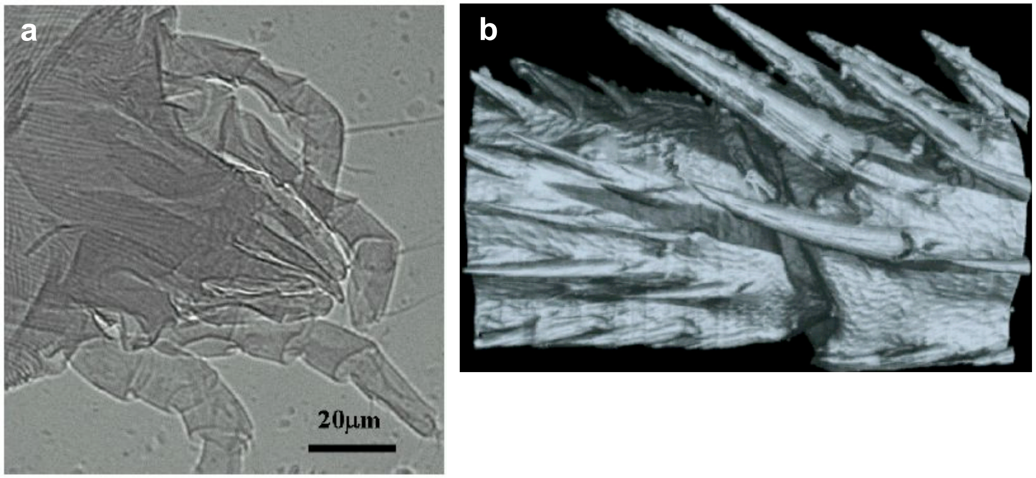

(a)Dust mite and (b) tomographically reconstructed fly leg joint, recorded with ~8 keV x-rays and propagation phase contrast.

S. Mayo, Opt. Express 11, 2289 (2003)

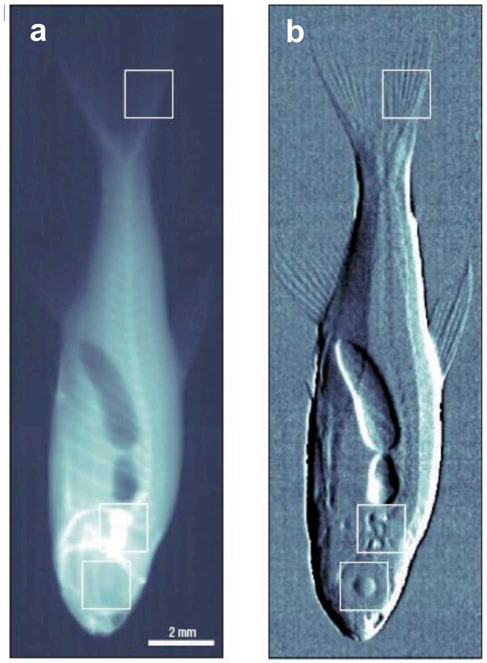

Small fish, recorded with three-grating method and a standard x-ray tube (40 kV/25 mA). (a) Transmission. (b) Differential phase contrast.

F. Pfeiffer, Nature Phys. 2, 258 (2006)

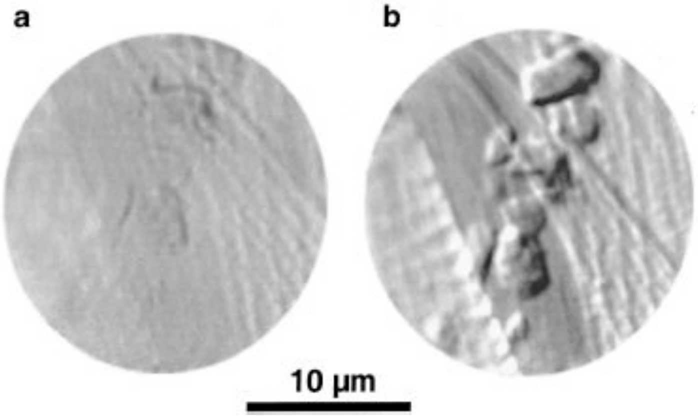

Moth wing, recorded with 4 keV x-rays.
(a) Bright-field. (b) Differential interference contrast.

B. Kaulich, T. Wilhein, J. Opt. Soc. Am. A19, 797 (2002)

Full-field and scanning x-ray microscopes

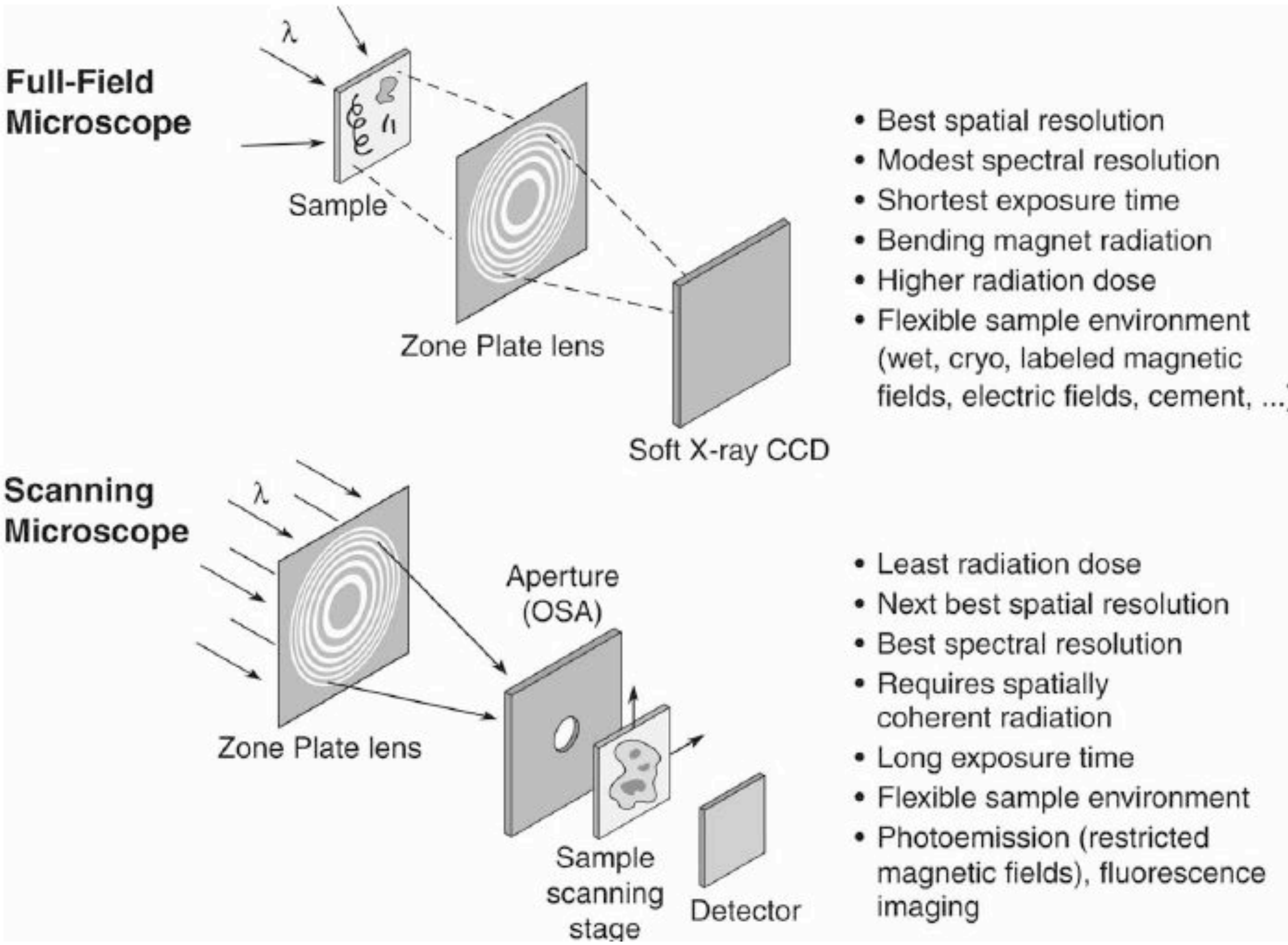

XM-1 microscope at the ALS

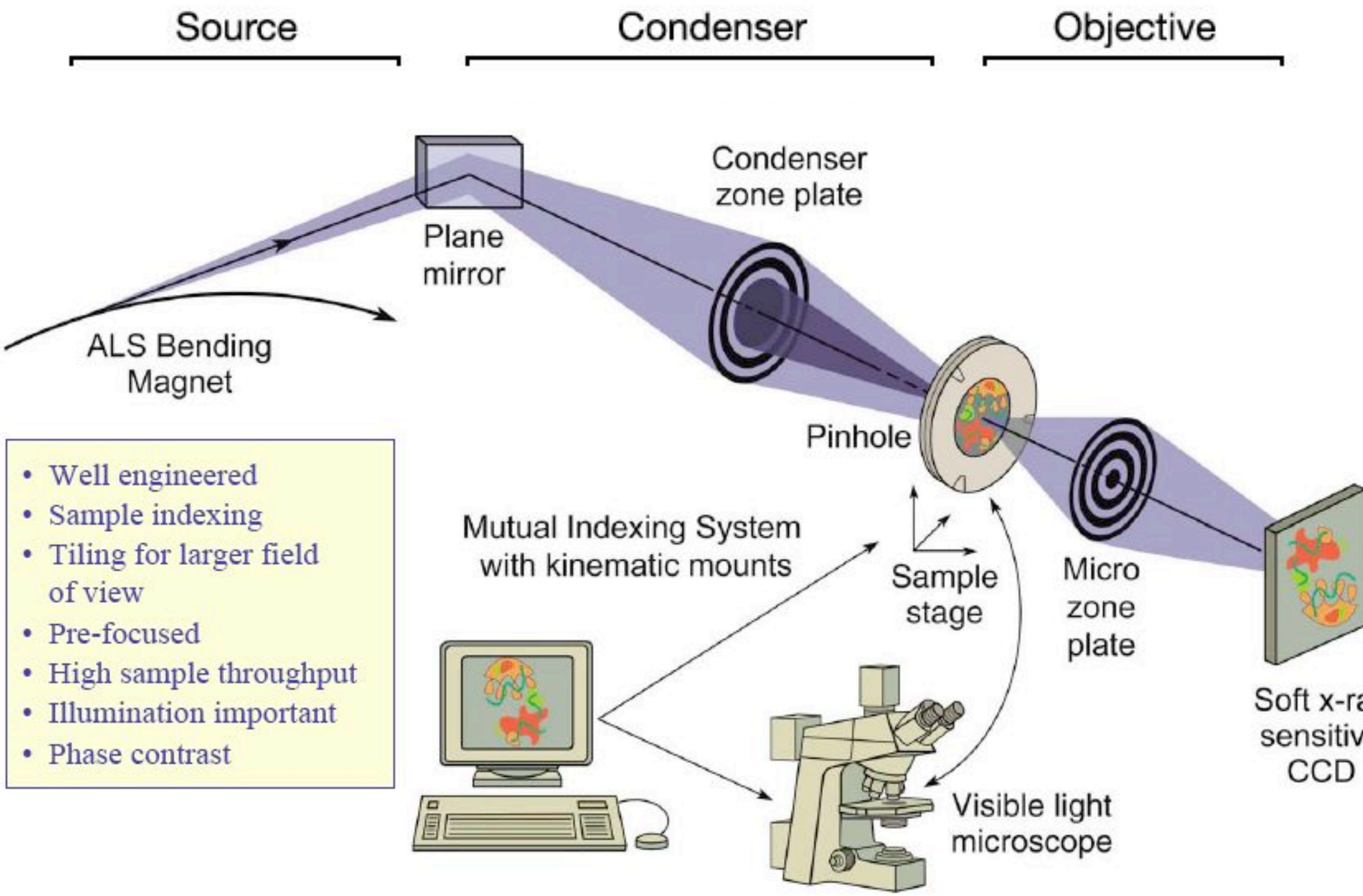

- Well engineered
- Sample indexing
- Tiling for larger field of view
- Pre-focused
- High sample throughput
- Illumination important
- Phase contrast

Wet specimens can be studied by x-ray microscopy

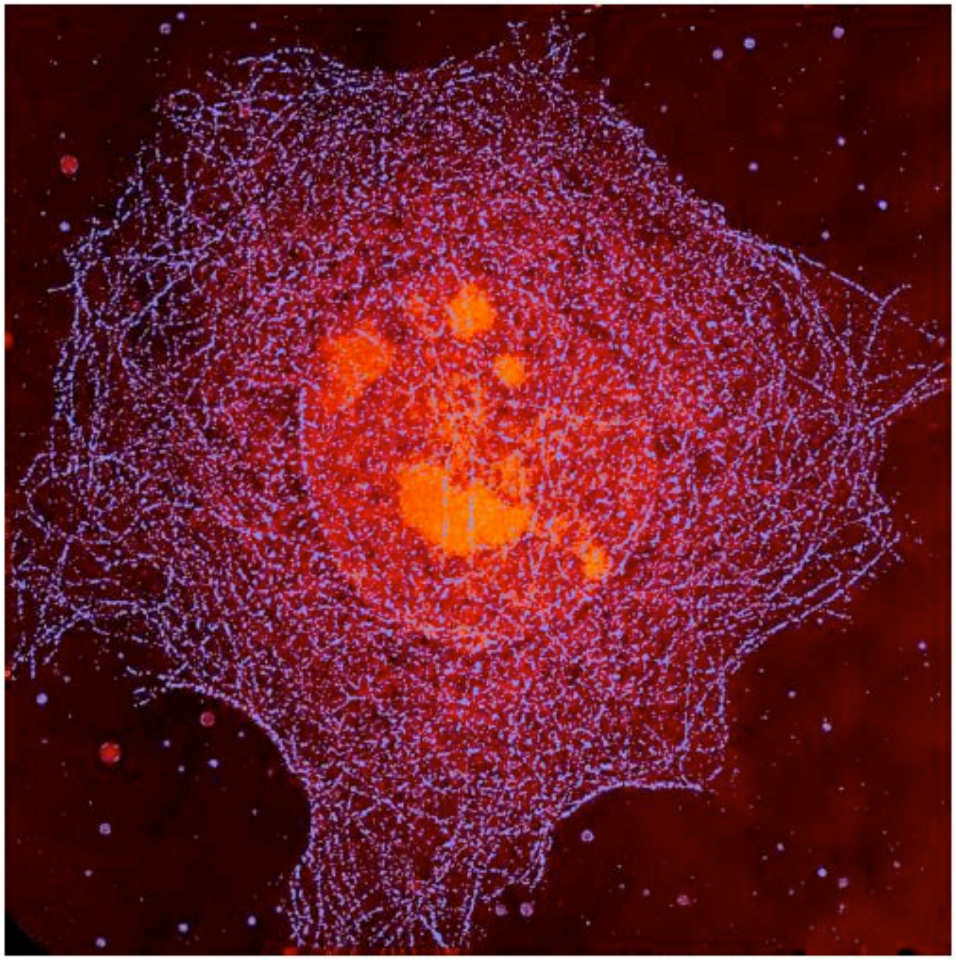

$\hbar w = 520$ eV

32 μm x 32 μm

Ag enhanced Au labeling of the microtubule network, color coded blue.

Cell nucleus and nucleoli, moderately absorbing, coded orange.

Less absorbing aqueous regions coded black.

W. Meyer-Ilse et al. J. Microsc. 201, 395 (2001)

Whole, hydrated mouse epithelial cell

Cryo-preparation of sample mitigates radiation damage

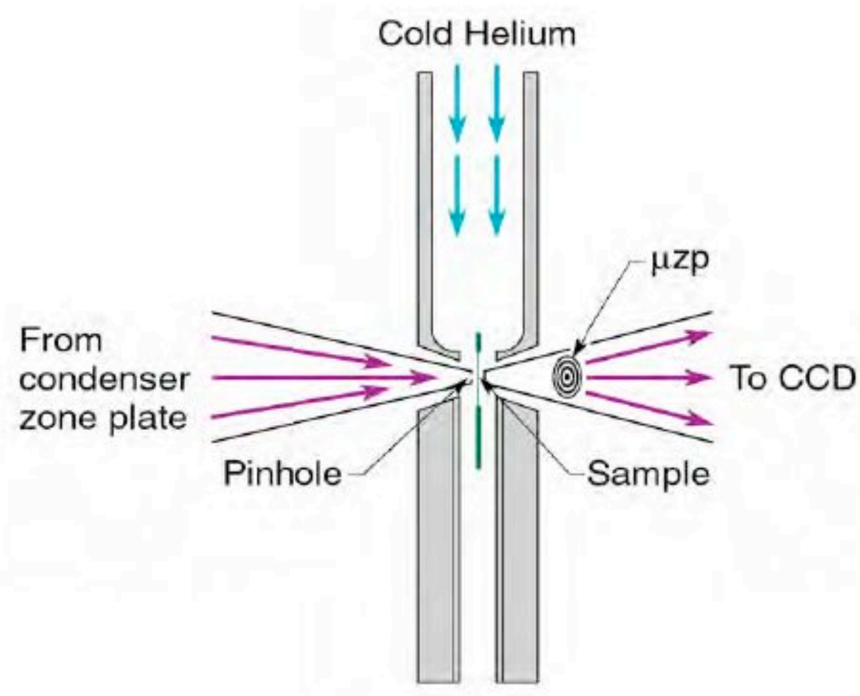

Helium passes through LN, is cooled, and directed onto sample windows

Fast Freeze

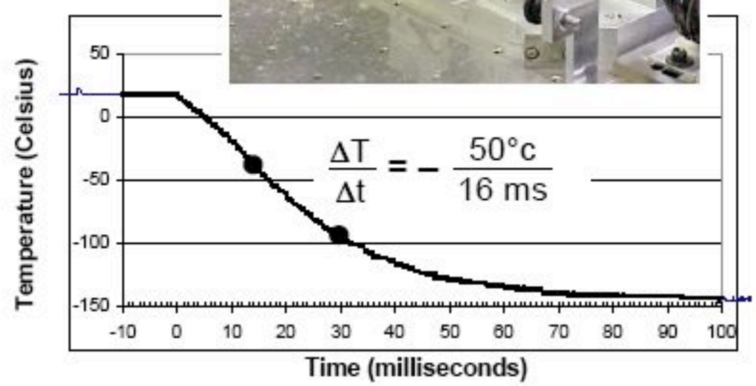

Interconnects in chips are more "hardy"

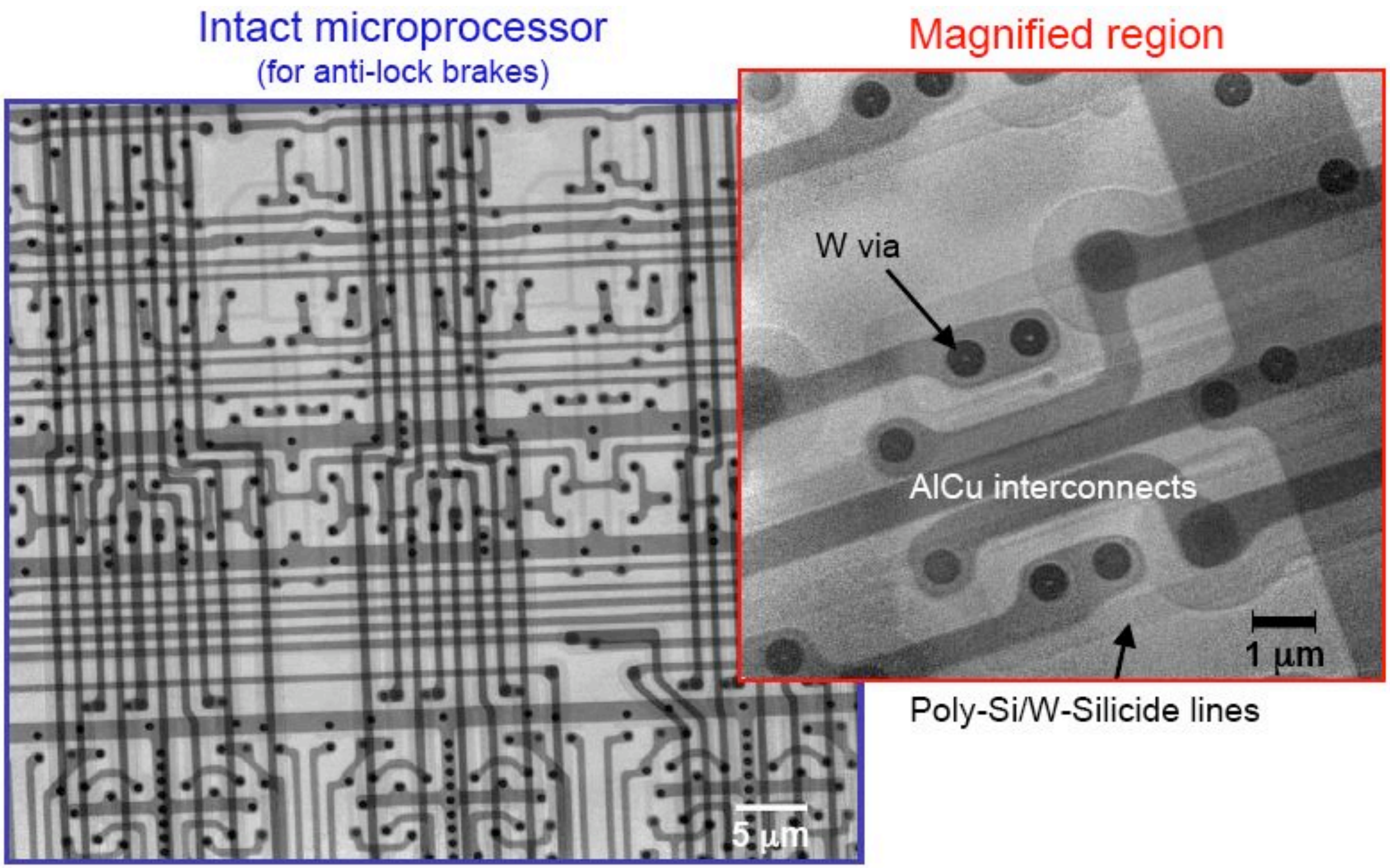

Circular dichroism contrast using polarized x-rays

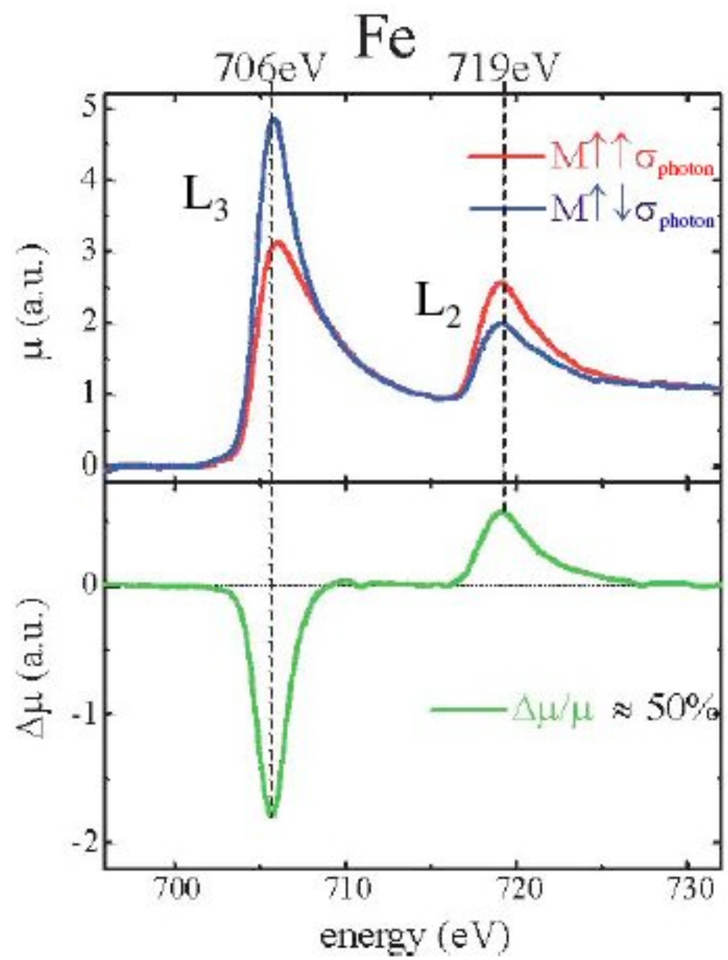

Magnetic x-ray microscopy

FeGd Multilayer

Contrast reversal

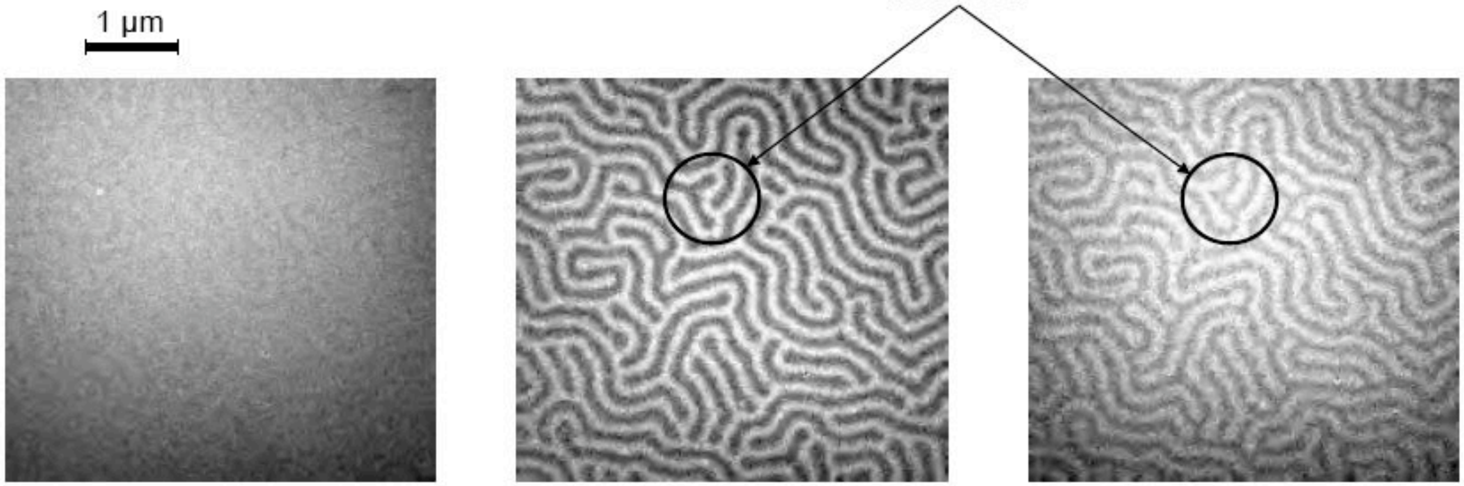

ħω = 704 eV
below Fe L-edges

ħω = 707.5 eV
Fe L_3-edge

ħω = 720.5 eV
Fe L_2-edge

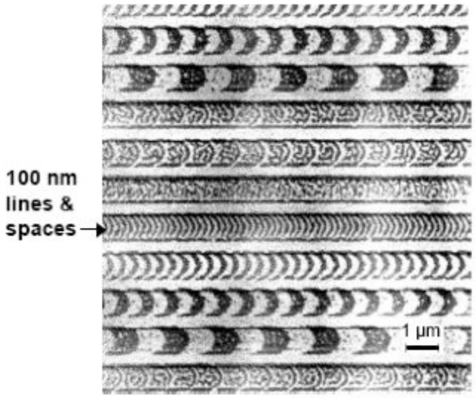

Magnetic recording materials:
FeTbCo multilayer with Al cap layer

P. Fischer (MPI), G. Denbeaux (CXRO)

3D imaging

$R \approx 0.61\ \lambda\ /\ NA$ $DOF \approx 1.22\ \lambda\ /\ (NA)^2 = 2\ R^2\ /\ (0.61\lambda)$

$|n| \approx 1 \quad \Rightarrow \quad NA \ll 1 \quad \Rightarrow \quad DOF \ll R$

Synthesize larger NA with multiple views

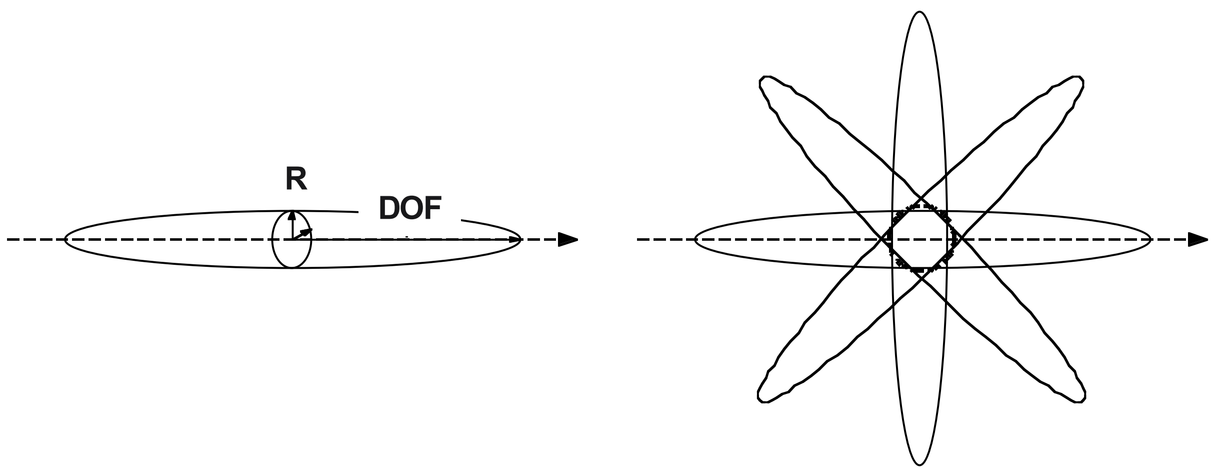

Cannot improve R, only DOF by tomography

Computed tomography

1 **Record many projections through sample over wide angular range. Projections at angles *q* contain:**

$$I(x,y,\theta) = I_0\, e^{-\int \mu_\theta (x',y',z')\,dz'}$$

2 **Reconstruct 3D sample density from suite *S* of projections**

$$\text{Invert } \; S\{I(x,y,\theta)\} \;\Rightarrow\; \mu(x,y,z)$$

Soft x-ray nanotomography

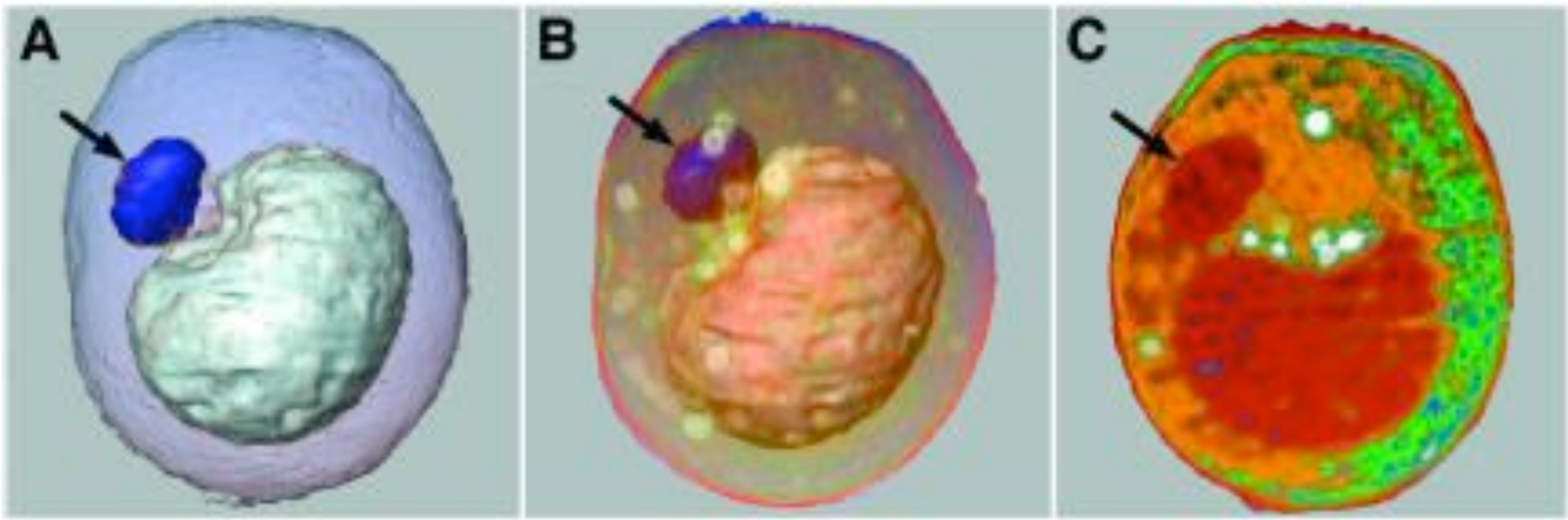

Frozen hydrated yeast Saccharomyces cerevisiae C. Larabell, M. Le Gros, *Mol. Biol. Cell* **15**, 957 (2004)

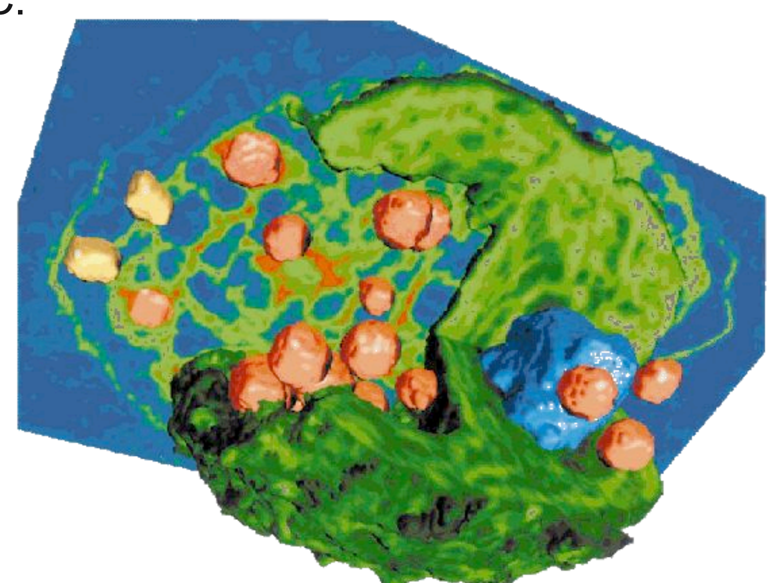

Frozen hydrated alga *Chlamydomonas reinhardtii*: D. Weiß, G. Schneider, *et al*., *Ultramicroscopy* **84**, 185 (2000)

Quantitative phase tomography

- **Defocus series (a, b, c) and phase (d) of a silicon AFM tip**
- **Quantitative 3D reconstructions of real part of refractive index from ±70° tomographic projections through tip**

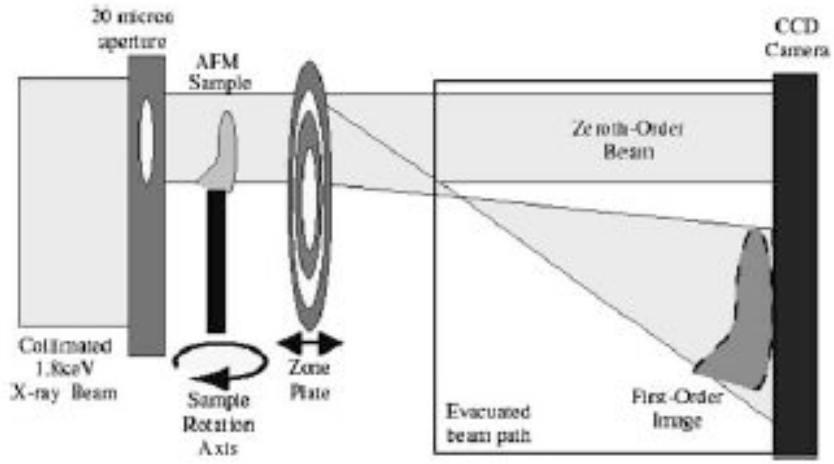

- **Calculated $\delta = 5.1 \times 10^{-5}$**

  Measured $\delta = 5.0 \pm 0.5 \times 10^{-5}$

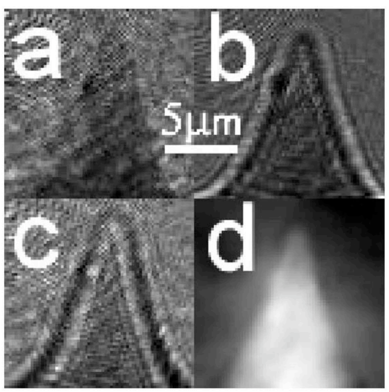

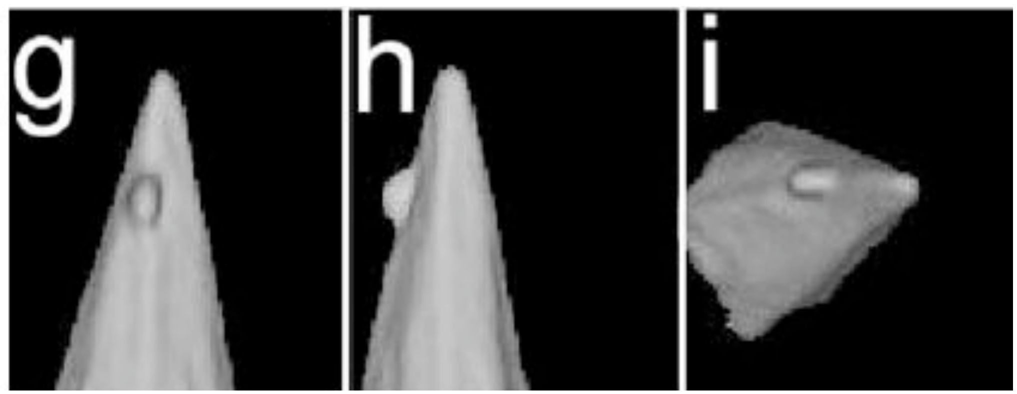

P. McMahon et al., *Opt. Commun.* 217, 53 (2003)

Full-field microscopy with hard x-rays

Beamline for scanning microscopy (soft x-ray)

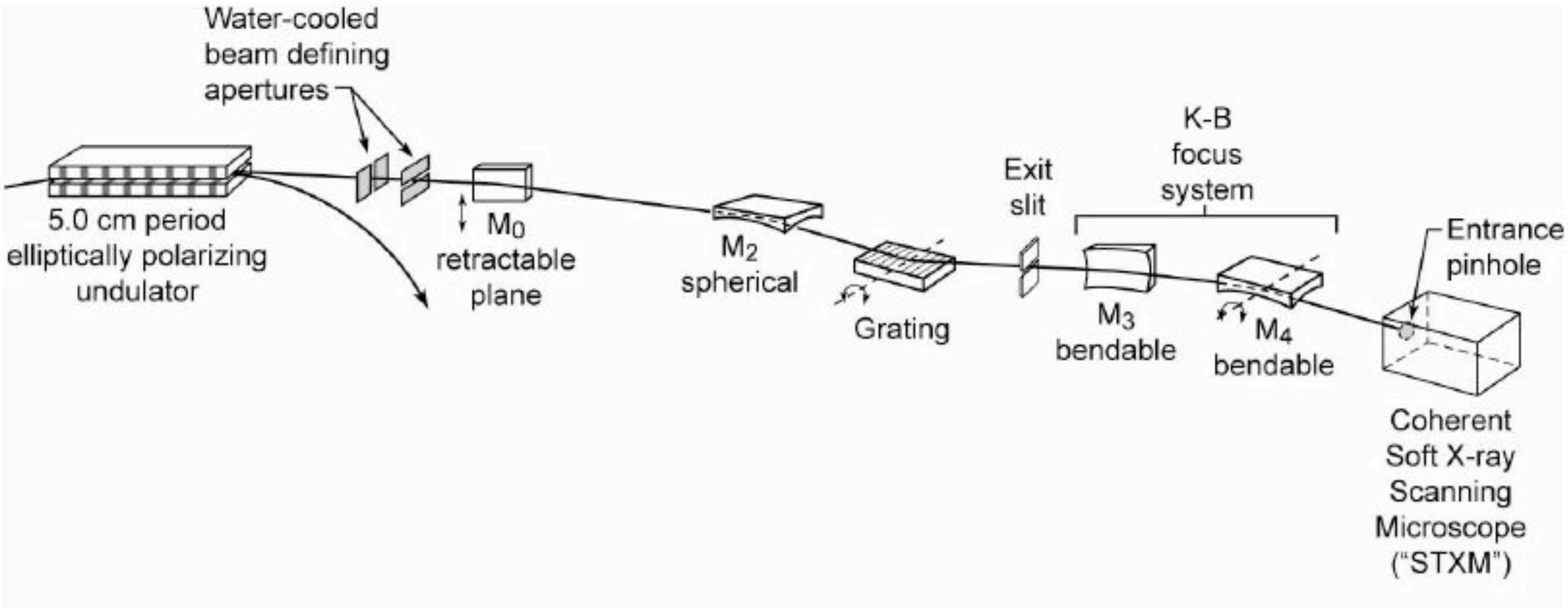

1-4 keV scanning x-ray microscope at APS 2-ID-B

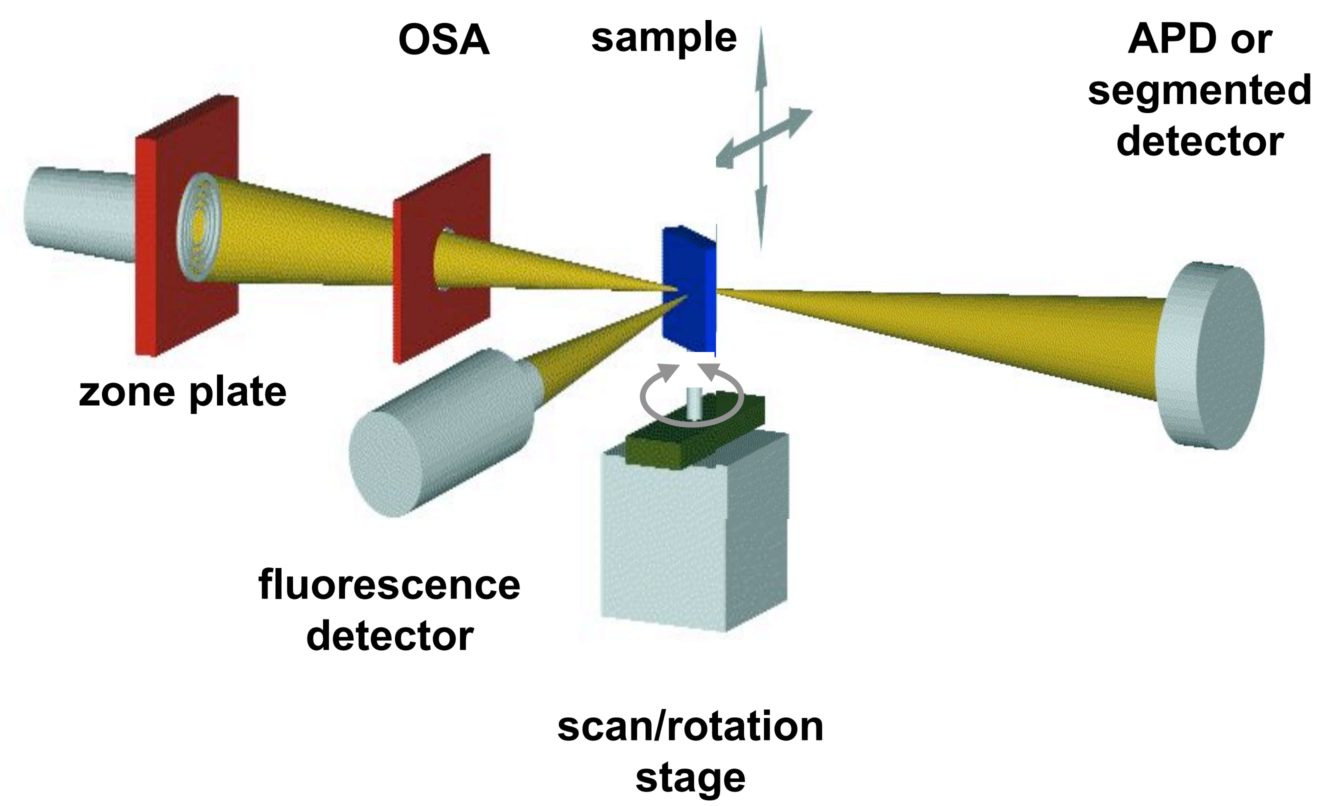

X-ray probe

- Fresnel ZP
- 60 nm spot
- 10^8-10^9 ph/s

Contrast modes

- Transmission
- Fluorescence
- Micro-XANES

Defects in buried interconnects

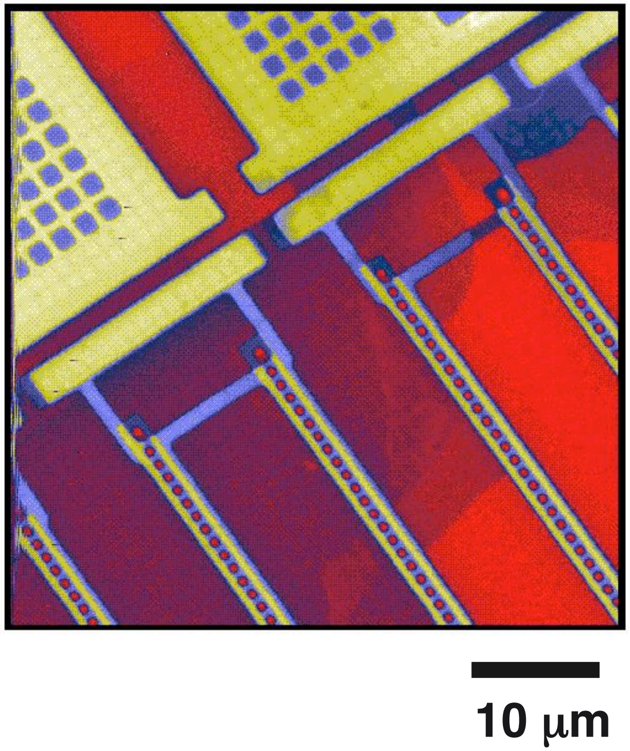

Example: Ta-lined Cu interconnect, W vias

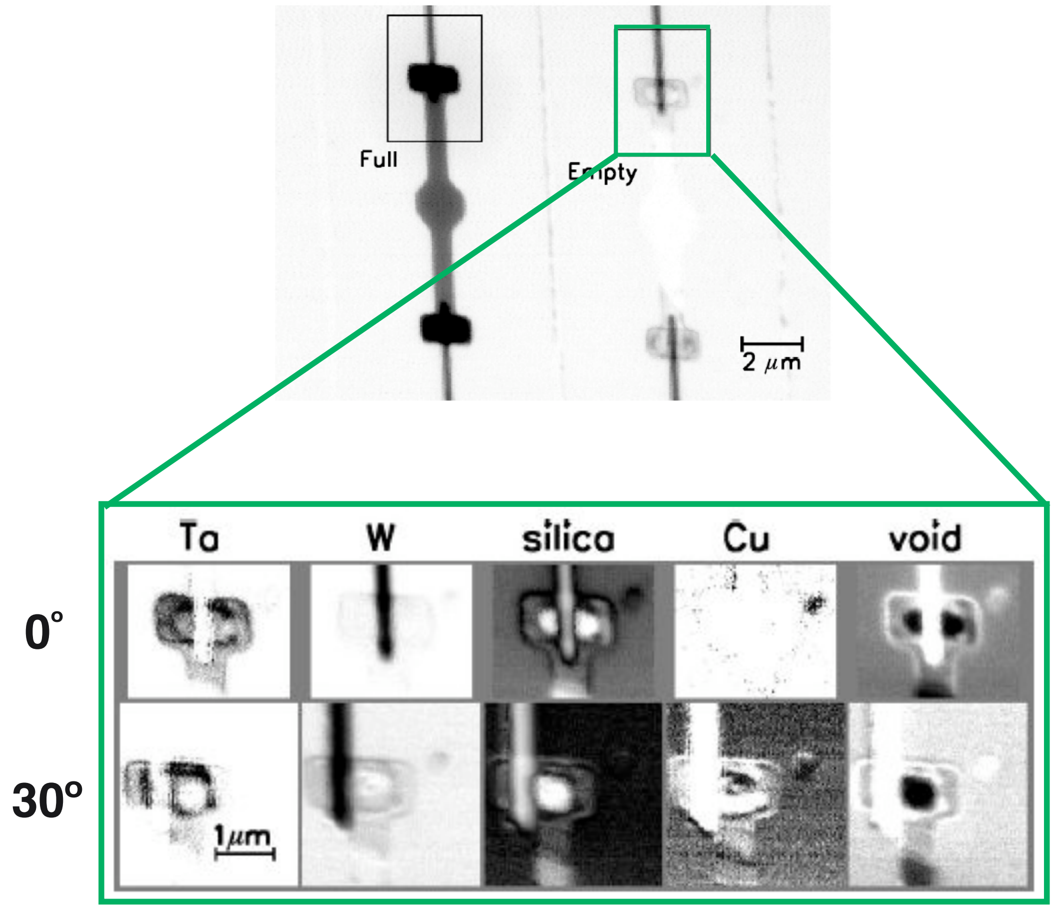

Z. Levine et al., *J. Appl. Phys.* 95, 405 (2004)

X-ray spectromicroscopy is valuable to study P speciation

Marine sediments contain complex, heterogeneous P chemistry.
P typically shows little covariance with most other elements.

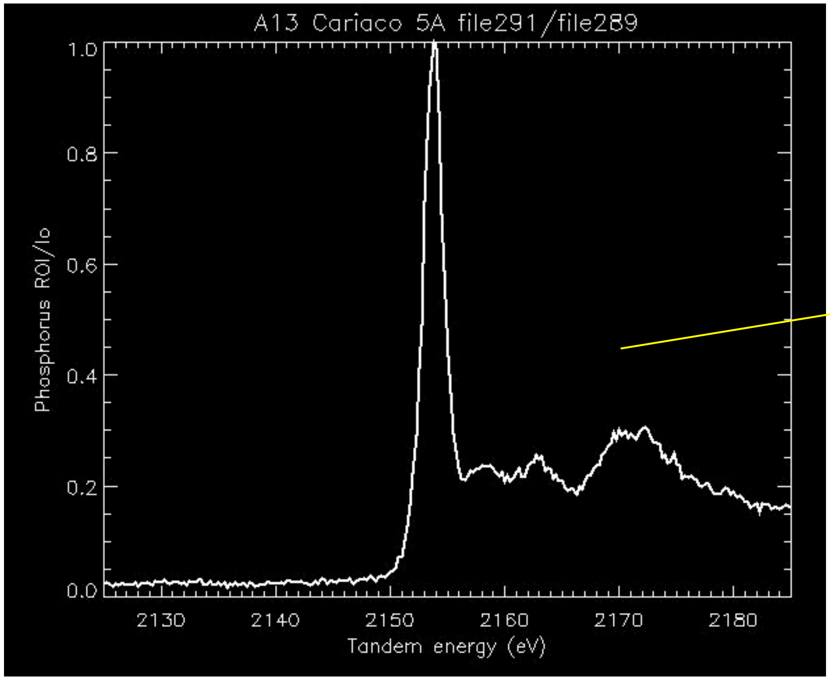

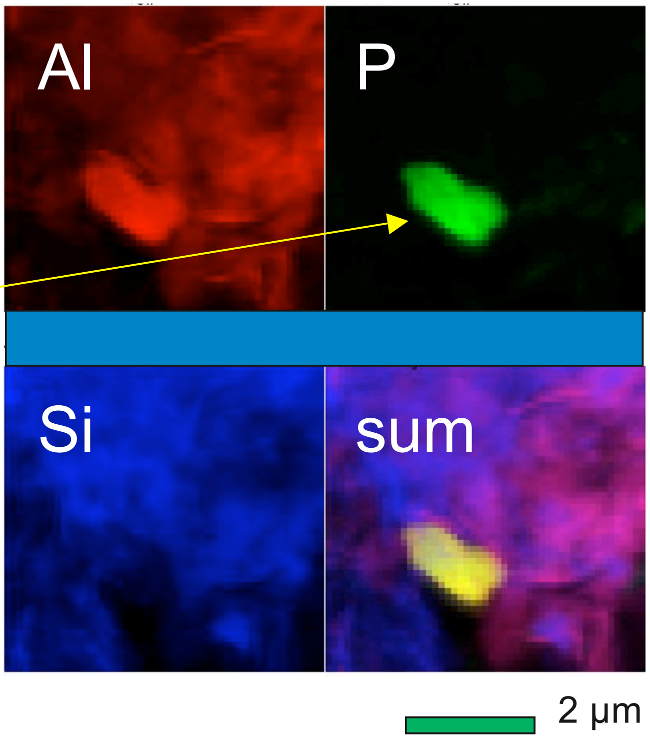

- **Occasionally find odd P-containing minerals with distinctive P-XANES that do not match closely with any known Al-phosphate mineral**
- **Previously unknown in marine samples - Riverine or Aeolian source?**

J. Brandes et al., *Marine Chem.* 103, 250 (2007)

Use phase contrast for biological specimens

Complex transmission function: $\exp(i\,\delta\,kt)\,\exp(-\,\beta\,kt)$

phase shift absorption

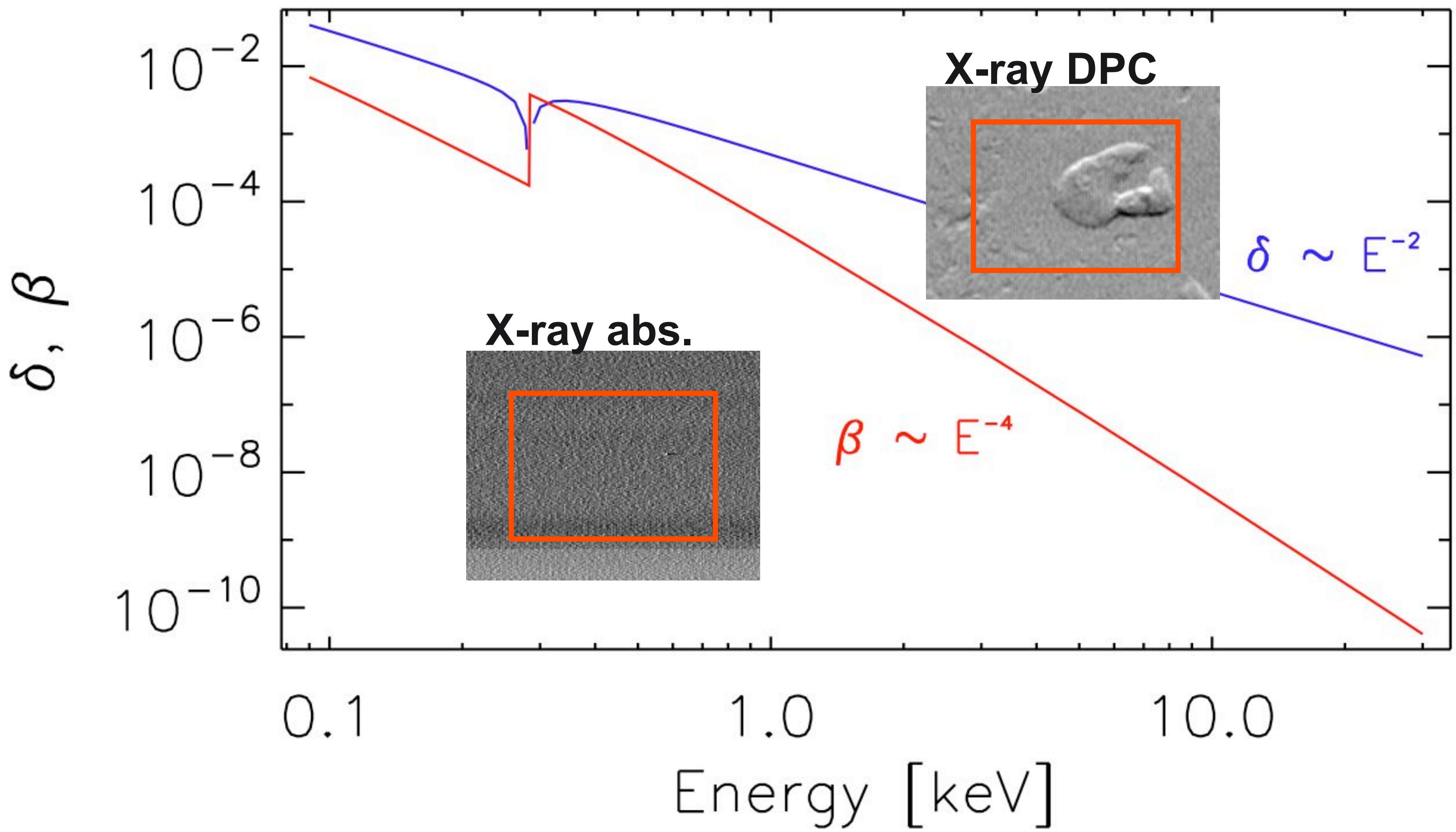

STXM: differential phase contrast

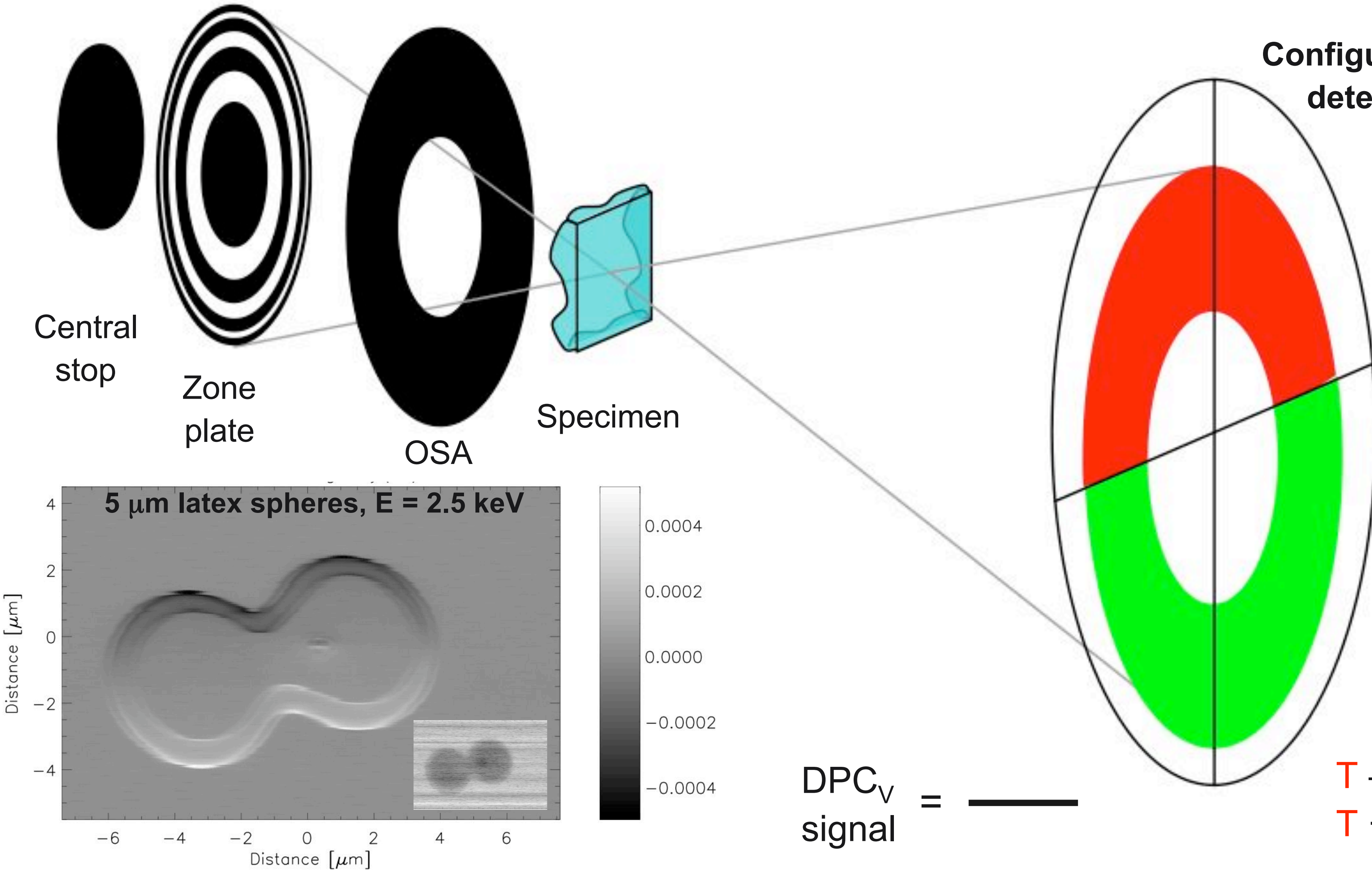

$$\text{DPC}_V \text{ signal} = \frac{T - B}{T + B}$$

M. de Jonge et al., *PRL* 163902, (2008)

Pennate diatoms

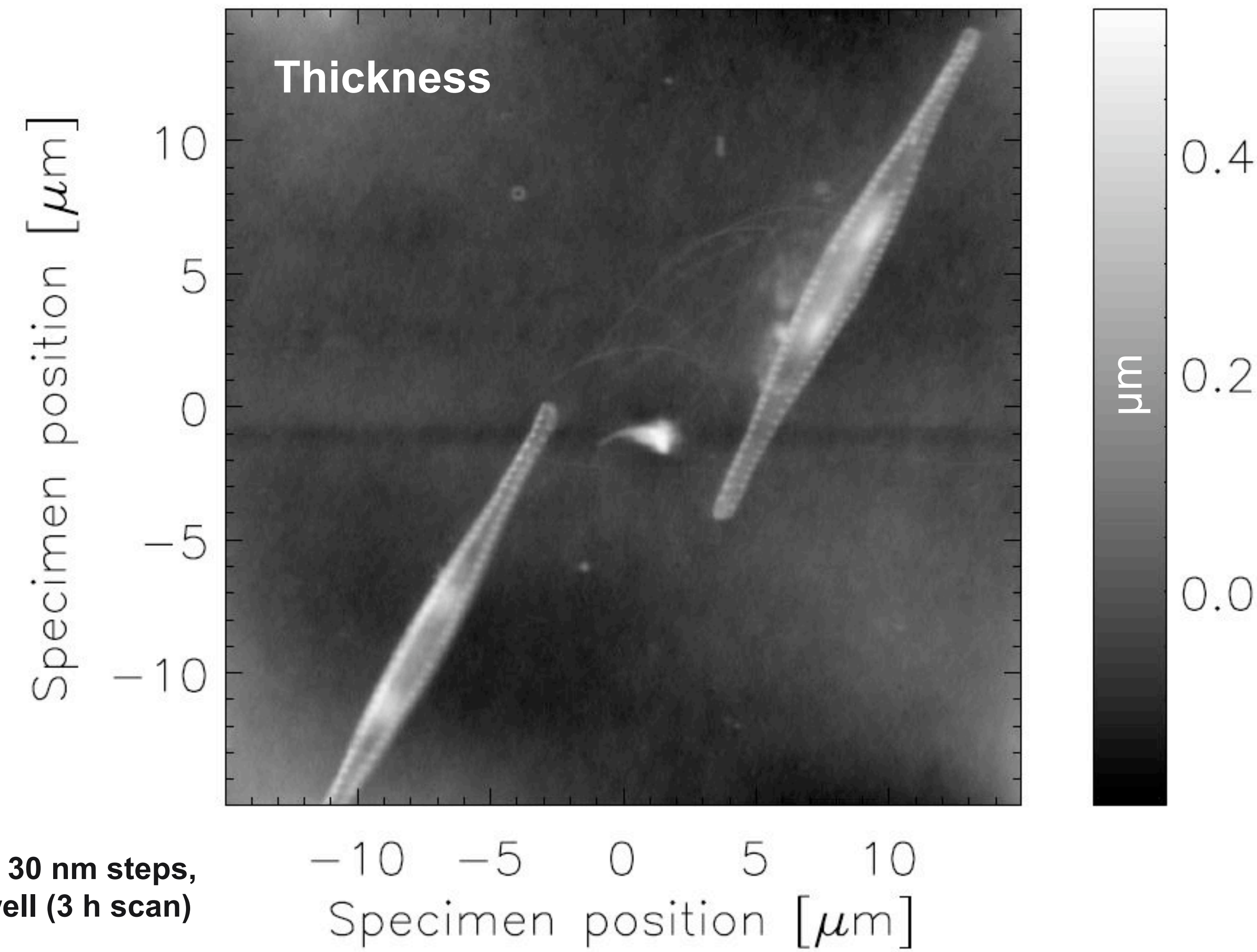

2535 eV, 30 nm steps, 5 ms dwell (3 h scan)

Hard x-ray scanning flourescence microscope

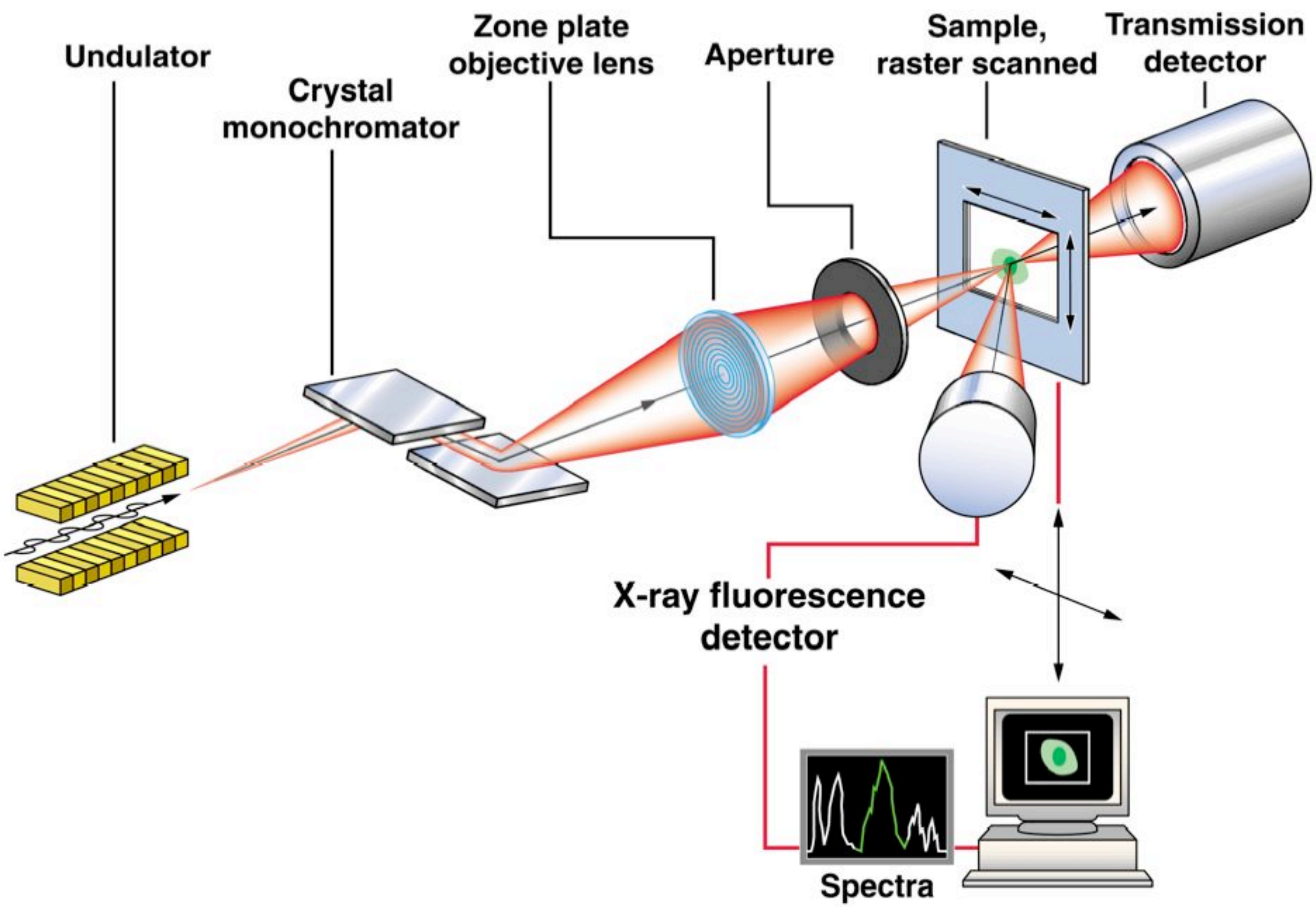

Copper is an essential trace element for all life forms

- **Catalyzes production of highly reactive oxygen species**

  ⇒ oxidative damage to lipids, proteins, DNA, etc

- **Defects in regulatory processes may led to:**
  - ✓ Menkes syndrome
  - ✓ Wilson's disease
  - ✓ Amyotropic lateral sclerosis (ALS)
  - ✓ Alzheimer's disease

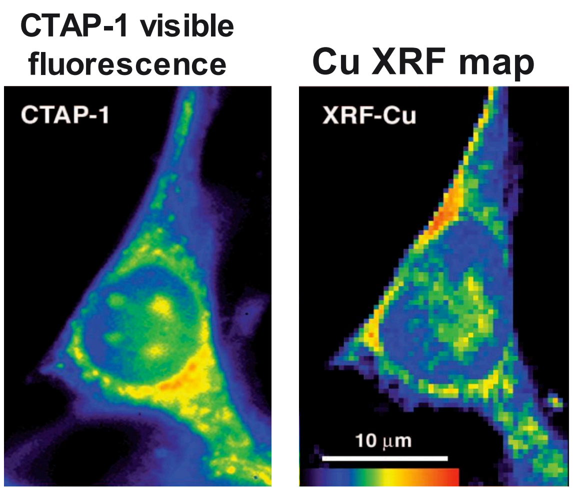

Mouse fibroblast cell + 150 µM $CuCl_2$

- **Need to be understand cellular uptake, trafficking, storage of Cu**
- **Novel Cu(I) fluorescent sensor (CTAP-1) was recently developed**

  ⇒ ***Does it reflect the true cellular distribution?***

μ-XANES indicates Cu(I) is present (reducing environment)

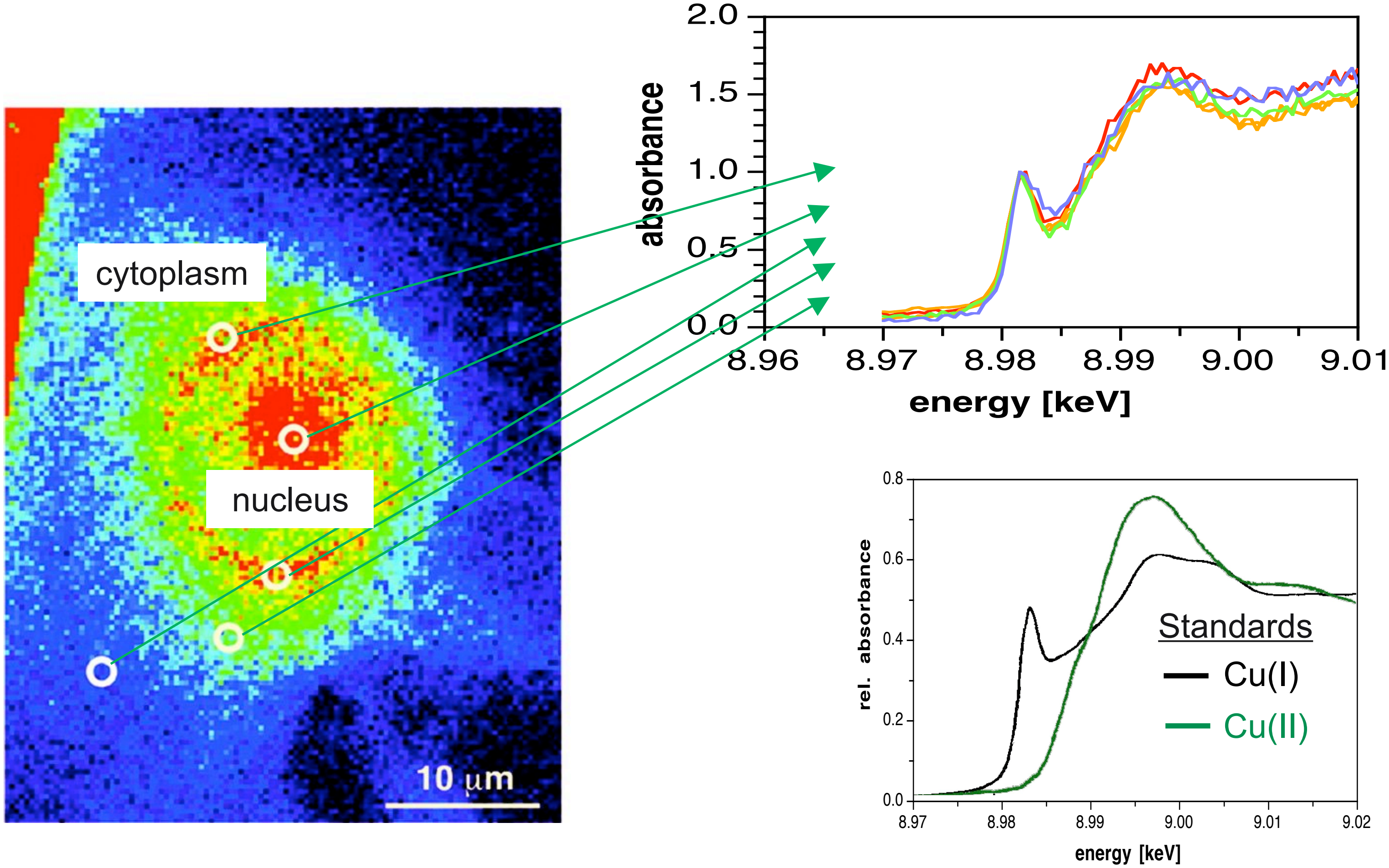

L. Yang et al., *Proc. Natl. Acad. Sci.* 102, 11179 (2005)

Arsenic distribution and speciation in rice grains

A. Meharg, E. Lombi, P. Williams, K. Scheckel, J. Feldmann, A. Raab, Y. Zhu, and R. Islam, *Environ. Sci. Technol.* 42, 1051 (2008)

- There is worldwide concern over elevated arsenic concentrations in regions where rice paddy fields are irrigated with As contaminated groundwater.
- Rice production increasingly occurs in As and metal contaminated soils in Asia
- S-XRF was utilized to locate As in polished (white) and unpolished (brown) rice grains from the United States, China, and Bangladesh
- As dispersed in white rice but localized in the pericarp and aleurone layer of brown rice - Cu, Fe, Mn, and Zn localization followed that of As in brown rice
- µ-XANES and bulk extraction revealed the presence of mainly inorganic As and dimethylarsinic acid (DMA)
- Percentage of DMA present in the grain increased along with total As.

US White Rice

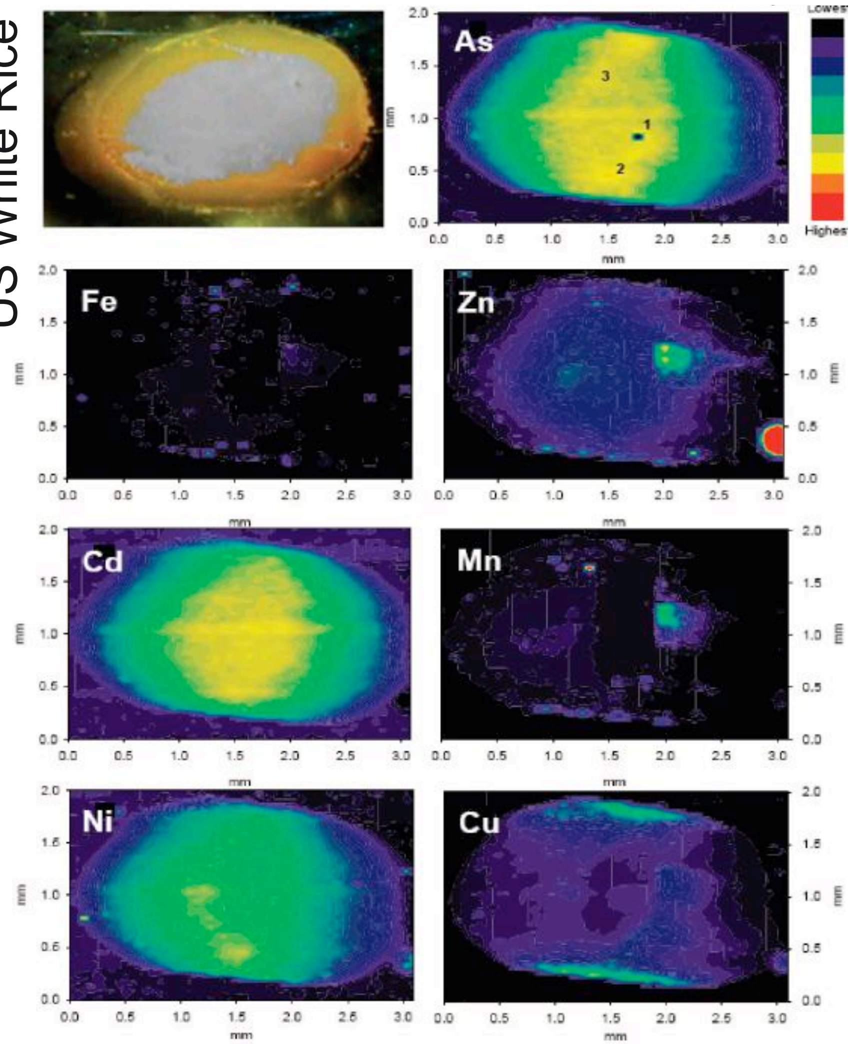

3. Indirect methods

- Microdiffraction
  - Scanning (monochromatic/Bragg)
  - 3D differential-aperture x-ray microscopy (white/Laue)
- Coherent diffraction imaging
- Holography

Is there lattice strain in zinc oxide nano-rings?

Termination at Zn (+) and O (-) results in spontaneous polarization along the c-axis resulting in formation of nano-rings

Internal lattice strain and distribution needed to study balance between mechanical and electronic configurations for nano-sensor applications.

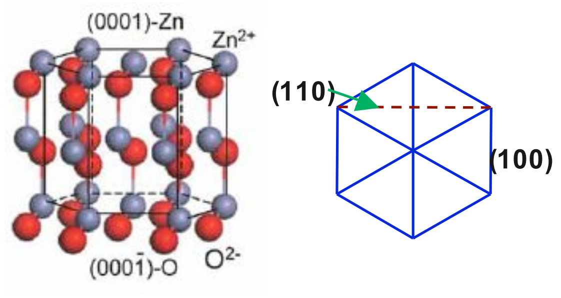

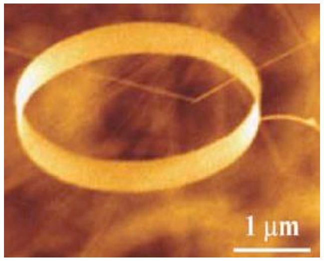

X-ray fluorescence (Zn Kα) map

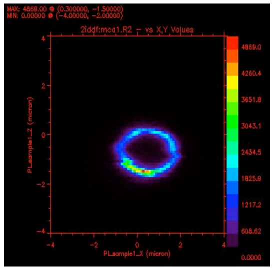

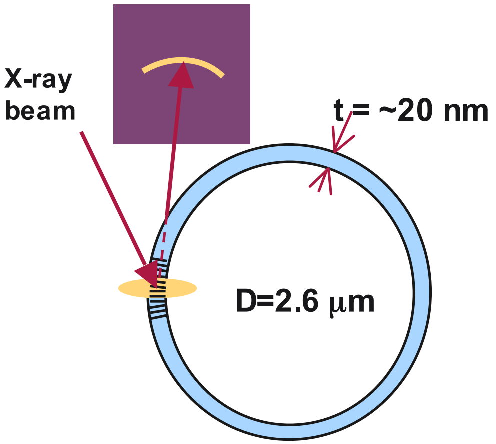

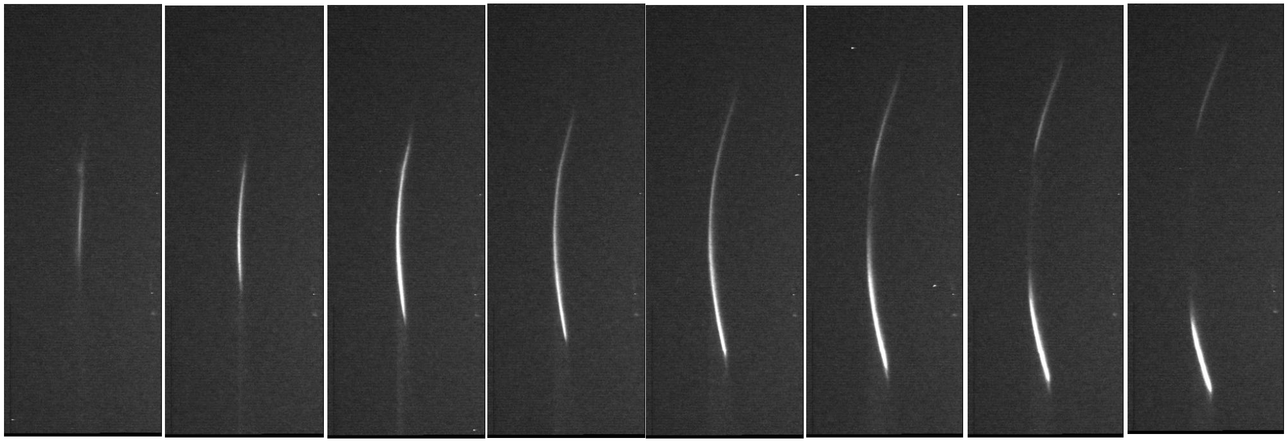

Diffraction of Zn (110) from a section of the ring. Patterns were taken at angles θ across the rocking curve width

X-ray nanodiffraction explains strains

Image (220) reflections from ZnO nano-ring with CCD using 10 keV x-rays

Patterns cover a θ angular range of 0.6°

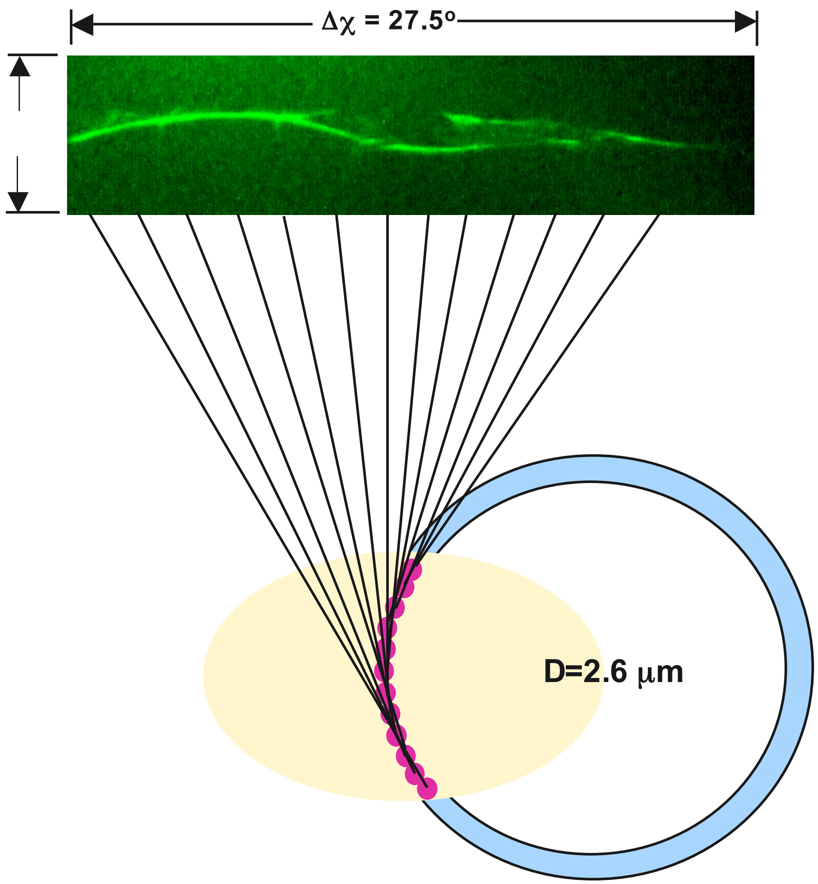

Y. Xiao et al., *JSR* 12, 124 (2005)

- **Might expect that coiling stress would cause a continuous strain distribution from compressive to tensile across the ring width.**
- **The two branches of the diffracted intensity indicate existence of two strain domains, with as much as 1.8% difference in the (220) plane spacing.**
- **Data show the structure either collapses into distinct domains across the ring width, or exhibits strain that varies little in width but continuously up to 2.4% along the ring arc.**

Differential-aperture x-ray microscopy

3D depth-resolved, white-beam Laue diffraction technique

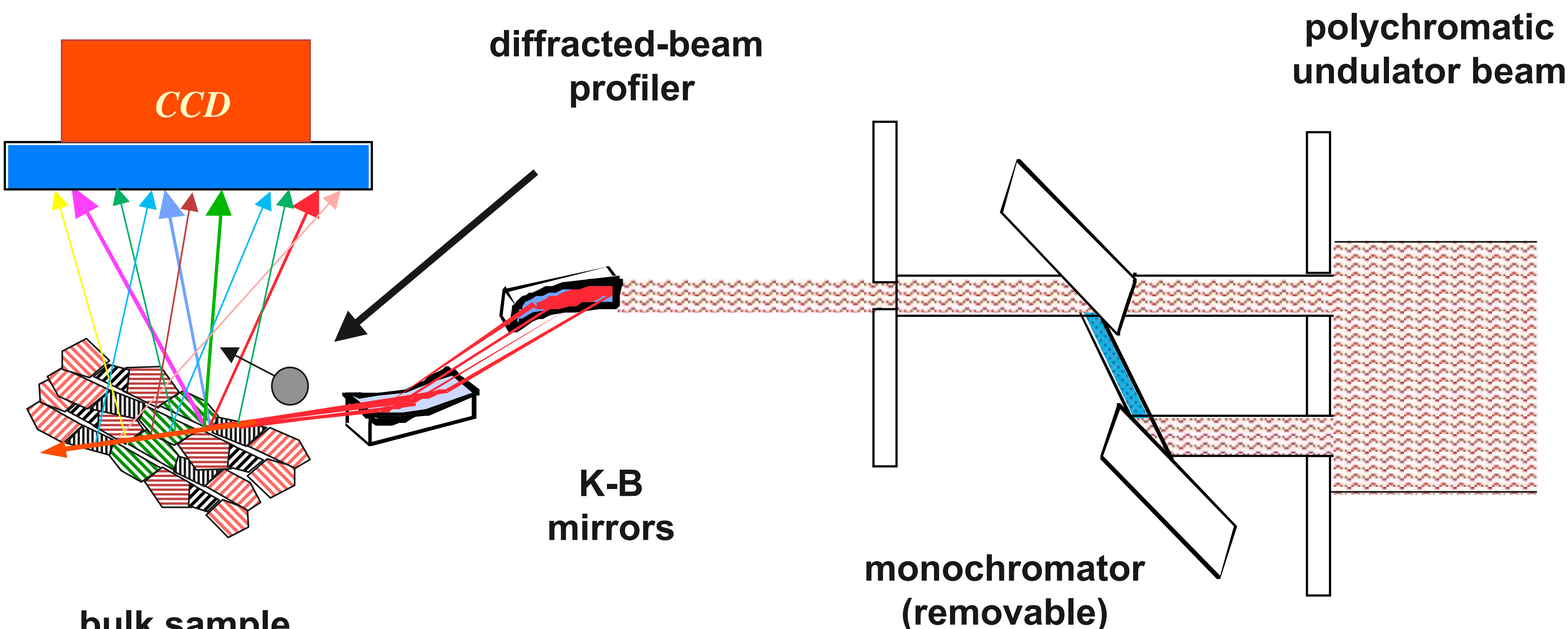

B. Larson et al., *Nature* 415, 887 (2002)

3D diffraction microscope at APS beamline 34-ID-E

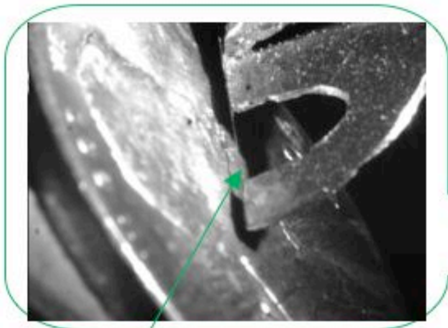

Differential aperture

(wire scan, ~ 200 mm above sample surface)

Sample stage

K-B focusing mirrors

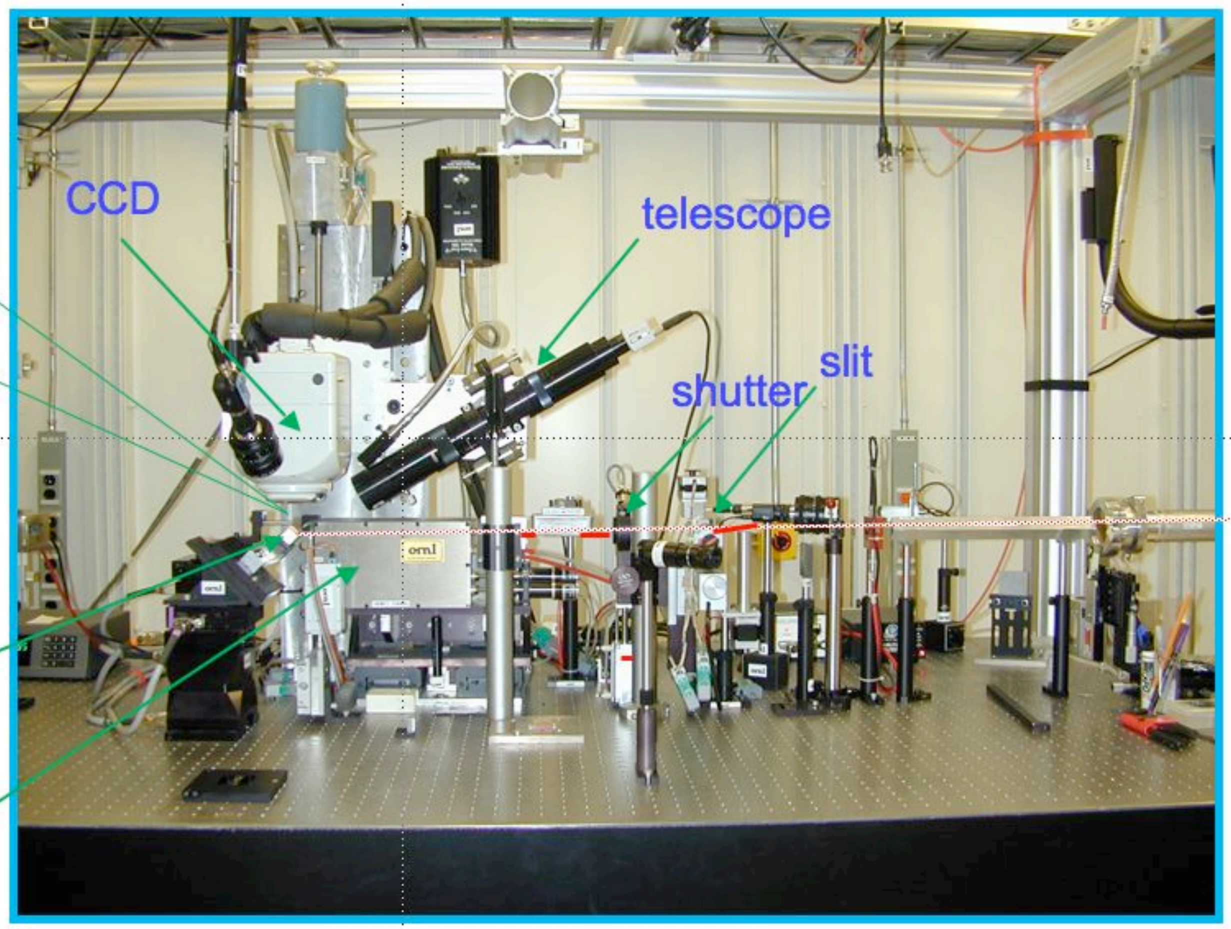

DAXM illuminates the 3D structure of aluminum

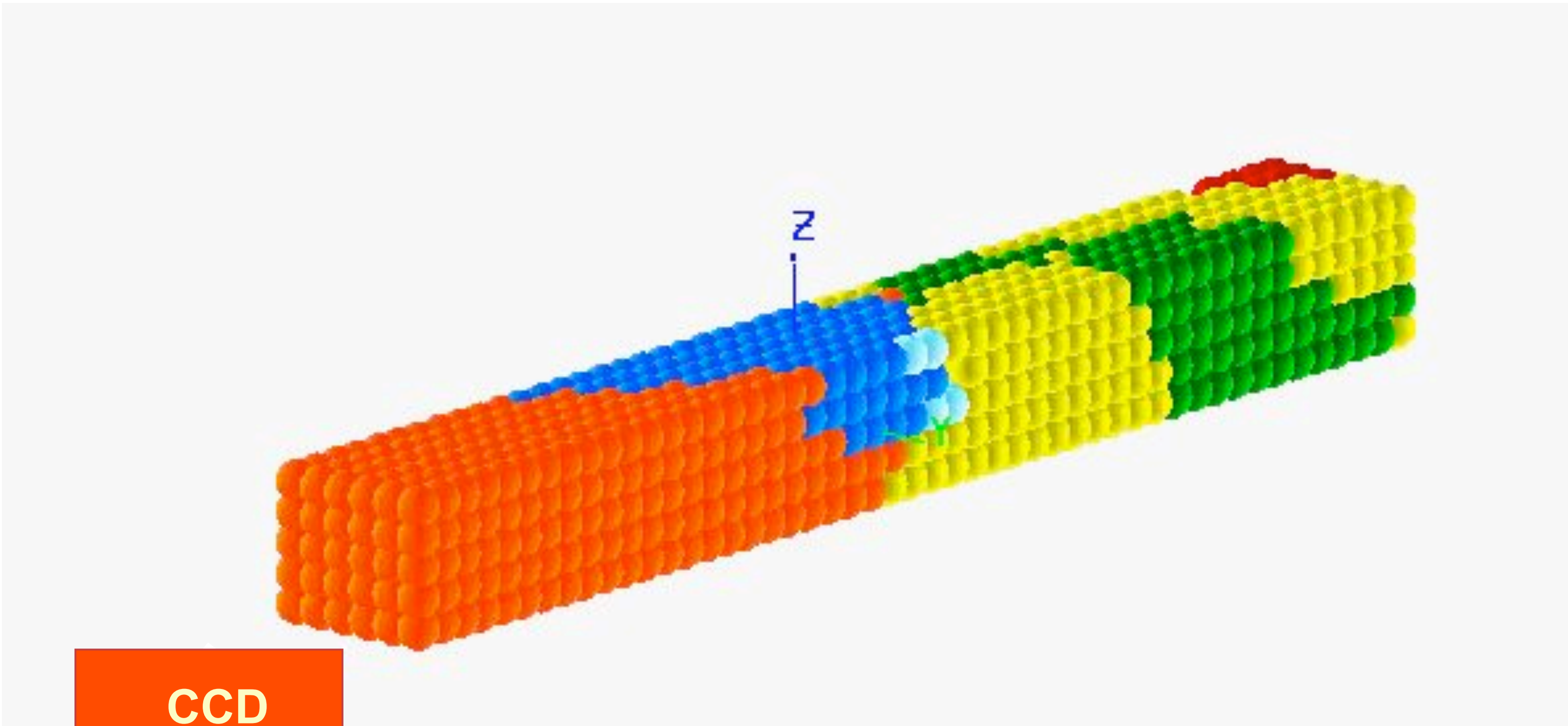

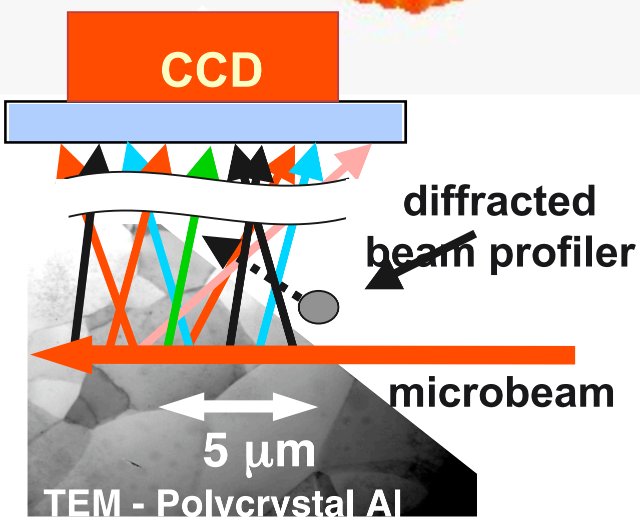

- Intra- and inter-granular information
- Grain boundary morphology and type
- Misorientation axis/angle between grains
- 3D microtexture
- Grain size-distribution

W. Yang, et al., *Micron* 35, 431 (2004)

Coherent diffraction and holography: "lensless" imaging

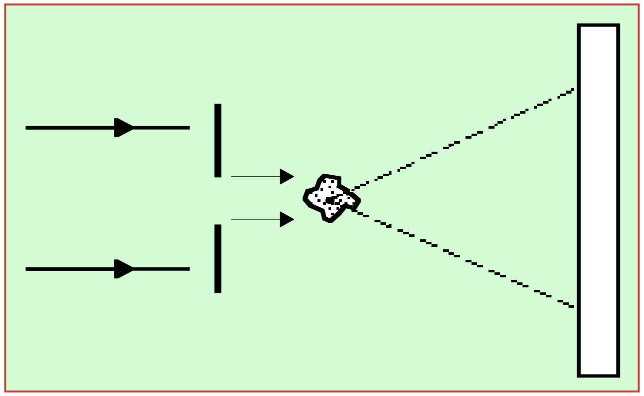

Coherent Diffraction

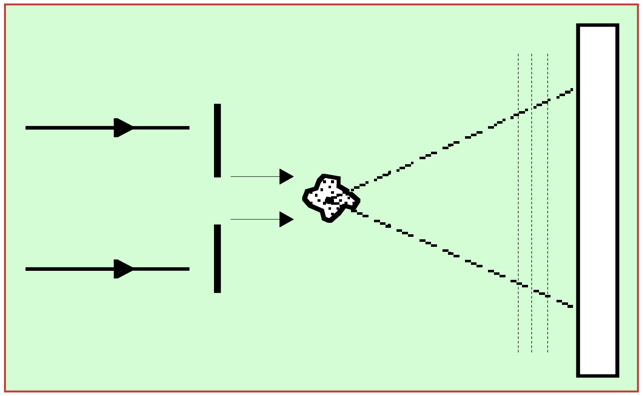

Holography

- **Object wave (diffraction) is detected directly**
- **Diffraction intensity corresponds to autocorrelation of object**

- **Coherent reference wave interferes with object wave to form hologram**
- **Hologram intensity corresponds to convolution of object and reference**

Resolution:	**transverse**	$\sim \lambda/NA$
	longitudinal	$\sim \lambda/(NA)^2$
Contrast:		$\propto \lvert f_1^2 + f_2^2 \rvert$

Coherent diffraction x-ray imaging

Lensless method - resolution limited only by wavelength, signal

- **Two-step process: record coherent diffraction pattern, recover object structure numerically (iterative phase retrieval)**
- **Sensitive to phase as well as absorption of the specimen**
- **Get 3D by tomographic methods; no depth of field limit**
- **But: must assume some *a priori* information to recover phase, e.g. known object extent or illumination profile**

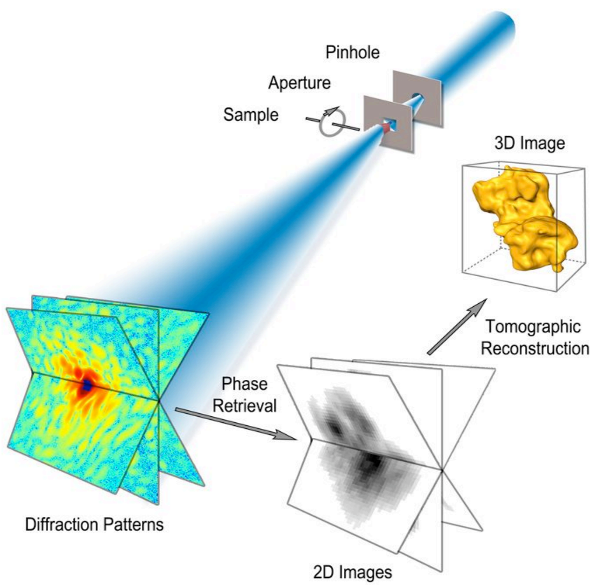

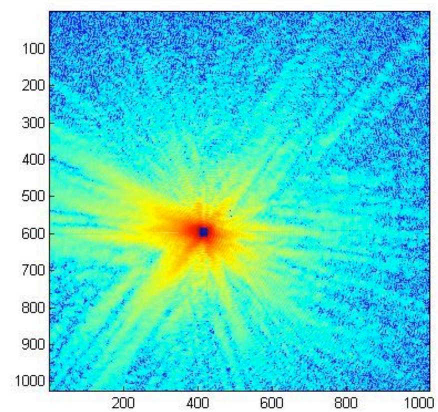

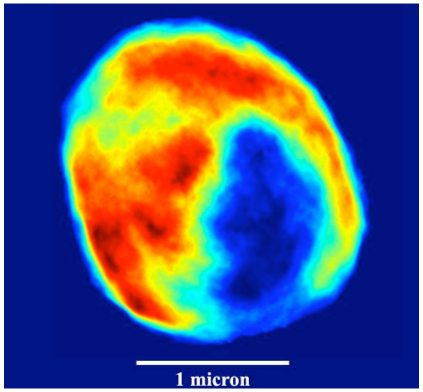

resolution ~ λ / angular size

J. Miao, et al., *Nature* 400, 342 (1999)

Iterative phase retrieval

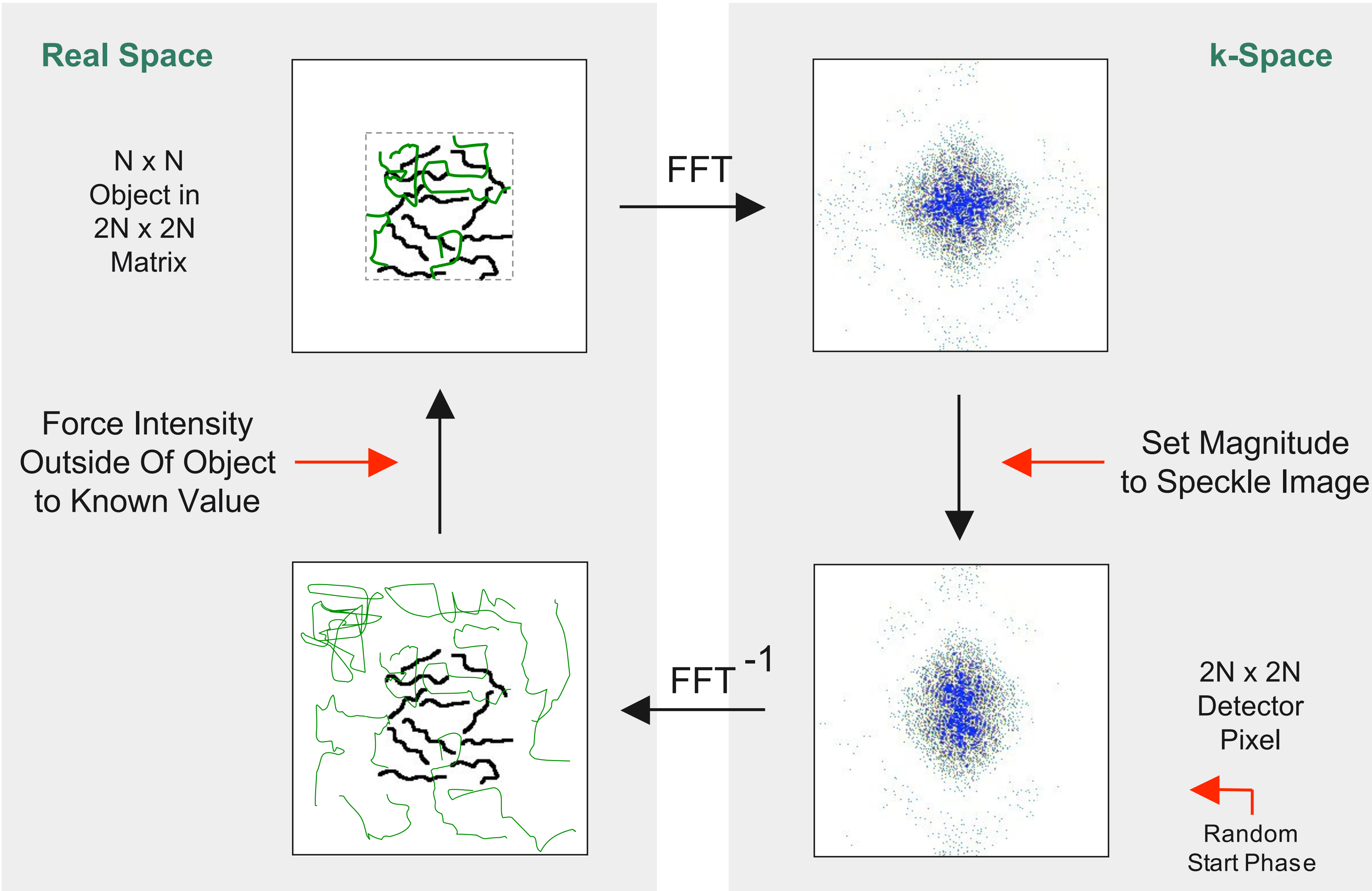

R. Gerchberg and W. Saxton, *Optik* 35, 237 (1972); J.R. Fienup, *Appl. Opt.* 21, 2758 (1982)

Freeze dried yeast cell imaged by coherent x-ray diffraction

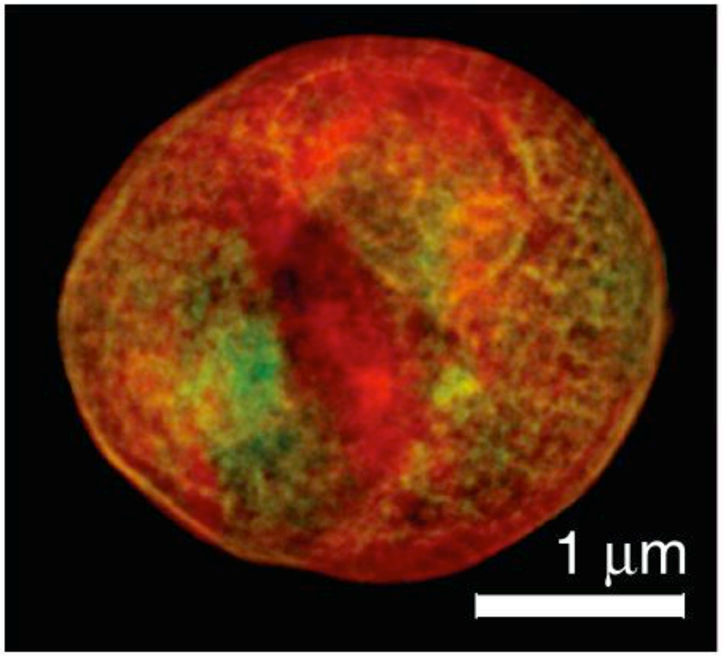

Diffraction reconstruction (data taken at 750 eV; absorption as brightness, phase as hue).

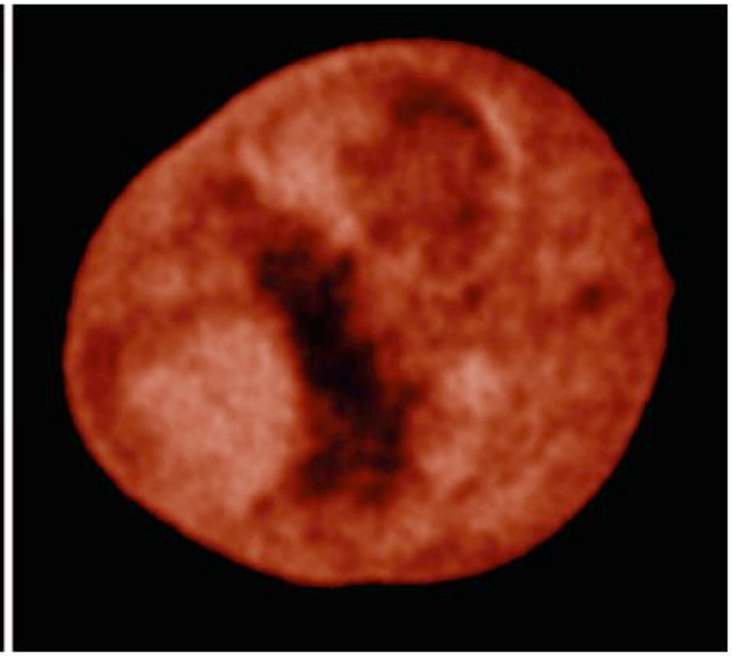

Stony Brook/NSLS STXM image with 45 nm Rayleigh resolution zone plate at 520 eV (absorption as brightness)

D. Shapiro et al., *PNAS* 102, 15343 (2005)

Diffraction microscopy in 3D

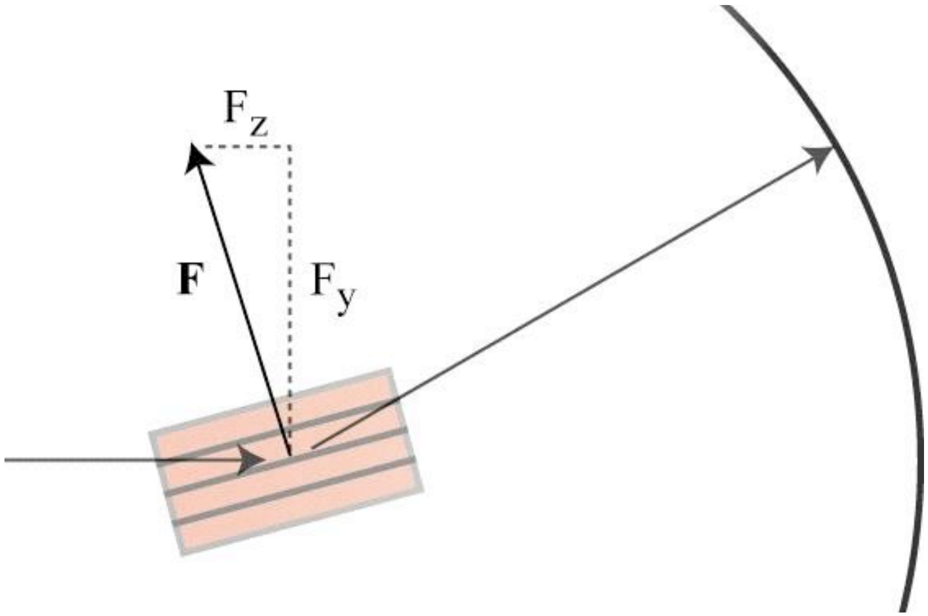

Bragg gratings that diffract to a certain angle represent a specific transverse and longitudinal periodicity (Ewald sphere)

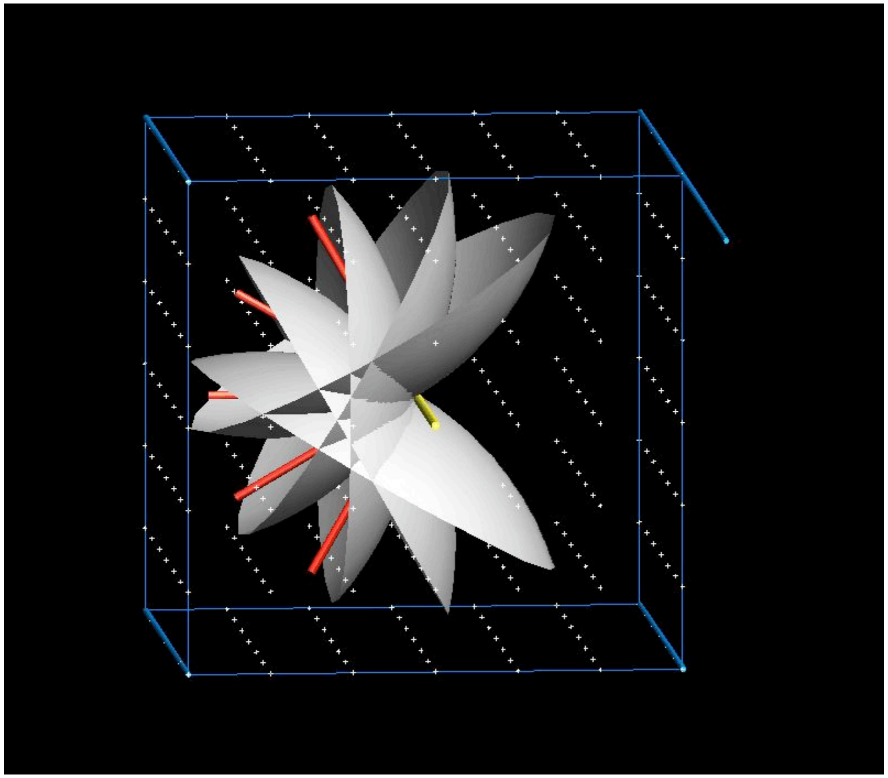

Data collection over a series of rotations about an axis fills in 3D Fourier space for phasing

3D coherent diffraction imaging

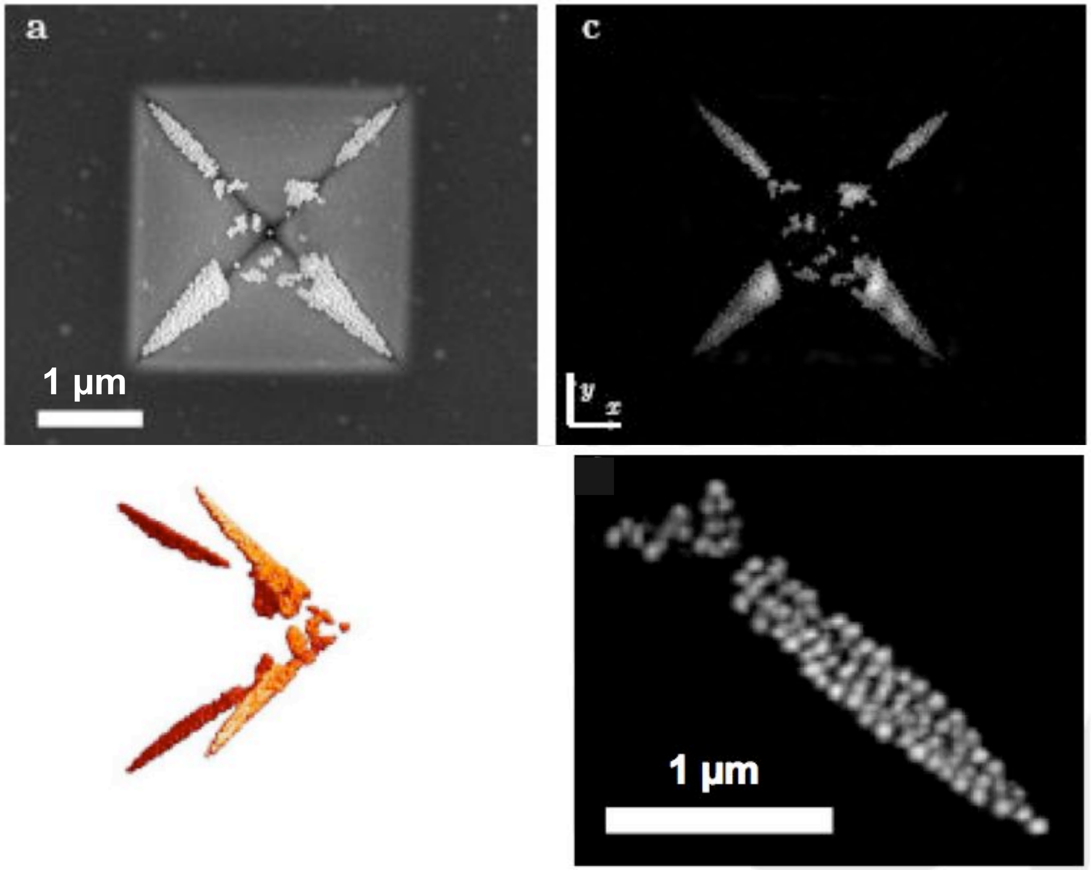

(a) SEM of pyramidal indentation in a 100-nm Si_3N_4 membrane lined with 50-nm Au spheres. (b) 3D image reconstructed from 123 diffraction projections spanning -57° to +66°, using reality and positivity constraints. (c) Large DOF projection. (d) Enlarged region of (c).

H. Chapman et al., JOSA A23, 1179 (2006)

Coherent x-ray diffraction can reveal strain in crystals

- **Double crystal monochromator selects temporal coherence**
- **Precision slits select spatially coherent fraction of hard x-ray beam**
- **Diffractometer is used to locate Bragg peaks from an isolated nanocrystal**
- **Rocking curves around Bragg peak are recorded to obtain 3D data**

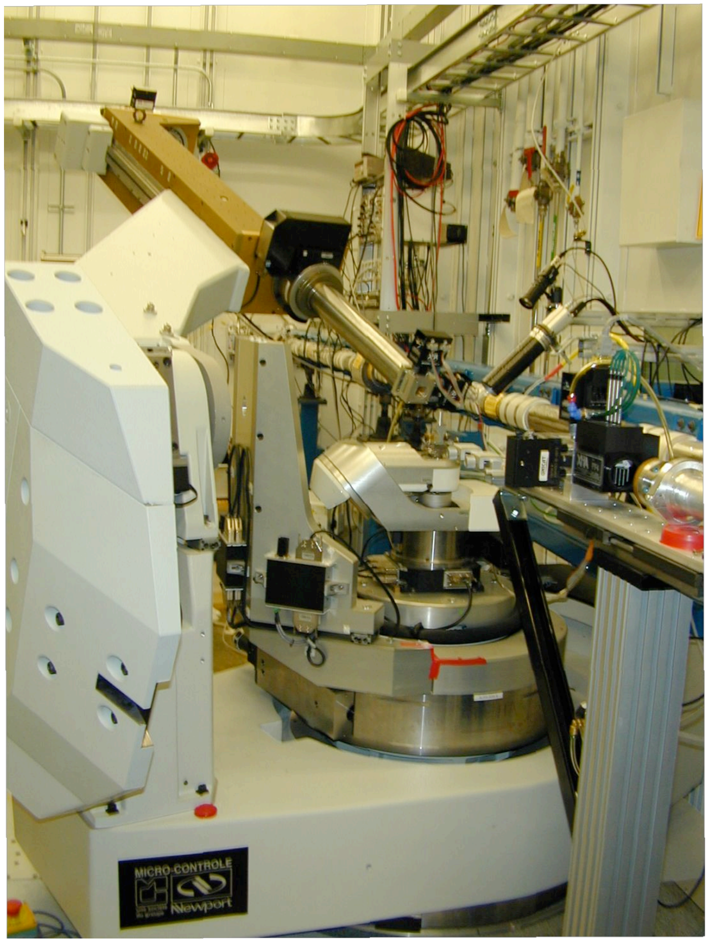

Setup at APS 34-ID-C beamline

Mapping crystal strain in 3D by CDI

0.5 µm Pb crystal grown on SiO_2 substrate

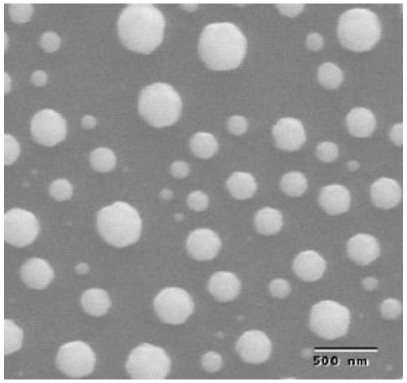

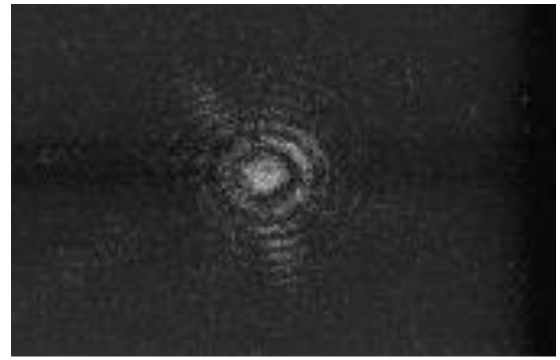

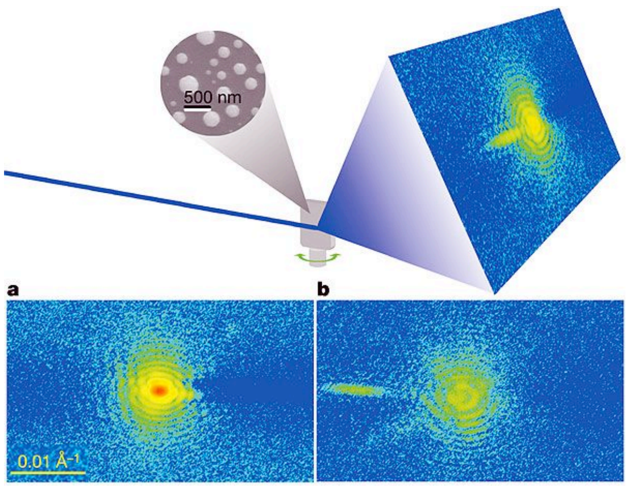

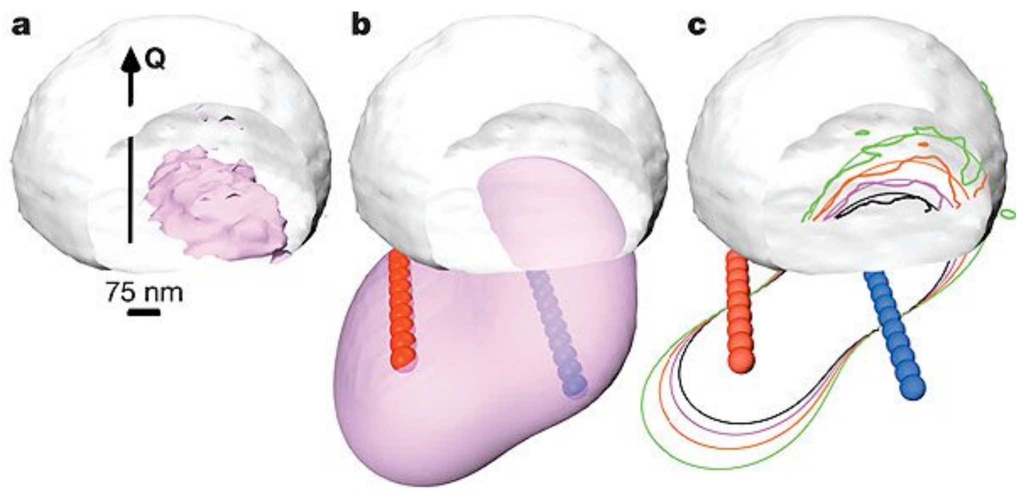

Map series of diffraction patterns about (111) Bragg peak

Diffraction data reconstructed by HIO

M. Pfeifer et al., *Nature* 442, 63 (2006)

CDI setup at APS beamline 2-ID-B (1-4 keV)

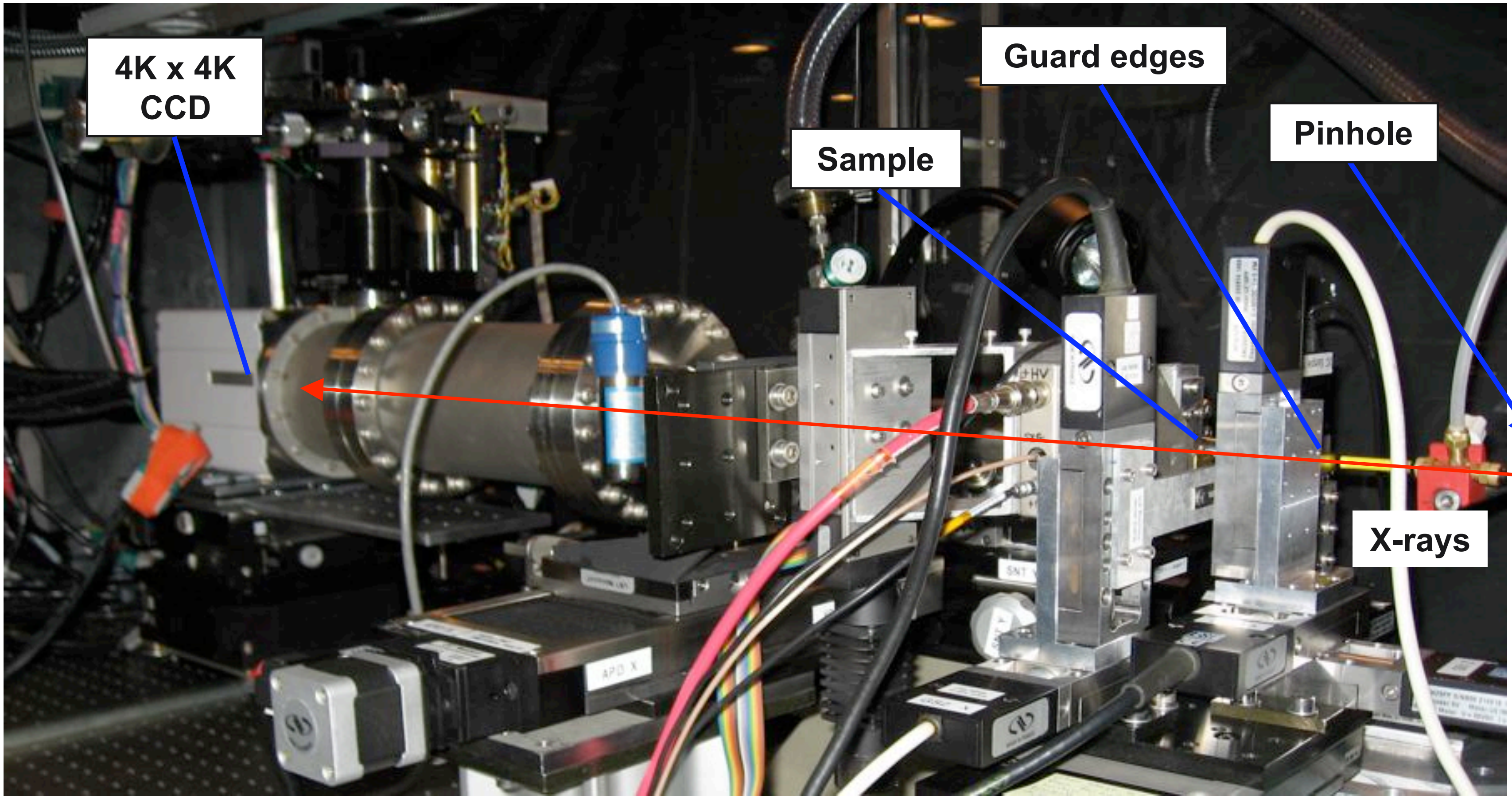

Buried structures can be probed with element specificity

In contrast to weak segregation theory, Bi is locally concentrated in Bi-doped Si crystals

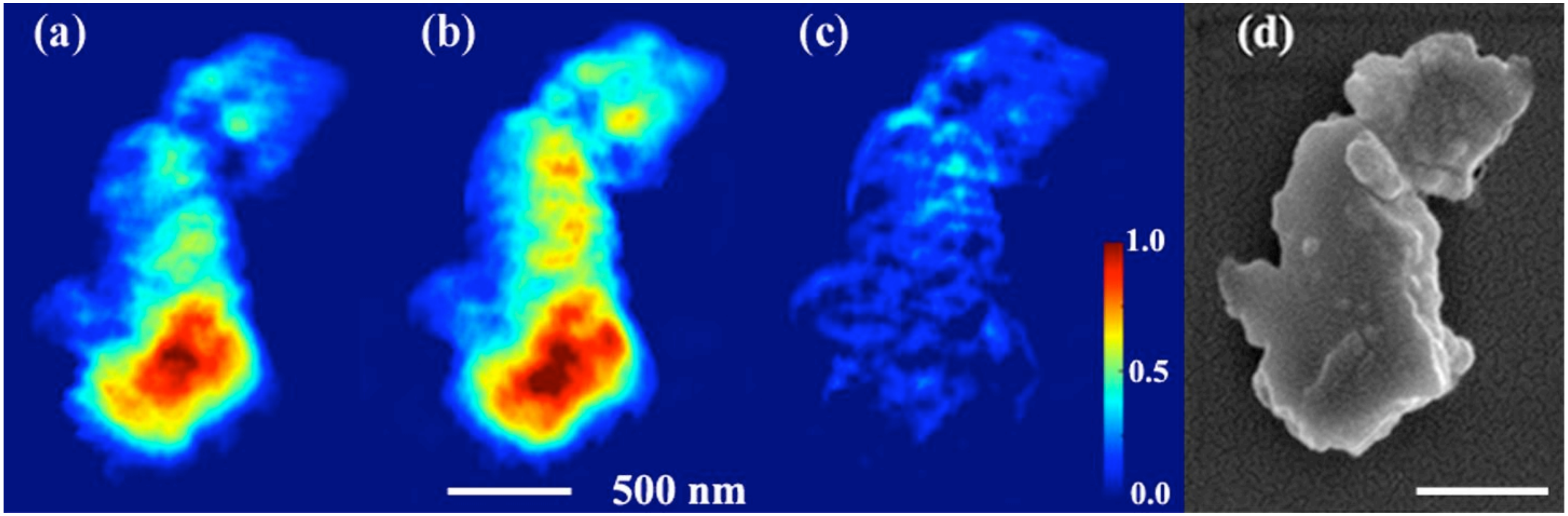

(a) Image below Bi M5 edge (2550 eV)
(b) Image above the Bi M5 edge (2595 eV)
(c) Difference
(d) SEM image

C. Song et al., *PRL* 100, 025504 (2008)

Curved object illumination aids unique phase recovery

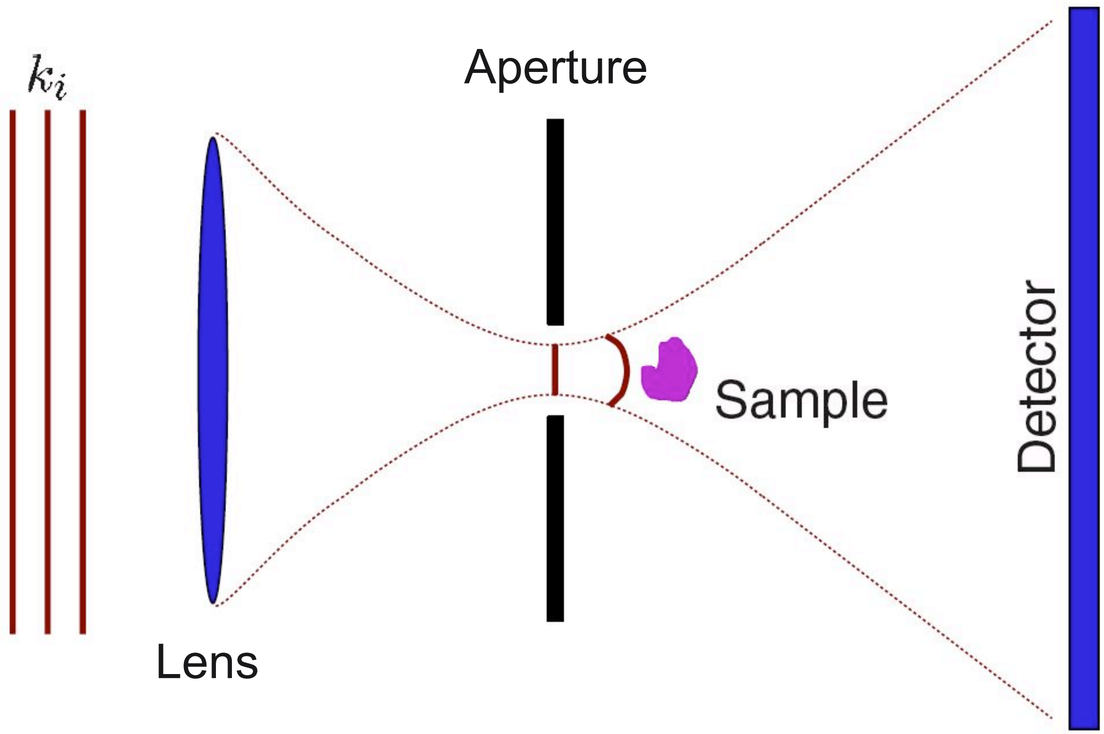

- Lens illuminates object with curved wavefront, defines field of view
- Object illumination is reconstructed by back-propagation, used to retrieve phase of object wave by iterative methods

K. Nugent et al., *PRL* 91, 203902 (2003)

... and converges faster

Original

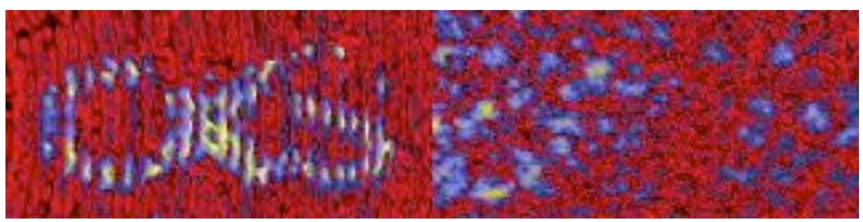

curved beam illumination | **plane wave illumination**

FCDI setup

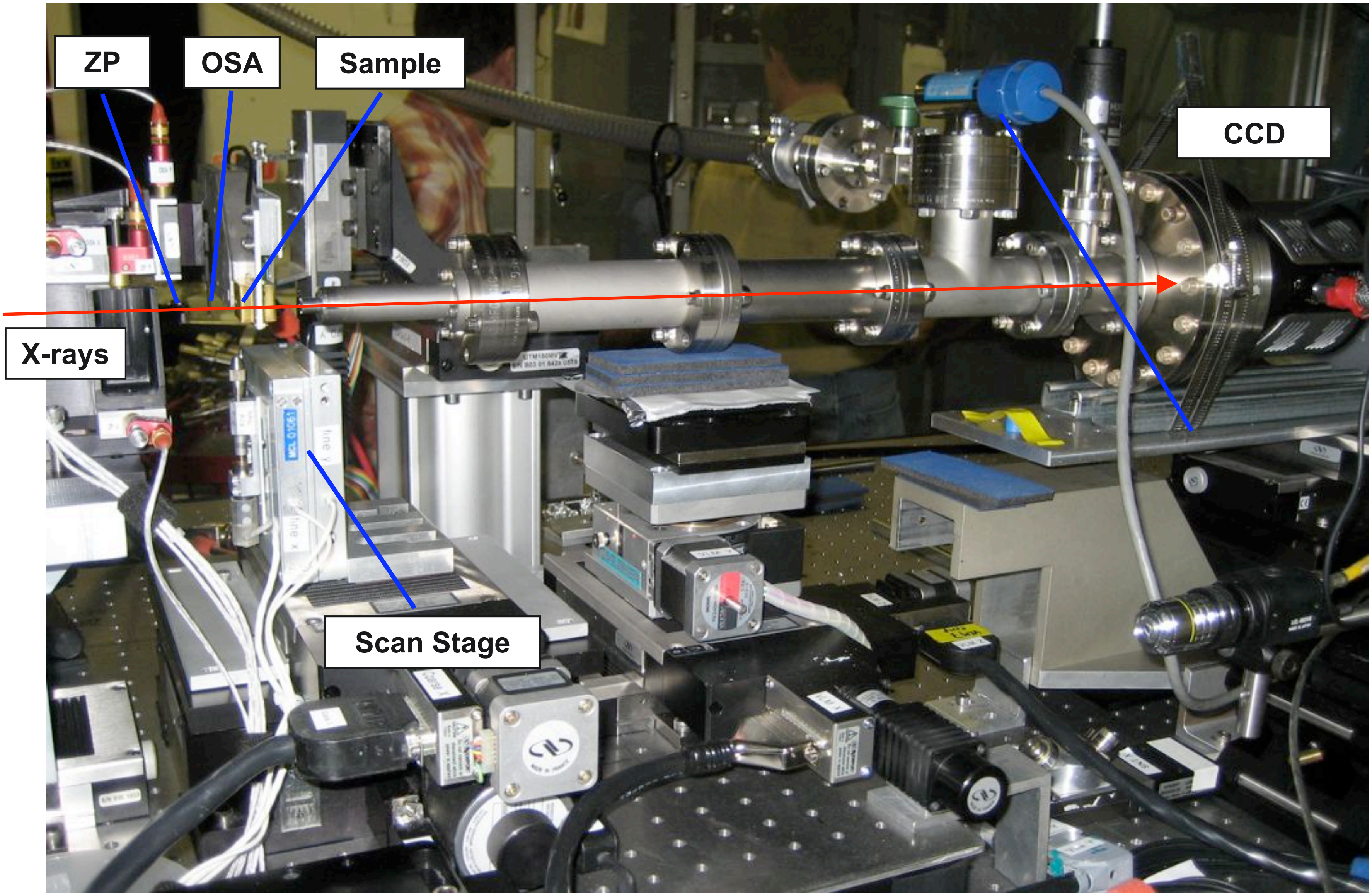

Fresnel coherent diffraction imaging of a gold test pattern

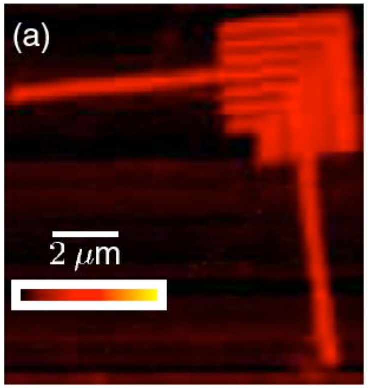

STXM image (1.8 keV)

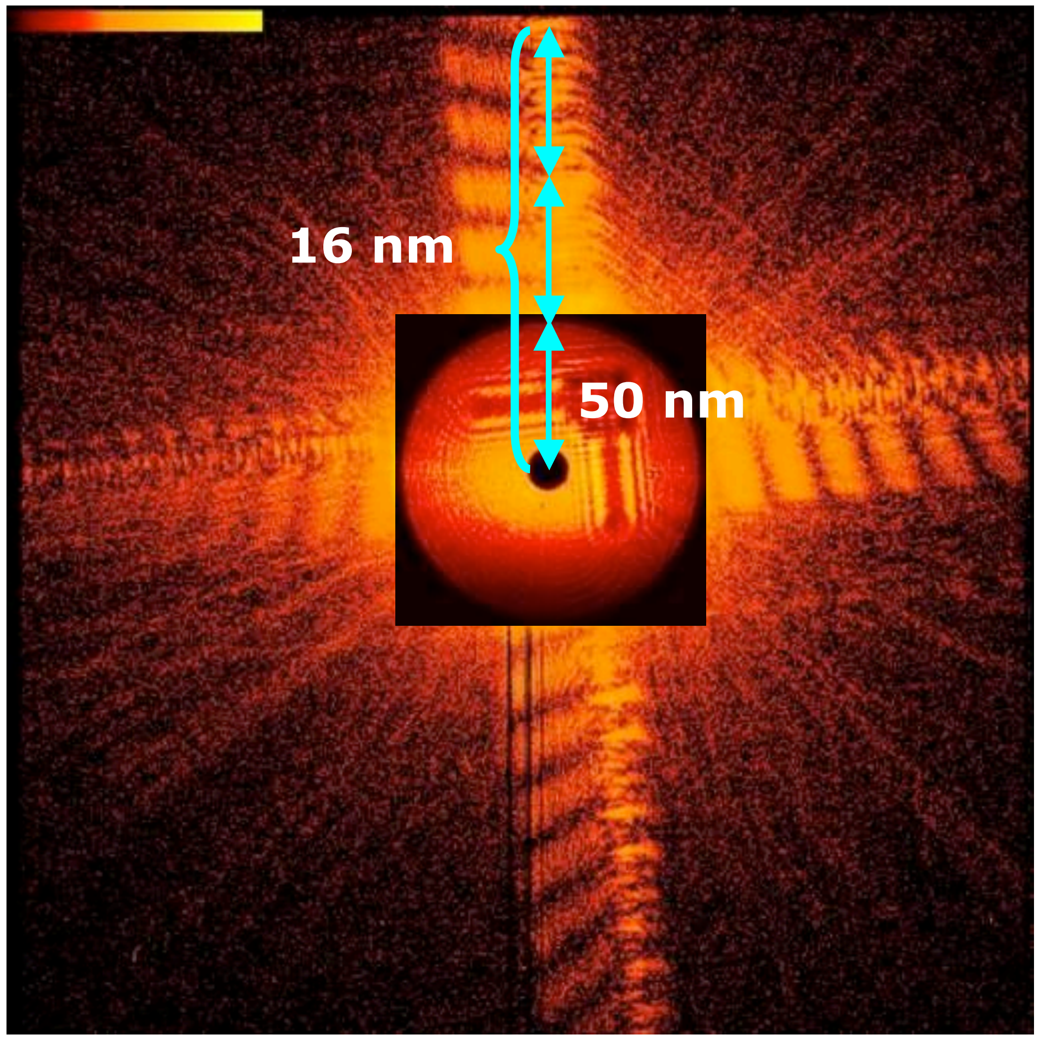

Images reconstructed by FCDI

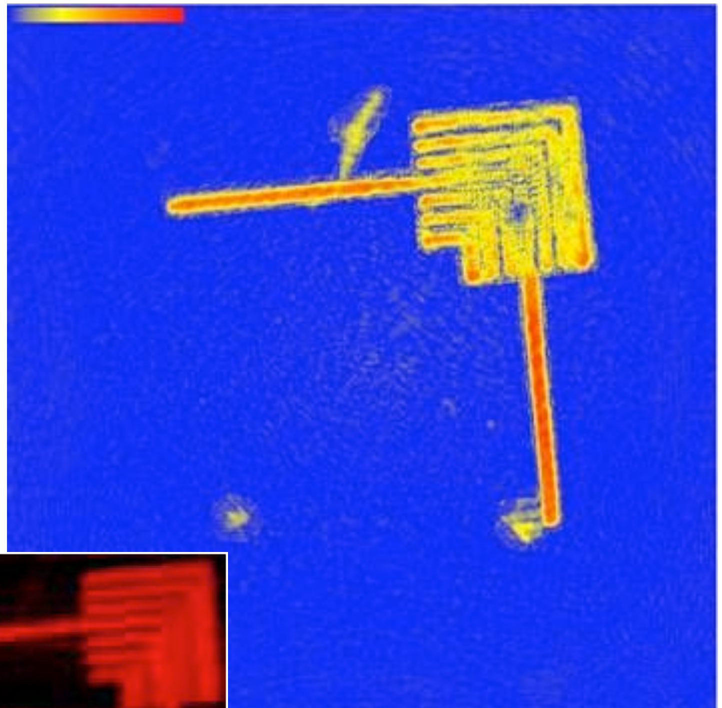

Phase

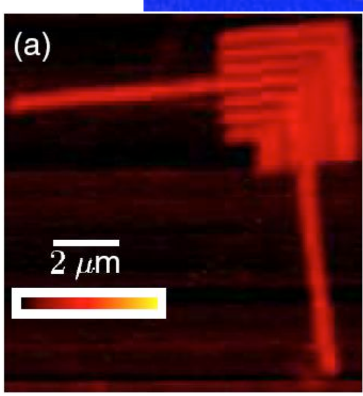

STXM image (1.8 keV)

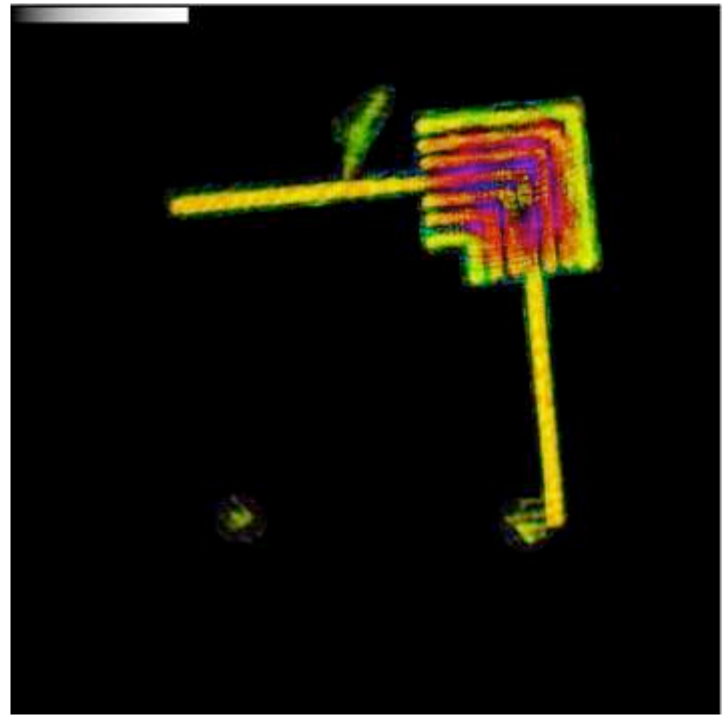

Magnitude with
color-encoded phase

G. Williams et al., *PRL* 97, 022506 (2006)

"Keyhole" FCDI

Use reconstructed illumination profile to determine support in extended sample

H. Quiney,
***Nature Physics* 2, 101 (2006)**

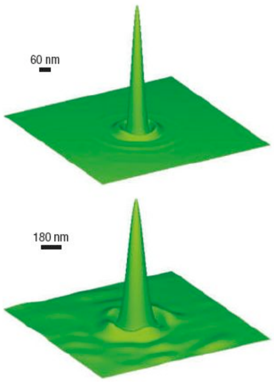

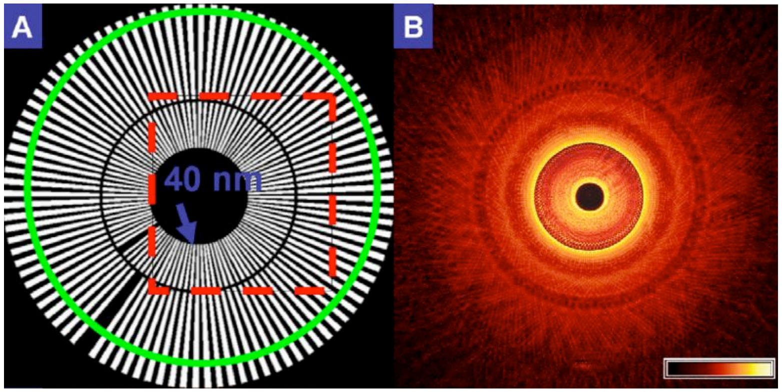

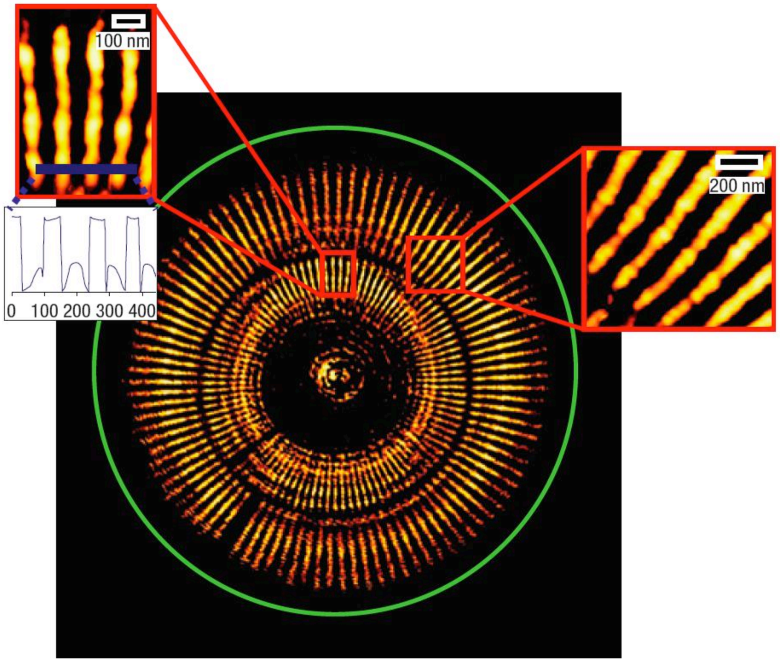

Ability to study extended samples is essential for many real-world problems!

B. Abbey et al., *Nature Physics* 4, 394 (2008)

Recent results ("fuse bay" structure)

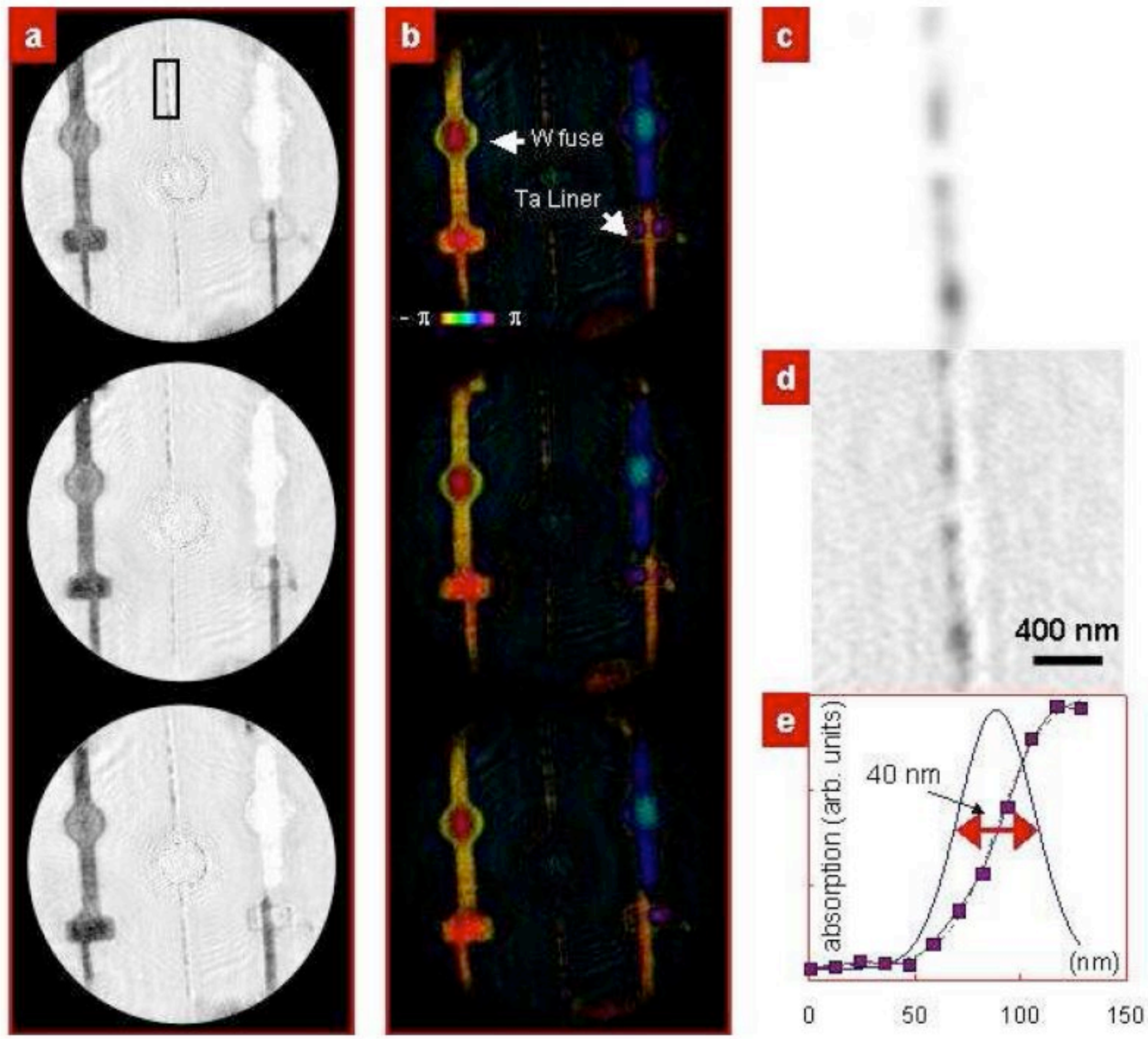

Alternative approach: ptychography

R. Hegerl et al., Phys. Chemie 74, 1148 (1970)
H. Faulkner and J. Rodenburg, PRL 93, 023903 (2004)
J. Rodenburg et al., Phys. Rev. Lett. 98, 034801 (2007)
P. Thibault et al., Science 321, 379 (2008)

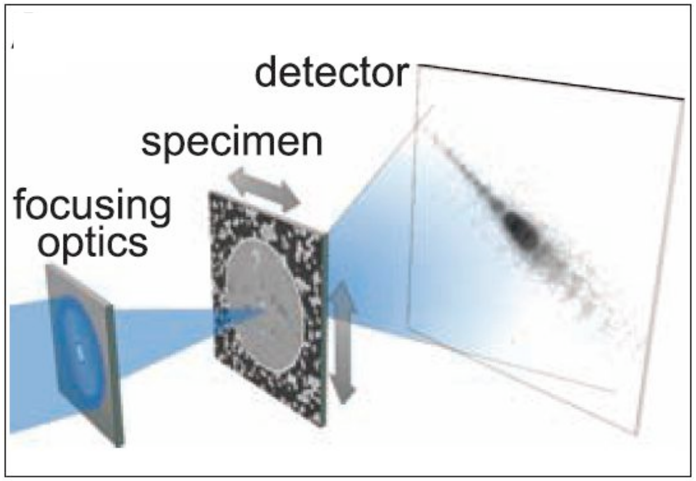

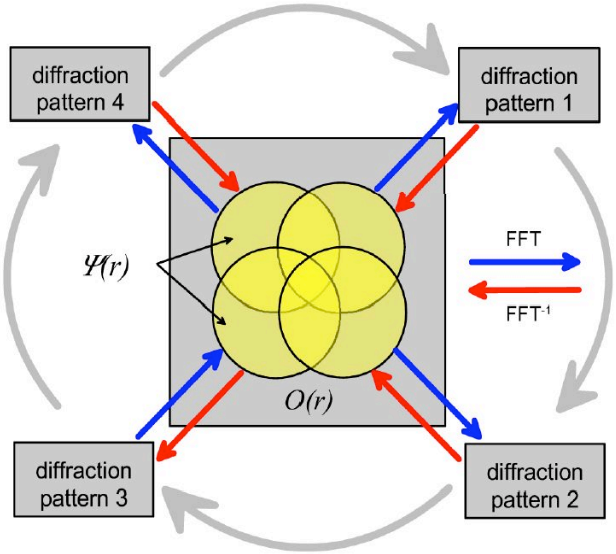

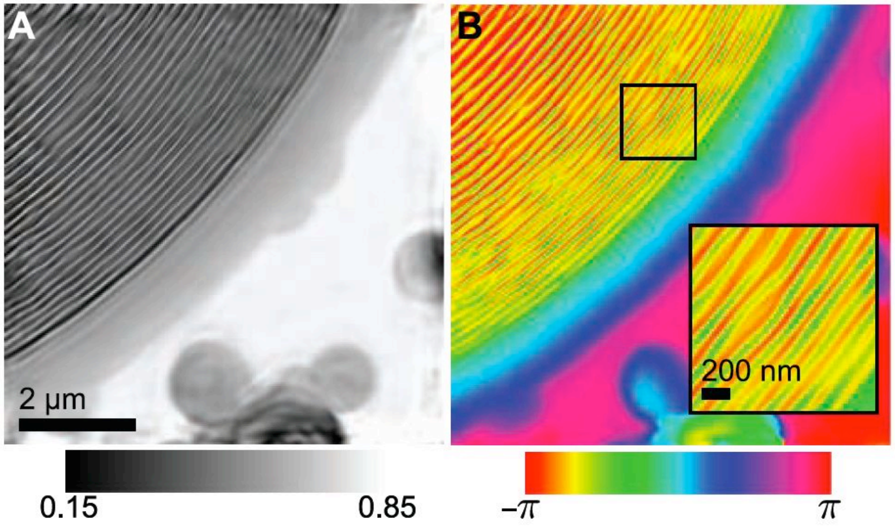

Holography

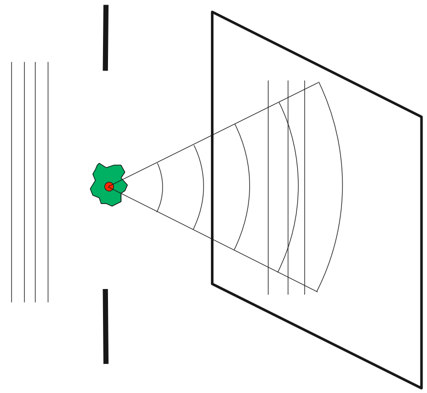

Gabor

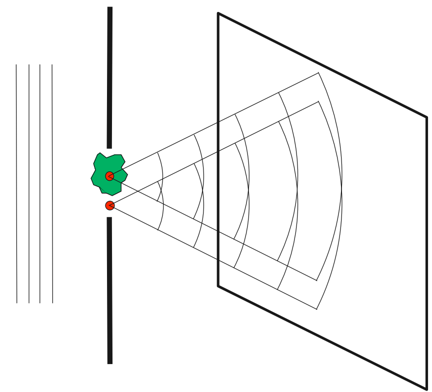

Fourier transform

Record hologram

$$I = |a+b|^2 = |a|^2 + |b|^2 + a^*b + ab^*$$

Reconstruct

$$\begin{aligned} bI &= b|a|^2 + b|b|^2 + a^*bb + abb^* \\ &= aI_b + b(I_a + I_b) + \text{background} \end{aligned}$$

- **Reference wave encodes magnitude and phase of object wave**
- **Reconstruct object wave by "re-illuminating" hologram with reference wave (or its C.C.)**

Gabor holography

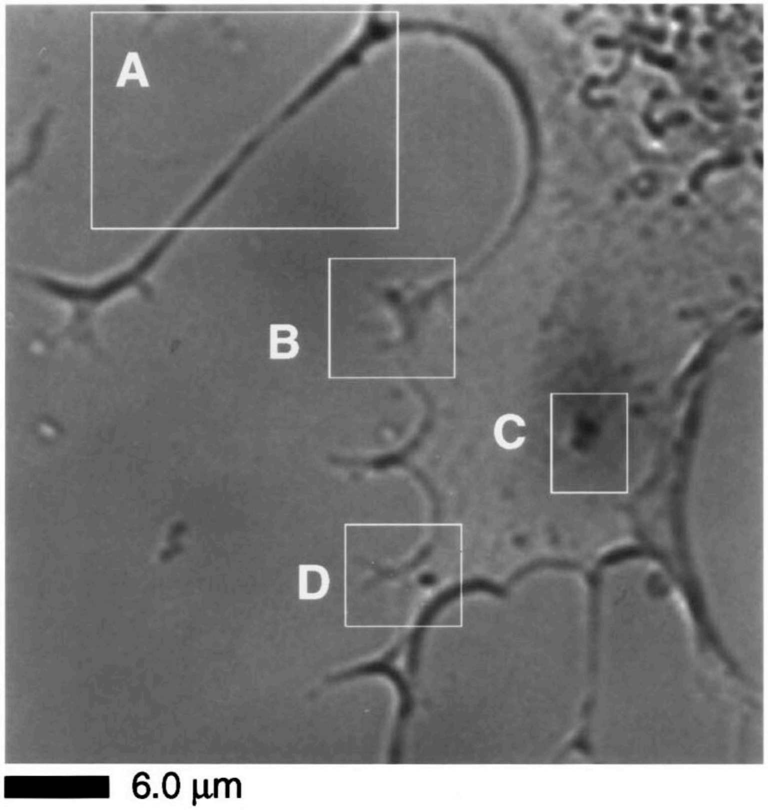

Visible light

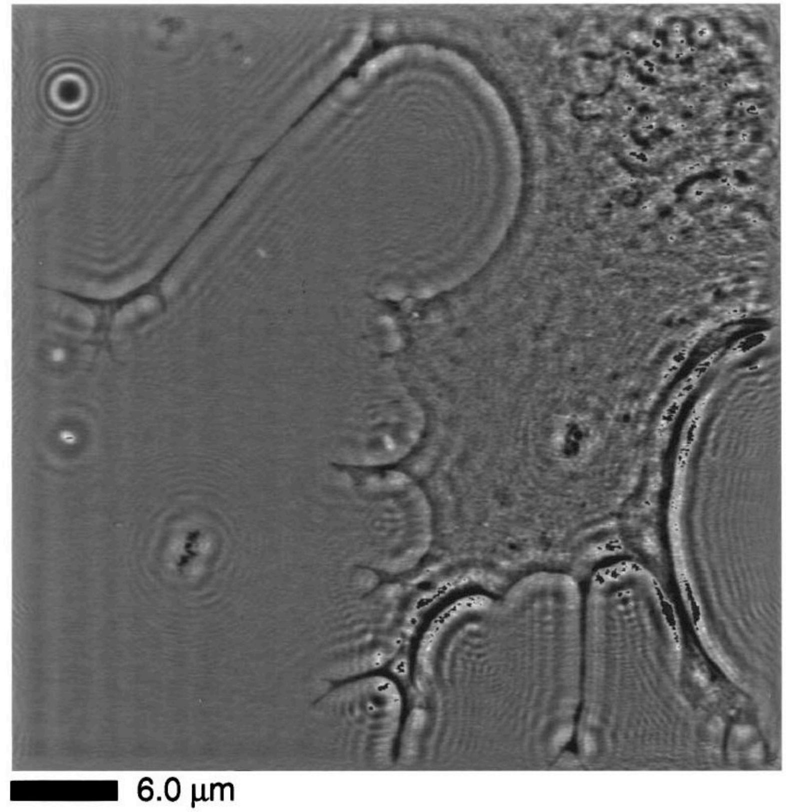

X-ray

Reconstructed hologram (right) of a NIL8 hamster neural fibroblast recorded with 656 eV x-rays. Estimated dose was 7.5 x105 Gy

S. Lindaas et al, *J. Opt. Soc. A.* 13, 1788 (1996)

Hard x-ray holotomography

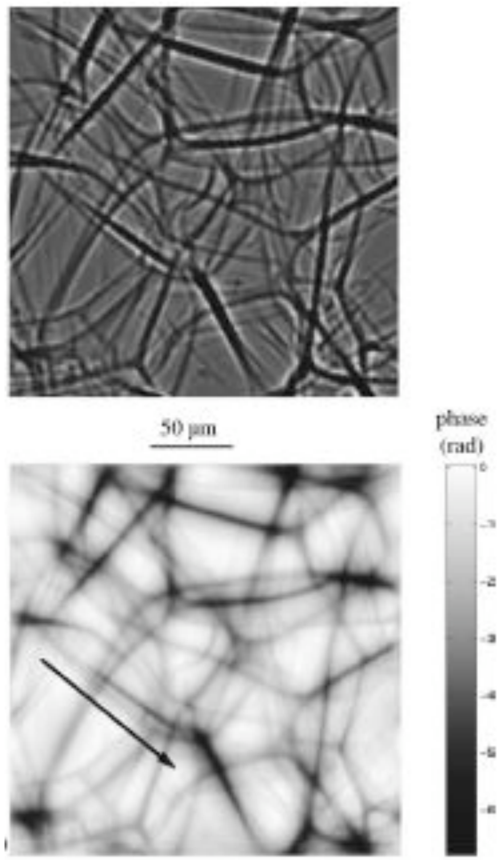

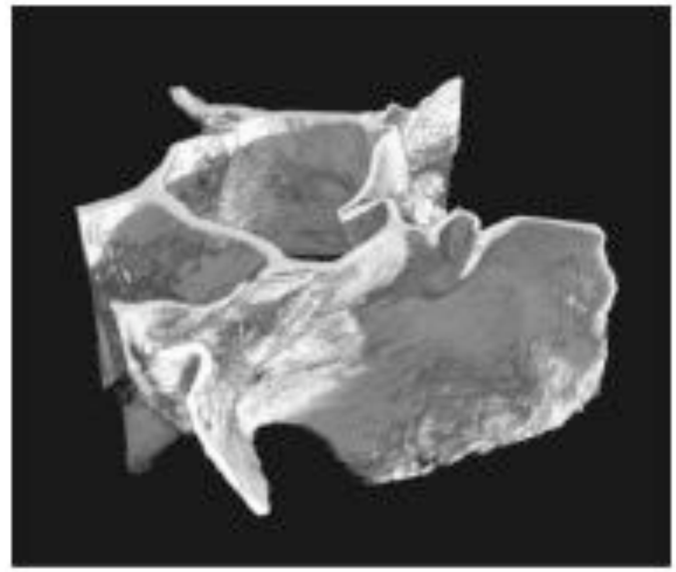

Phase-sensitive image quantitative phase map, and volume rendition of polystyrene foam (18 keV x-rays)

P. Cloetens et al., *Appl. Phys. Lett.* 75, 2912 (1999)

FT hologram formation

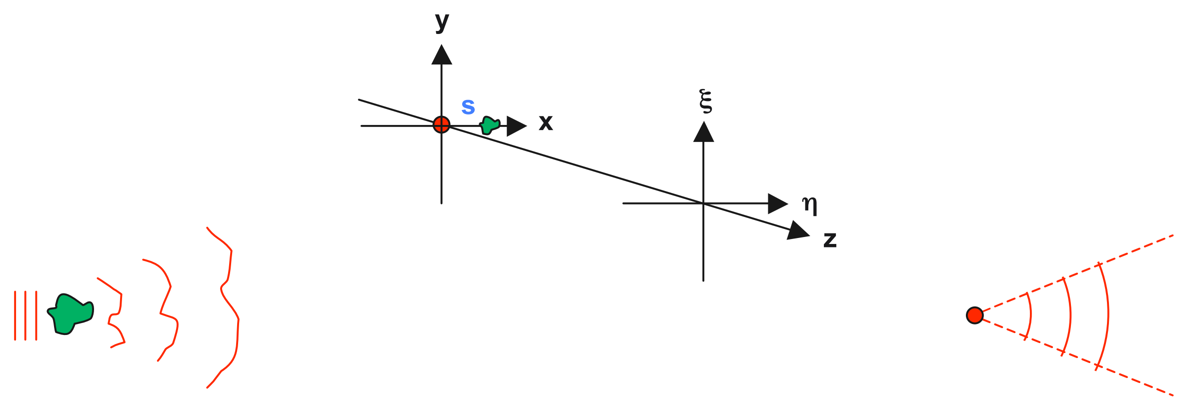

$$a(\xi,\eta) = \frac{e^{ikz}}{i\lambda z}\iint a(x-s,y)\; e^{\frac{ik}{2z}\left((x-\xi)^2+(y-\eta)^2\right)} dxdy$$

object wave

$$b(\xi,\eta) = \frac{e^{ikz}}{i\lambda z} b_0 e^{\frac{ik}{2z}\left(\xi^2+\eta^2\right)}$$

reference wave

$$I = |a+b|^2 = |a|^2 + |b|^2 + a^*b + ab^*$$

hologram intensity

Reconstruction

- **Numerically take FT of hologram intensity to reconstruct**
- **Spatially separated primary, conjugate object waves result**
- **Weak curvature f(x,y) on object wave can be ignored**

Image terms: $$a^{*}b+ab^{*} = \varphi(s\xi)F(\xi,\eta)+\varphi(s\xi)^{*}F(\xi,\eta)^{*}$$

where: $$F(\xi,\eta) = \frac{e^{ikz}}{i\lambda z} f(\xi,\eta)\iint a(x,y)f(x,y)e^{-\frac{ik}{z}(x\xi+y\eta)}\,dxdy \quad ,$$

$$\varphi(s,\xi) = e^{-\frac{ik}{z}s\xi}$$ **and** $$f(\xi,\eta) = e^{\frac{ik}{2z}(\xi^2+\eta^2)}$$

$$FT^{-1}\{a^{*}b+ab^{*}\} = \boxed{f(x-s,y)\,a(x-s,y)} + f(-(x-s),-y)^{*}\,a(-(x-s),-y)^{*}$$

CoPt magnetic labyrinth nanostructures

side view

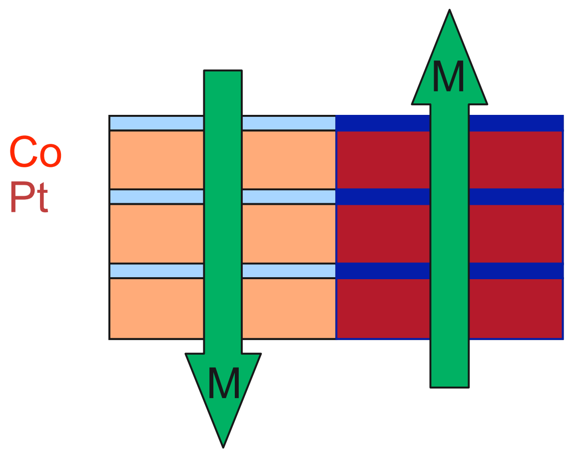

Sample: O. Hellwig (Hitachi)

MFM, top view

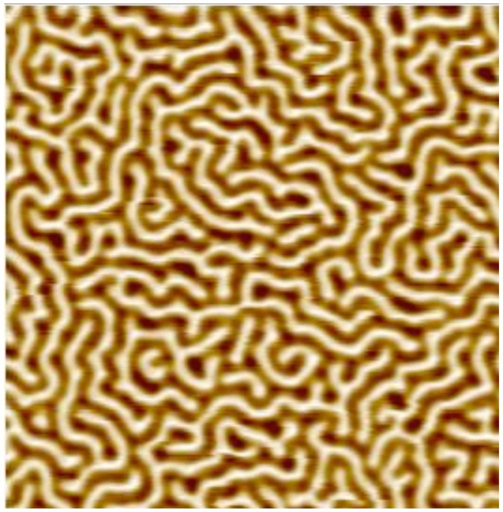

5 μm x 5 μm

continuous object

SiN_x / Pt (24 nm) /
[Co (1.2 nm) / Pt (0.7 nm)]$_{50}$ /
Pt (1.5 nm)

perpendicular anisotropy → magnetic storage media

UE56-SGM beamline and ALICE

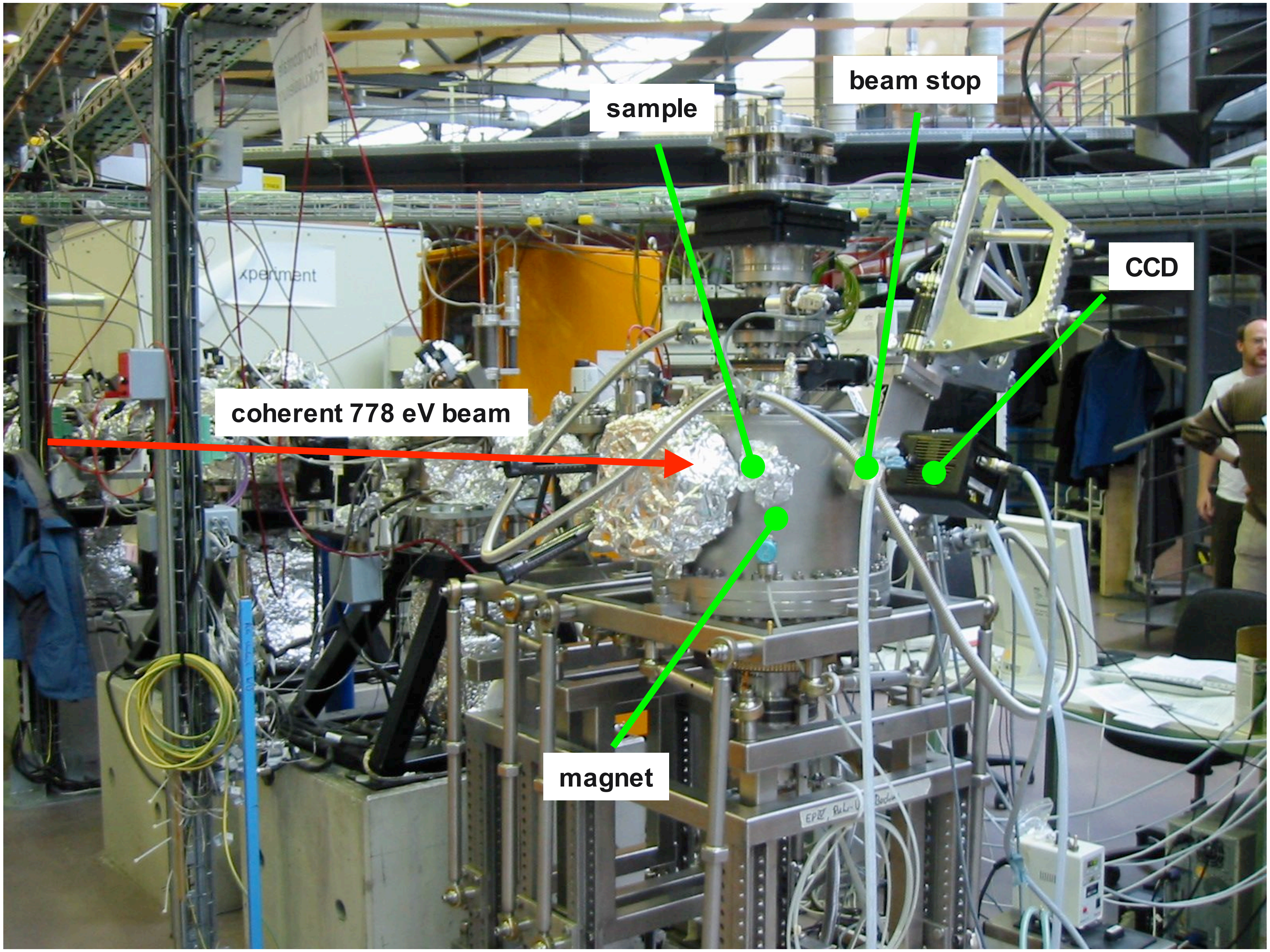

Pinhole mask method

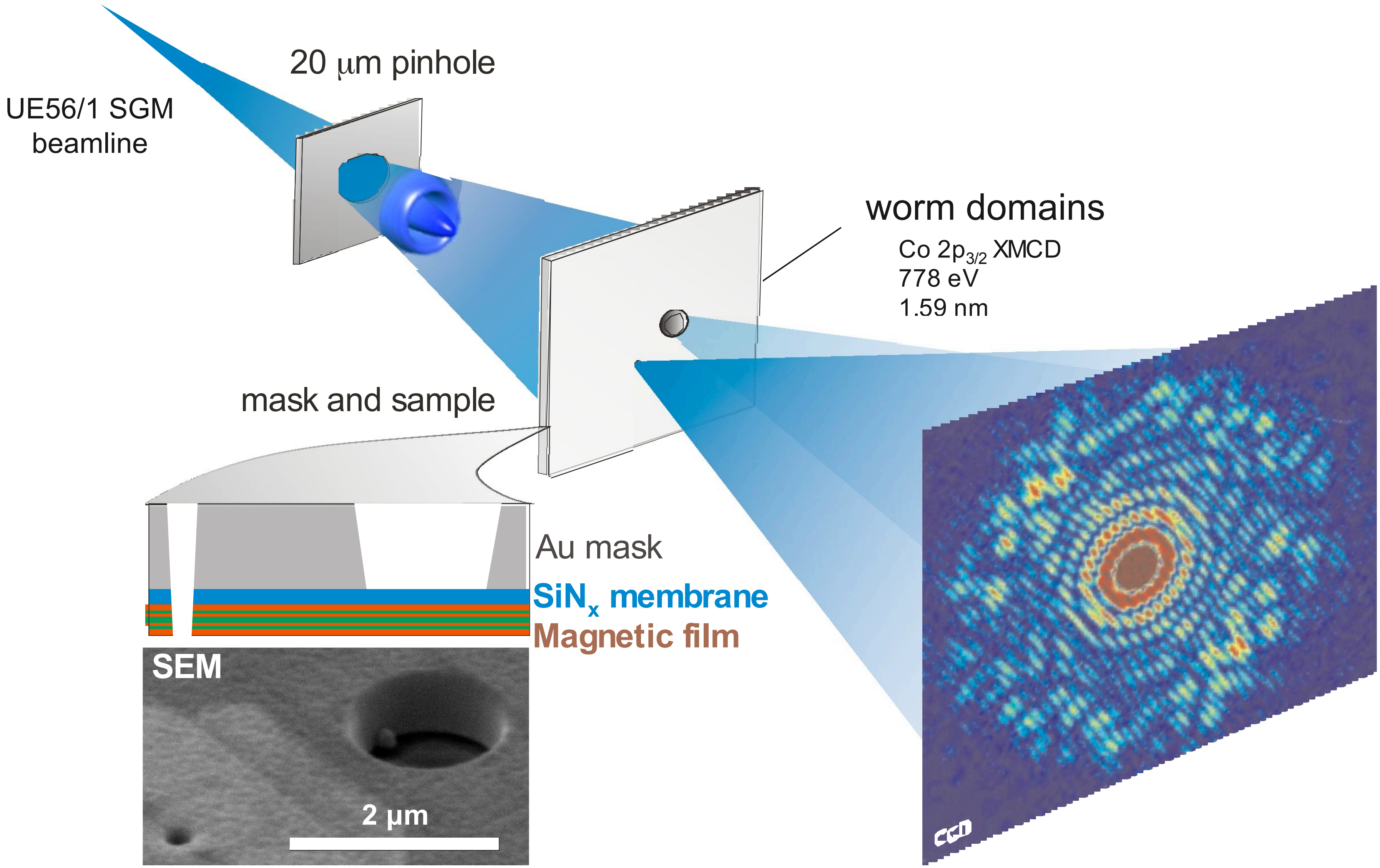

FTH

STXM

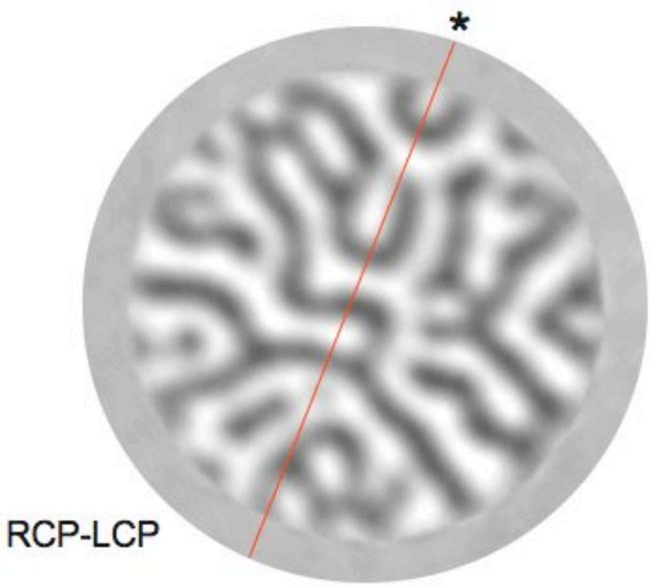

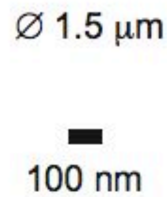

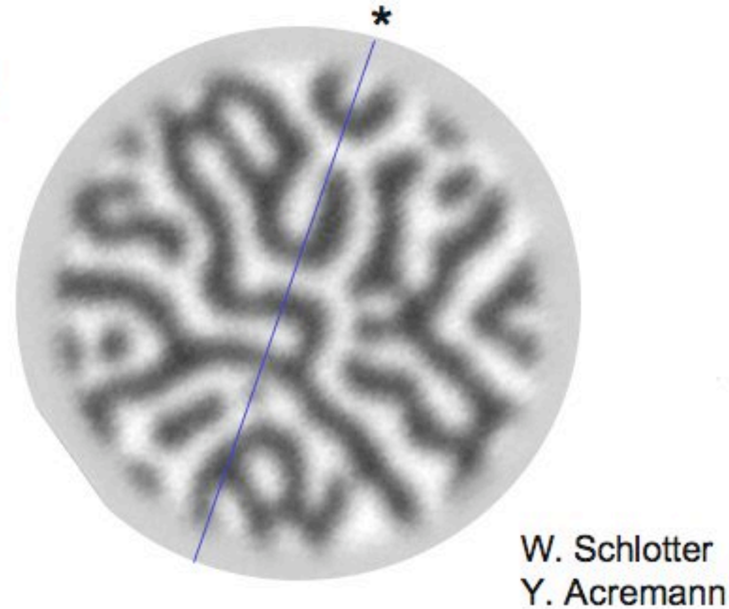

Reconstructed resolution ~50 nm

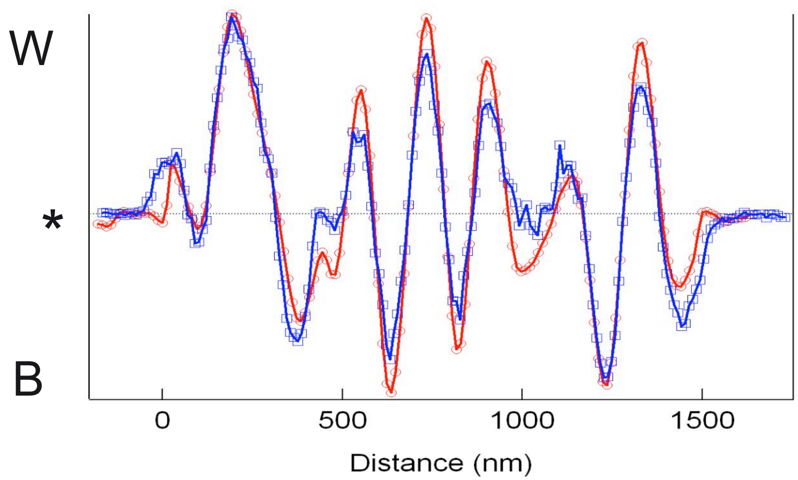

Resolution ~35 nm

S. Eisebitt, et al., *Nature* 432, 885 (2004)

Imaging resolution by x-ray holography

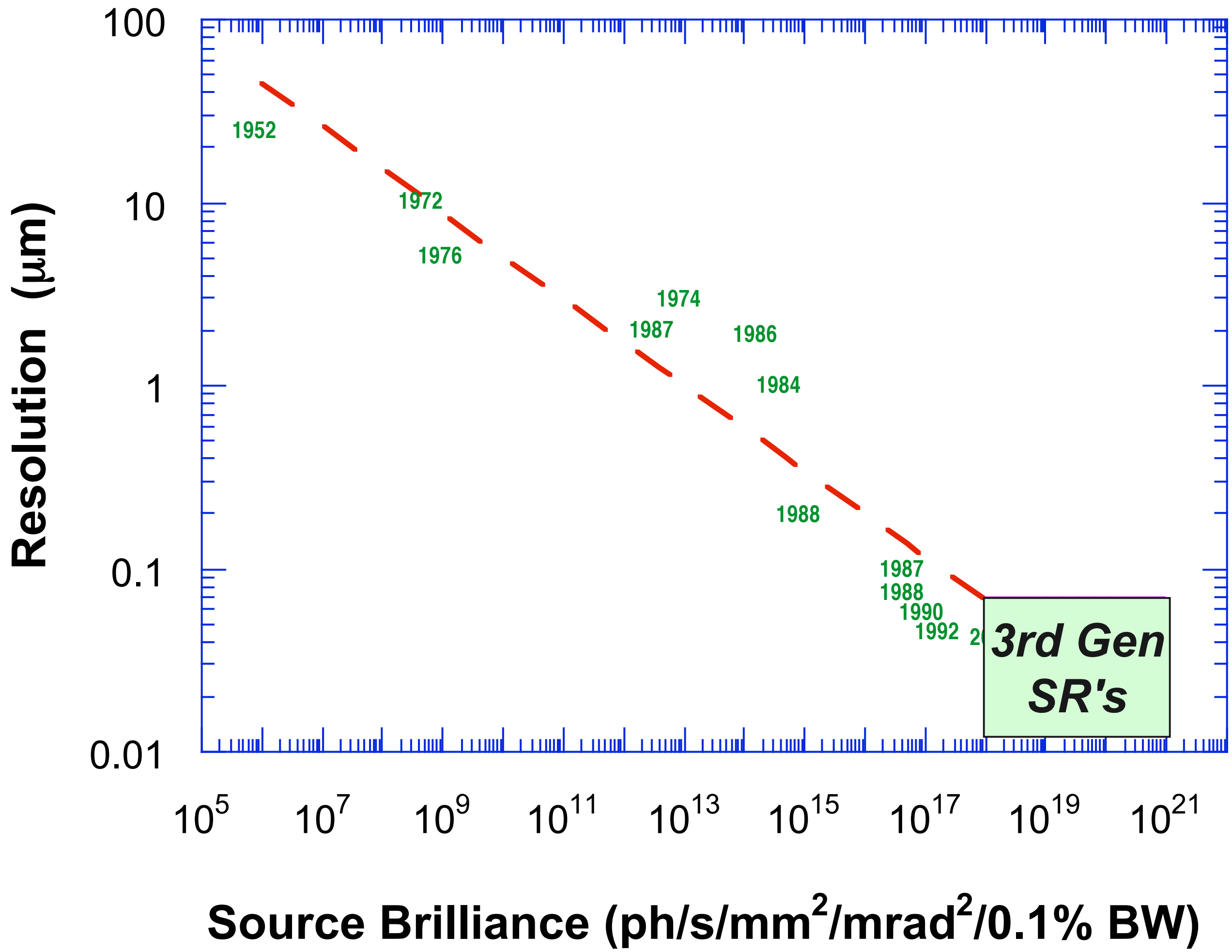

What's in store for the future?

- Resolution of x-ray optics is improving steadily
  - 30 nm is routine
  - < 5 nm looks possible using MLLs

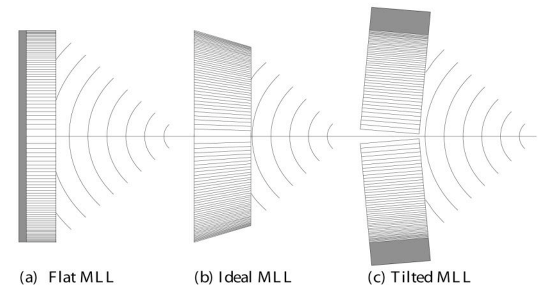

- Commercial x-ray microscopes are proliferating
  - Precision full-field and scanning instruments
  - Multiple contrast mechanisms available
  - Cryo-preparation will become standard (as for TEM)

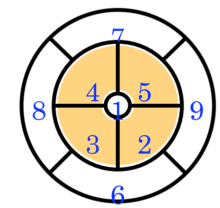

- Hybrid scanning (ptychography) and single-view (keyhole) coherent diffraction methods broaden range of applications

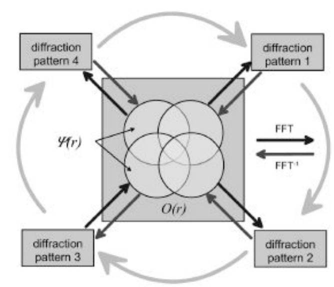

- Diffraction and holographic methods are attractive for x-ray lasers such as XFEL and LCLS !
  - Bypass radiation damage with a single few-fs flash
  - Use pump-probe methods to study ultrafast dynamics
  - No lens to limit resolution or get between sample, detector

Ultrafast coherent diffraction with a free-electron laser

The reconstruction is carried out to the diffraction limit of the 0.26 NA detector

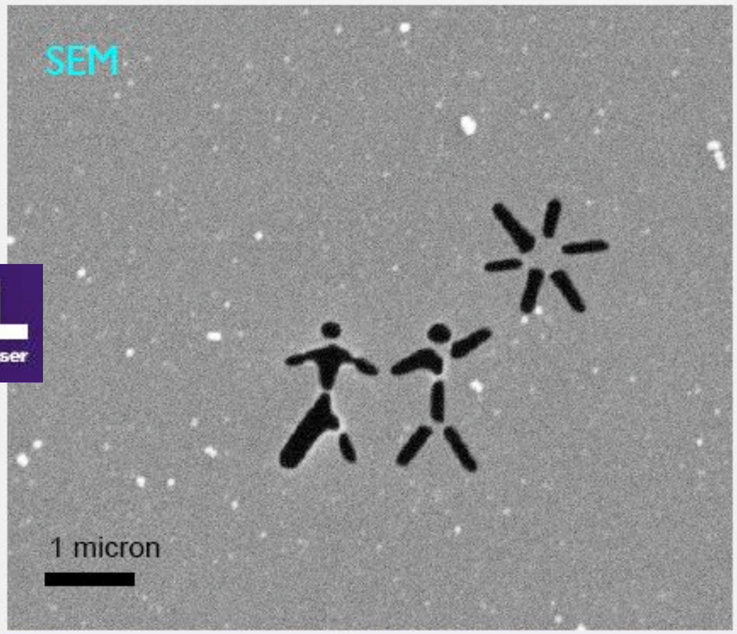

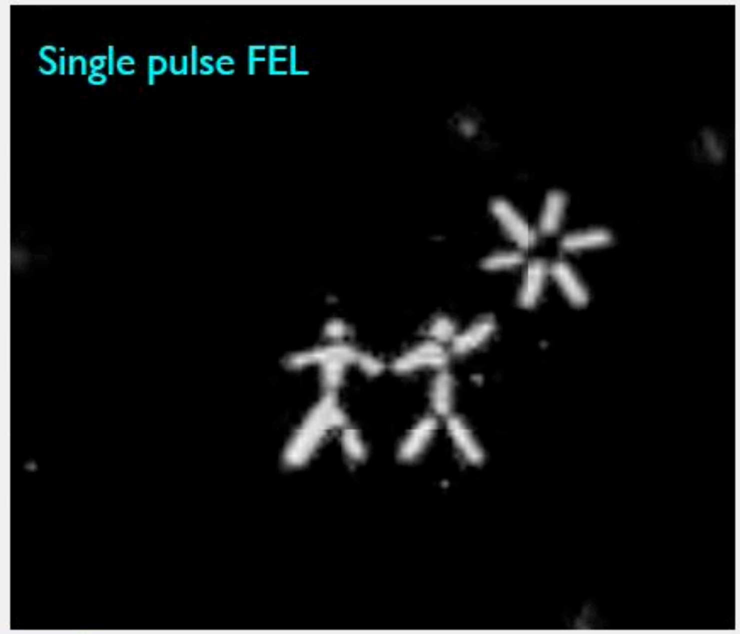

Phase-retrieval transfer function gives an estimate of the resolution of the reconstructed image

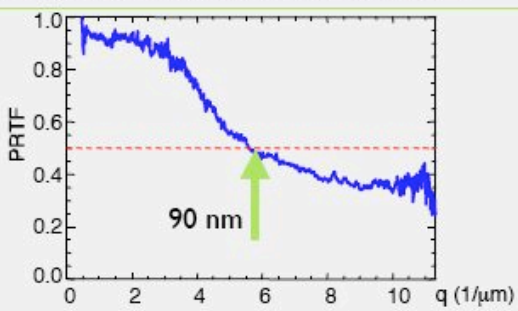

32 nm, one wavelength

λ / NA

H. Chapman et al., *Nature Physics* 2, 839 (2006)

Now it can be done on a tabletop!

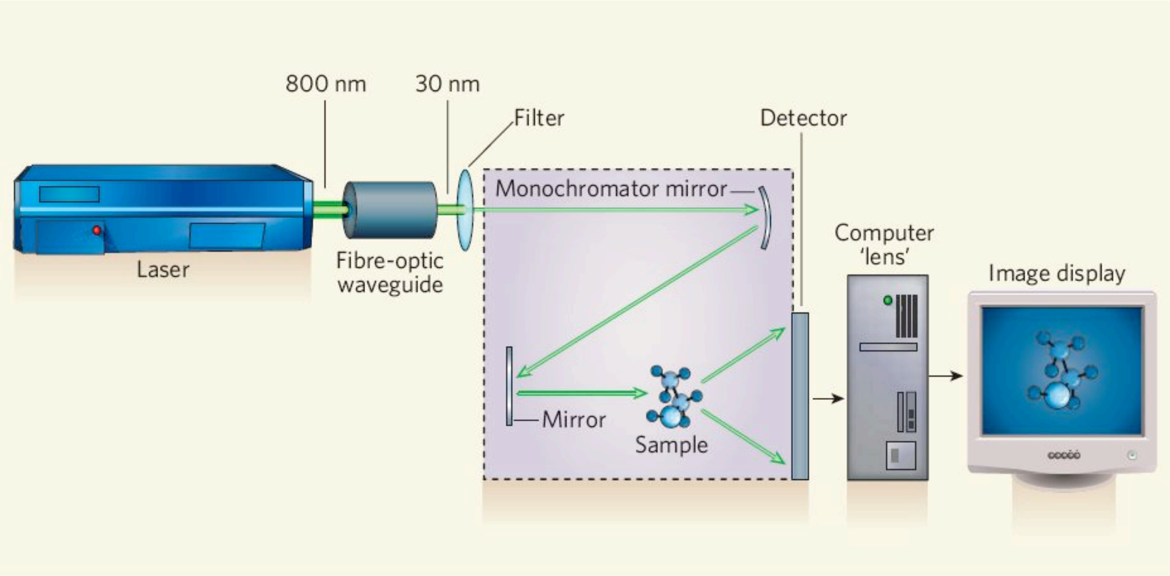

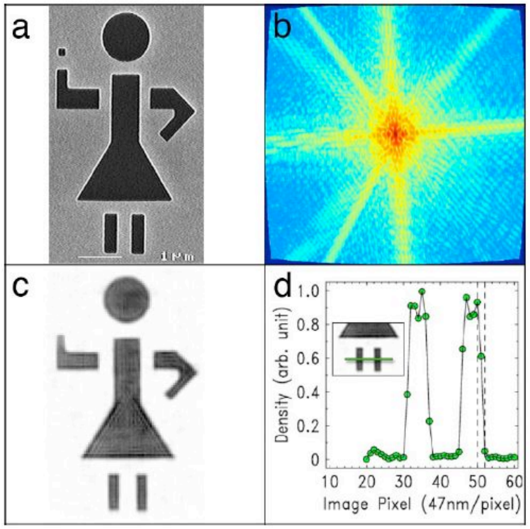

R. Sandberg et al., PRL 99, 098103 (2007)

J. Spence, *Nature* 449, 543 (2007)

R. Sandberg et al., PNAS 105, 24 (2008)

Summary

- **Resolution, contrast, sources, and optics for x-ray imaging**
- **Direct methods: projection, full-field, and scanning**
- **Indirect methods: microdiffraction, coherent diffraction, holography**

Many thanks to:

David Attwood Carolyn Larabell	LBNL/UCSF
Chris Jacobsen	Stony Brook University
Keith Nugent	Centre for Coherent X-ray Science
Stefan Eisebitt	BESSY
John Miao	UCLA
Qun Shen	NSLS-II
Karen Chen	Northwestern University
Jay Brandes	Skidaway Institute of Oceanography
Ellery Ingall	Georgia Institute of Technology
Ben Larson	Oak Ridge National Laboratory
Ross Harder Barry Lai Wenjun Liu Xianghui Xiao	Advanced Photon Source